UNIVERSITY OF LIVERPOOL

RECTENNAS FOR RF WIRELESS ENERGY HARVESTING

by

Jingwei Zhang

Submitted in accordance with the requirements for the award of the degree of Doctor of Philosophy of the University of Liverpool

September 2013

Copyright

To my parents: Anfu Zhang and Yunxin Xiong

ACKNOWLEDGEMENTS

This thesis would not be finished without the help and support of many people who are grateful acknowledged here. At a very first, I would like to express my deepest gratitude to my supervisor, Prof. Yi Huang. He has always given me valuable ideas, suggestions and comments with his profound knowledge and rich research experience and guided me in the right direction. He was easily available and accessible and willing to discuss whenever I needed his guidance and support. I also would like to thank Dr. Yaochun Shen for supporting and guiding me in my research. I have learnt from them a lot not only about research, but also about the professional ethics.

In addition, I would like to thank my parents. Without my parents' support during my whole research duration, I also would not be able to achieve my goals.

Last but not least, I wish to extend my thanks to the Department of Electrical Engineering and Electronics for its support of this study. I would like to thank my postgraduate friends, who never failed to give me great encouragement and suggestions. Special thanks should go to Dr. Di Li, Dr. Yang Lu, Mr. Ping Cao, Miss. Lei Xing and Mr. Qian Xu for their discussions with me during my research.

TABLE OF CONTENTS

LIST OF FIGURES

LIST OF PUBULICATIONS

1. **J. Zhang**, Y. Huang and P. Cao, “Wideband rectenna arrays for low input power energy harvesting,” *submitted to IET Microwaves, Antennas & Propagation.*2013.

2. **J. Zhang**, Y. Huang and P. Cao, “A high conversion efficiency wideband rectenna for wireless energy harvesting,” *submitted to IEEE antennas and wireless propagation Letters.*2013.

3. **J. Zhang**, Y. Huang, P. Cao, and H. T. Chattha, "Broadband unidirectional dipole antennas for wireless applications," in *Antennas and Propagation Conference (LAPC), Loughborough*, pp. 1-4, 2011.

4. **J. Zhang**, Y. Huang, and P. Cao, "Harvesting RF energy with rectenna arrays," in *Antennas and Propagation (EUCAP), 2012 6th European Conference on*, pp. 365-367, 2012.

5. **J. Zhan**g, Y. Huang, and P. Cao, "A wideband cross dipole rectenna for wireless harvesting," in *Antennas and Propagation (EuCAP), 2013 7th European Conference on*, pp. 3063-3067, 2013.

6. **J. Zhang** and Yi Huang, "Rectennas for wireless energy harvesting," in *IET Seminar: Electromagnetic in current and emerging energy and power systems*, 2012.

7. P. Cao, Y. Huang, X. Zhu and **J. Zhang**, “Pattern Diversity Based UWB MIMO monopole antenna,” *submitted to IET Microwaves, Antennas & Propagation.*2013.

8. P. Cao, Y. Huang, **J. Zhang**, X. Zhu and R. Alrawashdeh, “A UWB Monopole Antenna with Reconfigurable Band notched Characteristics,” *submitted to Microwave and Optical Technology Letters.*2013.

9. P. Cao, Y. Huang, **J. Zhang**, and N. Khiabani R. Alrawashdeh,“A UWB Planar Monopole Antenna with Quintuple Band Notched Characteristics,” *submitted to IET Microwaves, Antennas & Propagation.*2013.

10. P. Cao, Y. Huang, **J. Zhang**, and R. Alrawashdeh, "A compact super wideband monopole antenna," in *7th European Conference on Antennas and Propagation (EuCAP), Sweden*, pp. 3107-3110, April, 2013.

11. P. Cao, Y. Huang, **J. Zhang**, and Y. Lu, "A comparison of planar monopole antennas for UWB applications," in *Antennas and Propagation Conference (LAPC), 2011 Loughborough*, pp. 1-4, 2011.

12. P. Cao, Y. Huang, and **J. Zhang**, "A UWB monopole antenna for GPR application," in *Antennas and Propagation (EUCAP), 2012 6th European Conference on*, pp. 2837-2840, 2012.

ABSTRACT

There is an increasing interest in energy harvesting. The rectenna, which is a combination of a rectifier and an antenna, is a device to harvest wireless energy in the air. This thesis is concentrated on the analysis, design and measurement of compact rectennas for radio frequency (RF) wireless energy harvesting applications, and the thesis can be divided into three parts.

The first part is about broadband planar dipole antennas with an unidirectional radiation pattern which is suitable for wireless energy harvesting applications. With the rapid development of various wireless systems, there is a need to have a broadband rectenna for energy collection. The antenna is optimized by changing the dipole shape, diameter, feed gap and the spacing between the antenna and the ground plane. It is shown the optimized antenna has a broad (from 2.8 to at least 12 GHz) with the ability to produce unidirectional radiation pattern. It is a good candidate to form a wideband dual-polarized antenna array for applications such as the wireless power transmission and collection. In addition, a simple rectenna and duel-polarized rectenna arrays are presented. The measurement of the rectenna array is shown that the design has produced the desired DC power with reasonable efficiency. The study is confirmed that the more elements in the array, the higher output voltage although the bandwidth is not as wide as expected because of practical limits.

The second part is about a novel wideband cross dipole rectenna for RF wireless energy harvesting. The proposed device consists of a cross dipole antenna, low-pass filter (LPF) and voltage doubling rectifier circuit using Shottcky diodes as rectifying elements. It works over the frequency range from 1.7 to 3 GHz for the reflection coefficient less than -10 dB. Besides, the proposed rectenna can convert the RF energy into DC energy

with a good conversion efficiency of up to 75% for high input power density levels (>5 mW/cm^2). In addition, another wideband rectenna built on FR4 substrate is optimized for low input power and the rectenna is optimized, built and measured. A further investigation for the input impedance of rectifier is also conducted. Experimental results demonstrate the rectenna has wideband rectification performance and the maximum rectenna conversion efficiency at 1.7 GHz is more than 50% for the power density of 0.1 mW/cm^2.

The third part is about improving rectenna conversion efficiency for low input power density. Increasing the rectenna conversion efficiency for low power density is significant for improving rectenna performance. Currently, there are few of research focused on wideband rectenna arrays for low input power. A new wideband rectenna array with a reflector is developed to increase the rectenna conversion efficiency and output voltage through increasing the gain of the antenna. In addition, two connection methods are used to build the rectenna array and advantages and disadvantages for each method are presented. The RF to DC conversion efficiency of proposed rectenna arrays is much improved for low input power density over a wide bandwidth.

This research has produced some important designs and results for wireless energy harvesting, especially in wideband rectennas, and is a solid step towards possible widespread applications of rectennas in the near future.

CHAPTER 1

INTRODUCTION

1.1 Motivation

1.1.1 Introduction

Wireless communications have experienced a rapid development over the last two decades and have become an integral part of our daily lives. Cellular networks, wireless local networks (WLANs) and wireless personal area networks (WPANs) are just a few examples of the wireless technology that we are using every day. They enable us to be connected anywhere and anytime. These wireless systems also radiate a large amount of electromagnetic energy into the air but most of them are actually wasted.

Nowadays, the energy recycling has become a very significant issue all over the world. Thus, how to harvest and recycle the wasted ambient electromagnetic energy also has become an increasingly interested topic. In the past few decades, wireless power transmission (WPT) has become an interesting topic as one of the technologies for solving this problem.

There are many electronic devices or sensors that operate in conditions where it is costly, inconvenient or impossible to replace a battery, or deliver wired power. As a result there has been an increased demand for wireless power supplier for these devices. Let us take the low power sensor or device as an example; it normally works at a low duty cycle and in an environment with low-level of light or vibration. Thus RF wireless power suppliers offer a potential alternative for maintenance free operations.

The basic technology for wireless power supplier is the wireless power transmission which is a transmission of electrical power from one location to another without artificial conductor. In 1831, Michael Faraday discovered the electromagnetic induction. This discovery came from an experiment. He wrapped two insulated coils of wire around an iron hoop and when the current went through one of the coil, a current appeared in another coil [1]. This is called mutual induction. Later, Hertz used high frequency power to illustrate the generation and transmission of 500 MHz pulse energy in 1888. However, lacking of the device which can convert RF power to DC power, the WPT system cannot be realised.

Over 100 years ago, the concept of wireless power transmission was introduced and demonstrated by Tesla.[2], he described a method of "utilising effects transmitted through natural media". However, Tesla was unsuccessful to implement wireless power transmission systems for commercial use but he transmitted power from his oscillators. The reason for this unsuccessful attempt was that the transmitted power was used to

all directions with 150 kHz radio wave whose wavelength was 21 km and the efficiency was too low.

Based on the development of microwave tubes during the World War II, the rectifier of microwave signals for supplying DC power through wireless transmission was proposed and researched for high-power beaming since 1960s by B. C. Brown [3]. He finally laid the experiment foundation of WPT, and transferred the concept to reality.

The modern history of free space power transmission may be considered to have its origin in the late 1950s [3] with applications in microwave-powered aircraft and the solar power Satellite Concept. Since the first wireless transmission systems was demonstrated [4]it has become an increasingly interesting topic for the wireless energy community. This interest seems to have been initiated by short-range (< 2 m) radio frequency identification (RFID) applications, focusing on available industry, science and medical (ISM) frequency bands around 0.9 GHz, 2.4 GHz, 5.8 GHz and higher. Especially for the higher frequencies, the wavelengths are small enough for the realisation of miniature wireless products [5].

One of the most important and main requirement of WPT system is the efficient transfer of the electrical power. The key component for the system consists of an antenna coupled to a rectifying unit. The combination of an antenna and a rectifier is commonly called a rectenna and it can convert electromagnetic energy to direct current (DC) energy. A good review of rectification of microwave signals for supplying DC power through wireless transmission has been given in [4].

1.1.2 Motivation of This Work

There are at least two advantages for using rectennas to harvest the wasted energy in the air: (1) the lifetime for the rectenna is almost

unlimited and it does not need replacement (unlike batteries). (2) It is "green" for the environment (unlike batteries, no deposition to pollute the environment).

Recently, some narrowband rectennas using such as dipoles, patches and slot antennas were designed for rectenna devices [3, 5-20]. For example, a dual-frequency dipole rectenna was developed for dual-band (2.45 and 5.8 GHz) wireless power transmission, the rectenna with dual band is more attractive to use than a single-band one for the power transmission. It can receive power at either frequency depending on the availability of power. The main part of this rectenna is constructed by a receiving dual-frequency dipole antenna, a co-planar strip-line (CPS) input low-pass filter, two CPS band-stop filters, a rectifying diode, and a microwave block capacitor [8]. Its energy conversion efficiency was greater than 80%.

A few wideband rectennas were also investigated [21-24], such as a broadband (2 to 18 GHz) circularly polarised spiral rectenna array was presented in [22]. In this work, each antenna is connected to a rectifying diode, keeping the non-directive properties of each element. In addition, the power is collected from any arbitrary polarisation incident on the rectifying antenna array. However, these wideband rectennas had low RF to DC conversion efficiencies. For example, the conversion efficiency around 20% was presented in [22].

Generally speaking, there are three common limits of most of current rectenna designs. The first one is that most of rectennas were performed for narrowband, especially a single frequency. The second limit is that high RF to DC conversion efficiency needs high input power level. The final problem is wideband rectennas had low RF to DC conversion efficiency or DC output voltage.

The first motivation of this research is to overcome these limitations. Successfully increasing the rectenna bandwidth and improving the RF to

DC conversion efficiency for wideband rectennas at low input power density are the main motivation. The wideband rectenna is able to be integrated into different wireless devices, where the rectenna can capture and rectify larger amount of energy in the air at different frequencies. Low input power rectennas can efficiently use in low power density area with consistent high conversion efficiency performance.

To supply high DC output voltage, the rectenna array is also an important and necessary method for rectenna designs. The rectenna array can be built by using different interconnections of rectenna elements [22, 23, 25]. Each connection has its own output features. However, they all concern about optimum output voltage. There is lacking in design to improve RF to DC conversion efficiency for lower input power densities. Hence, the second motivation of this work is to develop a rectenna array which is able to effectively improve the rectenna conversion efficiency for low input power densities.

1.2 Organisation of The Thesis

The contents of this thesis are organised as follows:

Chapter 2 reviews the literature in rectennas in the past decades and identifies objectives and presents the state of art achievements on rectenna designs.

Chapter 3 presents three shapes of planar broadband antenna with unidirectional radiation patterns. Additionally, a simple dual-polarized rectenna array design is proposed and investigated.

Chapter 4 describes a novel wideband cross dipole rectennas for RF wireless energy harvesting. A newly developed planar integrated rectenna is used to validate this design. Results prove that the wide-band cross

dipole rectenna can have relatively high conversion efficiency for low input power density over the whole operational frequencies.

Chapter 5 explains a wideband rectenna array which further improves RF to DC conversion efficiency for low power density levels. It can overcome the limitation of the diode characteristics.

Chapter 6 finalises the thesis, reviews the work undertaken and draws conclusions about core parts of the research. Future work is also discussed.

1.3 Aim and Objectives

The aim of the research presented in this thesis is to develop wideband rectennas for RF wireless energy harvesting.

The objectives are:

- To investigate various shapes of broadband dipoles with reflector and develop a simple rectenna and rectenna arrays for wireless energy harvesting.
- To develop a wideband dipole antenna with good performance through different geometries and improving feed connection. Also, to integrate the wideband antenna with a rectifier as a wideband rectenna. It has relatively high RF to DC conversion efficiency to harvest RF energy.
- To develop a wideband antenna array with high gain and integrate with rectifiers as a rectenna array to improve the rectenna conversion efficiency for low power density levels.

1.4 Contribution of This Research

The following chapters of this thesis aim to highlight these contributions made towards the advancement and development of the rectennas for RF wireless energy harvesting.

The key contributions are summarized as follows:

i. *Development of broadband planar dipole antennas with unidirectional radiation patterns above a reflector*

Planar dipole antennas with unidirectional radiation patterns are investigated. The investigation compares various dipole antennas. With the aid of a reflector, the proposed planar dipole antenna can produce broadside unidirectional radiation patterns and a good gain. It is a good candidate for a duel-polarised rectenna array for RF wireless energy harvesting.

ii. *Development of a simple circular dipole rectenna and dual polarised rectenna array for RF wireless energy harvesting.*

A new simple planar circular dipole rectenna and rectenna arrays are designed, fabricated and measured. Results show the simple rectenna can convert the electromagnetic energy to DC electricity. In addition, it is presented the measured DC output voltage of the rectenna is sensitive to measured positions due to the distributed characteristic of antenna. Moreover, the cascade interconnection method for rectenna array can effectively combine output DC voltage from each rectenna element.

iii. *Development of a wideband cross dipole rectenna with relatively high conversion efficiency for RF wireless energy harvesting*

A novel wideband (> 50%) cross dipole antenna fed by a parallel strip-line is designed on different substrate and the high conversion efficiency of the double-sided rectenna is simulated at high power density

levels. Another planar integrated cross dipole rectenna on FR4 substrate is designed and optimised for low input power density and it is fabricated and measured. This antenna is connected with a low-pass filter and matched with the rectifier. The integrated rectenna shows that it is able to effectively convert the RF wireless energy to DC power with high conversion efficiency over a wide bandwidth.

iv. Improving cross dipole rectenna array conversion efficiency for low power density levels.

A new wideband rectenna array above a reflector is designed, fabricated and measured. The double-sided rectenna on a thin FR4 substrate with reflector is optimised and demonstrated to get good antenna gain performance. In addition, two types of rectenna array connection methods are discussed and compared. Results show that both of rectenna array connection method can successfully improve conversion efficiency for low power density level and RF power combiner rectenna array can achieve wider bandwidth.

References

[1] *Aechives Biographies: Michael Faraday*: The Institution of Engineering and Technology.

[2] Nicolas Tesla., *Experiments with Alternate Current of High Potential and High Frequency*: McGraw, 1904.

[3] W.C.Brown, "The history of power transmission by radio waves," *IEEE Trans. Microwave Theory Tech.*, vol. MTT-32, pp. 1230-1242, Sept. 1984.

[4] William C. Brown, "The technology and application of free-space power transmission by microwave beam," *Proceedings of the IEEE*, vol. 62, pp. 11-25, 1974.

[5] Hubregt J. Visser, *Approximate Antenna Analysis for CAD*: WILEY, 2009.

[6] G. Monti, L. Tarricone, and M. Spartano, "X-Band Planar Rectenna," *Antennas and Wireless Propagation Letters, IEEE,* vol. 10, pp. 1116-1119, 2011.

[7] Suh Young-Ho and Chang Kai, "A novel dual frequency rectenna for high efficiency wireless power transmission at 2.45 and 5.8 GHz," in *Microwave Symposium Digest, 2002 IEEE MTT-S International*, 2002, pp. 1297-1300 vol.2.

[8] Y Suh and K. Chang, "A high-efficiency dual-frequency rectenna for 2.45- and 5.8-GHz wireless power transmission," *Microwave Theory and Techniques, IEEE Transactions on,* vol. 50, pp. 1784-1789, 2002.

[9] Ren Yu-Jiun and Chang Kai, "5.8-GHz circularly polarized dual-diode rectenna and rectenna array for microwave power transmission," *Microwave Theory and Techniques, IEEE Transactions on,* vol. 54, pp. 1495-1502, 2006.

[10] C. H. K. Chin, Q Xue, and C.H Chan, "Design of a 5.8-GHz rectenna incorporating a new patch antenna," *Antennas and Wireless Propagation Letters, IEEE,* vol. 4, pp. 175-178, 2005.

[11] B. Strassner and Chang Kai, "5.8 GHz circular polarized rectenna for microwave power transmission," in *Energy Conversion Engineering Conference and Exhibit, 2000. (IECEC) 35th Intersociety*, 2000, pp. 1458-1468 vol.2.

[12] H. Takhedmit, B. Merabet, L. Cirio, B. Allard, F. Costa, C. Vollaire, *et al.*, "A 2.45-GHz low cost and efficient rectenna," in *Antennas and Propagation (EuCAP), 2010 Proceedings of the Fourth European Conference on*, 2010, pp. 1-5.

[13] T. Yoo, J. McSpadden, and K. Chang, "35 GHz rectenna implemented with a patch and a microstrip dipole antenna," in *Microwave Symposium Digest, 1992., IEEE MTT-S International*, 1992, pp. 345-348 vol.1.

[14] J. A. G. Akkermans, M. C. van Beurden, G. J. N. Doodeman, and H. J. Visser, "Analytical models for low-power rectenna design," *Antennas and Wireless Propagation Letters, IEEE,* vol. 4, pp. 187-190, 2005.

[15] A. Alden and T. Ohno, "Single foreplane high power rectenna," *Electronics Letters,* vol. 28, pp. 1072-1073, 1992.

[16] G. Andia Vera, A. Georgiadis, A. Collado, and S. Via, "Design of a 2.45 GHz rectenna for electromagnetic (EM) energy scavenging," in *Radio and Wireless Symposium (RWS), 2010 IEEE,* 2010, pp. 61-64.

[17] Y. Hiramatsu, T. Yamamoto, K. Fujimori, M. Sanagi, and S. Nogi, "The design of mW-class compact size rectenna using sharp directional antenna," in *Microwave Conference, 2009. EuMC 2009. European,* 2009, pp. 1243-1246.

[18] T. W. Yoo and Chang Kai, "Theoretical and experimental development of 10 and 35 GHz rectennas," *Microwave Theory and Techniques, IEEE Transactions on,* vol. 40, pp. 1259-1266, 1992.

[19] J. Zbitou, M. Latrach, and Serge Toutain, "Hybrid rectenna and monolithic integrated zero-bias microwave rectifier," *Microwave Theory and Techniques, IEEE Transactions on,* vol. 54, pp. 147-152, 2006.

[20] L. W. Epp, A. R. Khan, H. K. Smith, and R. P. Smith, "A compact dual-polarized 8.51-GHz rectenna for high-voltage (50 V) actuator applications," *Microwave Theory and Techniques, IEEE Transactions on,* vol. 48, pp. 111-120, 2000.

[21] A. Slavova and A. S. Omar, "Wideband rectenna for energy recycling," in *Antennas and Propagation Society International Symposium, 2003. IEEE,* 2003, pp. 954-957 vol.3.

[22] J. A. Hagerty, F. B. Helmbrecht, W. H. McCalpin, R. Zane, and Z. B. Popovic, "Recycling ambient microwave energy with broad-band rectenna arrays," *Microwave Theory and Techniques, IEEE Transactions on,* vol. 52, pp. 1014-1024, 2004.

[23] J. A. Hagerty and Z. Popovic, "An experimental and theoretical characterization of a broadband arbitrarily-polarized rectenna array," in *Microwave Symposium Digest, 2001 IEEE MTT-S International,* 2001, pp. 1855-1858 vol.3.

[24] Pham Binh, J. C. S. Chieh, and Pham Anh-Vu, "A wideband composite right/left hand rectenna for UHF energy harvesting applications," in *Antennas and Propagation Society International Symposium (APSURSI), 2012 IEEE,* 2012, pp. 1-2.

[25] N. Shinohara and H. Matsumoto, "Experimental study of large rectenna array for microwave energy transmission," *Microwave Theory and Techniques, IEEE Transactions on,* vol. 46, pp. 261-268, 1998.

CHAPTER 2

LITERATURE REVIEW OF RECTENNAS

2.1 System Review

2.1.1 Wireless Power Transmission Systems

A wireless power transmission system shown in Fig. 2.1 consists of three main functional blocks. The first block is to convert the electricity into microwaves (DC to AC). After radiating through the transmitting antenna, the RF power is carried within a focused microwave beam that travels across free space towards a receiver. This receiving block will convert the RF energy back to the DC electricity [1].

The efficiency of the system is basically equivalent to its transfer function. The general definition of any efficiency (η) used hereafter is the

ratio of output power P_{out} over input power P_{in}, The overall efficiency (η_{all}) of a wireless power transmission system is the ratio of the DC output power at the receiver end over the DC or AC input power at the transmitter end, which is given by

$$\eta_{all} = \eta_t \cdot \eta_c \cdot \eta_r \tag{2.1}$$

This end to end efficiency includes all the sub-efficiencies starting from the DC supply feeding the RF source in the transmitter to the DC power interface at the receiver. Where η_t is the electric to the microwave conversion efficiency or transmitter efficiency; η_c is the collection efficiency; and η_r is the microwave to electric conversion efficiency or RF to DC conversion efficiency of rectennas.

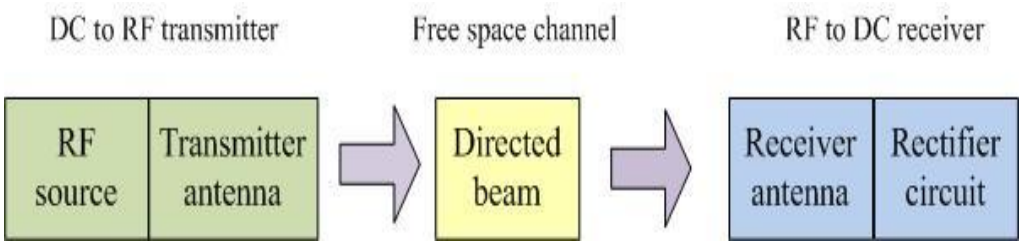

Fig.2.1: Wireless power transmission system diagram

The first term (η_t) equals to the product of the magnetron efficiency (η_{mag}) and the transmitter antenna efficiency (η_a). The magnetron efficiency is used to express how efficient the RF source works. The antenna efficiency at the transmitter described here is the antenna total efficiency which takes the antenna mismatching factor into account. It is assumed that both magnetron efficiency and transmitter efficiency are 100%, which means the generator is an ideal device that can provide wanted transmitting power.

The collection efficiency (η_c) is the ratio of the received power over the transmitted power. For maximum collection efficiency, an optimum power density distribution must be selected for the transmitting antenna aperture. The collection efficiency should be very high when the

impedance looking into the receiver is matched to the free space impedance. The collection efficiency is proportional to a design parameter τ, which is expressed as Goubau's relation [1, 2]

$$\tau = \frac{\sqrt{A_r A_t}}{\lambda D} \qquad (2.2)$$

Where, A_r and A_t are the receiving and transmitting effective aperture areas respectively; λ is the wavelength of the radiation; D is the distance between the transmitting and receiving apertures.

The function of receiver is to collect the incoming RF power and convert it back to DC electricity. An appropriate choice of devices to accomplish these tasks is the diode type rectenna.

A 'traditional' rectenna system is shown in Fig. 2.2. The wireless energy can be collected by the antenna attached to rectifying circuit through filters and a matching circuit. The rectifying circuit converts the received wireless energy into DC through a low-pass filter and a DC pass filter before and after the circuit. The low-pass filter can match the antenna with the rectifier and block the high order harmonics generated by the rectifying diode in order to achieve high RF to DC conversion efficiency. The rectifying diode is the core element of the rectifier circuit. A load resistor is placed at the output terminal to measure the DC output voltage [3].

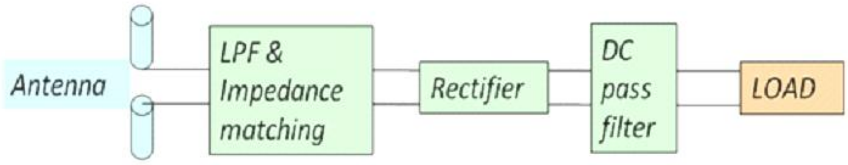

Fig. 2.2: Rectenna black diagram

2.1.2 Rectenna Conversion Efficiency

The RF to DC conversion efficiency of the rectenna is basically defined as the ratio of the output power P_{out} over the input power P_{in},

which means the conversion efficiency of the whole system is the DC power at the receiver end over the AC input power captured by the rectenna.

$$\eta_r = \frac{P_{out}}{P_{in}} = \left(\frac{{V_{DC}}^2}{R_{load}}\right)\frac{1}{P_d A_{eff}} \tag{2.3}$$

This conversion efficiency strongly depends on the power density (P_d) distribution across the receiver aperture. The effective area of the receiving antenna (A_{eff}) can be calculated by using the gain (G_r) and wavelength

$$A_{eff} = \left(\frac{{\lambda_0}^2}{4\pi}\right) G_r \tag{2.4}$$

The maximum incident power density can be derived as follows. Assuming an antenna which has a gain of G_t at the transmitter, the directivity of

$$D_0 = \frac{4\pi A_t}{{\lambda_0}^2} \tag{2.5}$$

is obtained [4], which means the power of the main beam is magnified by D_0 in a certain direction. A_t is the effective area of transmitting antenna. In addition, the distance d which is the distance between transmitting antenna and the receiving antenna needs to be relatively large for the rectenna to operate in the far field. Therefore, the maximum power density at the center of an aperture is obtained

$$P_d = \frac{P_t G_t}{{\lambda_0}^2 d^2} \tag{2.6}$$

Form this equation, a higher P_d requires a larger G_t.

2.2 Overview of Rectennas

2.2.1 Early Stage Rectennas

At the early stage, In order to complete the wireless power transmission system rectennas were developed to receive and convert the electromagnetic wave into DC power.

The first rectenna was conceived at Raytheon Company in 1963 as shown in Fig. 2.3; it was built and tested by R.H. George at Purdue University. It was composed of 28 half-wave dipoles, each terminated in a bridge rectifier made from four 1N82G point- contact, semiconductor diodes above a reflecting plane. In addition, a power output of 7 W was produced at an estimated 40% efficiency. To increase the power output suitable for helicopter experiment, a matching network was added into this structure and the measured output power was increased to 270 W [5].

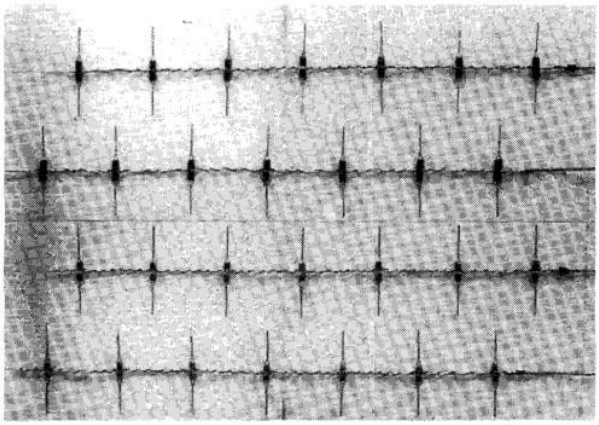

Fig. 2.3: views of the first rectenna made by Raytheon Co. (1963) [5]

Later, other dipole type rectennas, shown in Fig. 2.4, experiment at frequency of 2.45 GHz was demonstrated as well. The highest conversion efficiency record of 90.6% was made by W.C. Brown in 1977 using a GaAsPt Schottky barrier diode with input microwave power level of 8W [5-8].

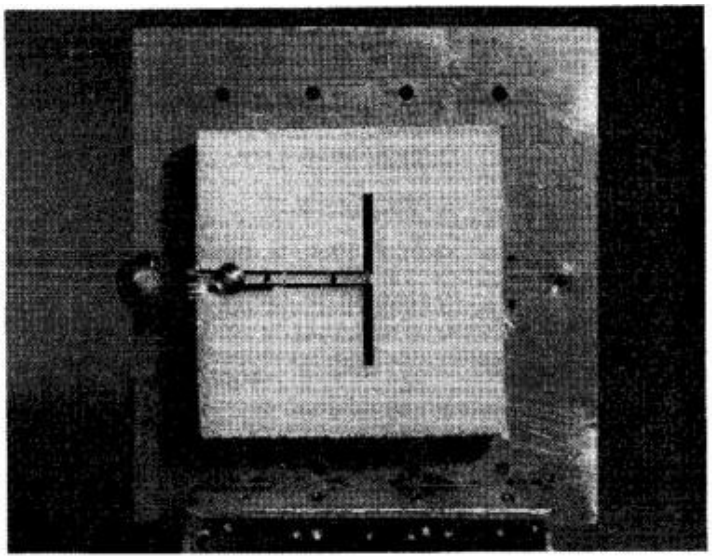

(a) A rectenna element above a reflecting plane

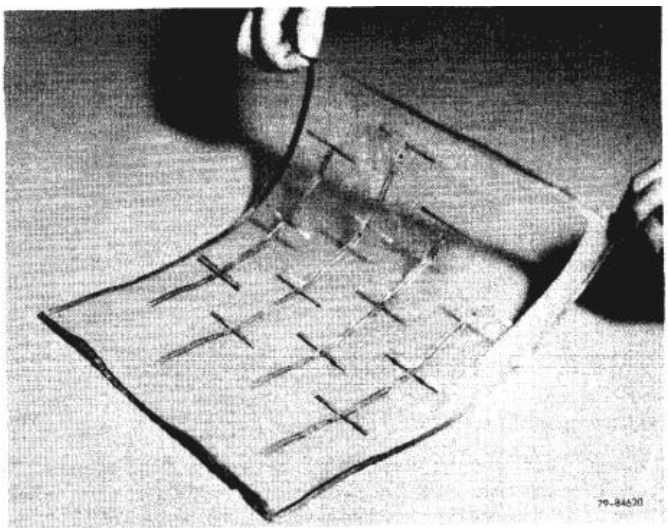

(b) A rectenna fore-plane made in the new thin film etched- circuit format (1982).

Fig. 2.4: Some early rectennas [7]

2.45 GHz was usually used as the transmitting frequency due to its advanced and efficient technology, location at the centre of an industrial scientific, and medical (ISM) band, and its small attenuation through the atmosphere even in heavy rainstorms.

Components for microwave power transmission were traditionally focused at 2.45 GHZ. To reduce the transmitting and rectenna aperture area and increase the transmission range, APCP Power Technologies

developed a 72% efficient rectenna element at 35 GHz in 1991 [9]. 35 GHz was targeted caused by a decrease in the atmospheric absorption around this frequency. However, components for generating high power at 35 GHz were expensive and inefficient.

To decrease the aperture sizes without sacrificing component efficiency, technology developed at the next higher ISM band centred at 5.8 GHz has been investigated. This frequency is appealing for beamed power transmission due to smaller component sizes and a greater transmission range over 2.45 GHz.

In 1992, the first C-band printed dipole rectenna achieved a 70% overall efficiency and an 80% conversion efficiency at 5.87 GHz [10]. These efficiencies were measured in a waveguide simulator with an input power level of approximately 700 mW by element. However, little information is provided on the design and testing of this rectenna.

In wireless power transmission, antennas in rectenna systems have well-defined polarisation, high rectification efficiency enabled by single frequency and high power density incident on an array of rectennas. Applications for this type of power transfer has been proposed for microwave power helicopter, solar-powered satellite to ground transmission, inter-satellite power transmission and short-range of wireless power transfer. [5, 11-13].

In 1991, Brown investigated a 2.45 GHz rectenna that absorbs small amounts (mW) of microwave power at incident density levels. With this new technology which will convert wireless power at very low levels into DC power at useful voltage levels, a new application for rectenna was firstly mentioned, which is RF wireless power harvesting. The potential application area is where the device is inaccessible to replace batteries and where solar or other light is not available for photovoltaic power suppliers [6]. The rectenna would receive and convert ambient wireless power to DC power as a power supplier.

In RF energy harvesting, rectennas should be available to harvest ambient RF power. Thus, the rectenna desires arbitrary polarisation, relative high rectification efficiency at wide bandwidth and good performance at low incident power density.

some of the researches for wireless power harvesting has been done In early 2000's. A Planar rectenna array for rectification of broadband electromagnetic waves of arbitrary polarisation was designed and characterised in 2001 [14]. In addition, a new rectenna based on aperture coupled micro-strip dipole and wideband band-pass filter inserted between the antenna and the rectifying diode was presented in 2003 [15]. However, both of them only given the DC output voltage and lacked the result of conversion efficiency (which is a key performance indicator).

Recently, most of rectenna researches were still focused on the wireless power transmission. Due to the big challenge of designing wideband rectennas only a few of rectennas were designed for the RF energy harvesting.

2.2.2 Current Rectennas

Currently, other types of rectenna were proposed to sufficient various application requirements such as dipoles [7, 16-22], Yagi-Uda antennas [23], micro-strip patch antennas [2, 24-32], monopoles[33, 34], loops [35], spiral antennas[14, 36] and slot antennas [37-41]. The rectenna also take any type of rectifying circuit such as single shunt rectifier [15, 26, 35, 40, 42-44], full-wave bridge rectifier [5] or other hybrid rectifiers [45]. The details of some of these rectennas are introduced as follows.

2.2.2.1 Planar Dipole Rectennas

In [46], the planar dipole rectenna with 39% conversion efficiency at 35 GHz were developed for wireless power transmission shown in Fig. 2.5.

The length and the width of a resonance dipole at the fundamental frequency have been determined as 0.46 λ and 0.02λ respectively. A micro-strip line low-pass filter and a GaAs Schottky diode DMK6606 used in Ka-band mixers were connected to the antenna.

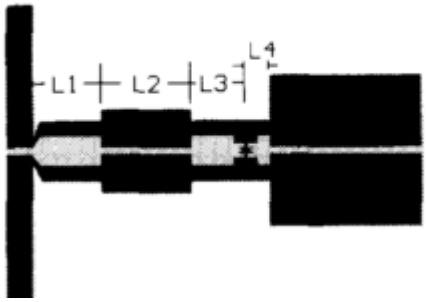

Fig. 2.5: The planar dipole rectenna at 35 GHz [46]

In [16], A high efficiency dual-frequency dipole rectenna for 2.45 and 5.8 GHz wireless power transmission was investigated. The rectenna consists of a receiving dual-frequency dipole antenna, a CPS input low-pass filter, two CPS band-pass filters, a rectifying diode and a microwave block capacitor which is shown in Fig. 2.6. The measured conversion efficiencies achieved at free space are 84.4% and 82.7% at 2.45 GHz and 5.84 GHz, respectively.

In [21], a decoupled dual dipole rectenna with a novel micro-strip decoupling structure was presented for wireless battery charging at 2.4 GHz shown in Fig. 2.7. The rectenna consists of decoupling dual dipole antenna and a Villard's voltage doubler rectifier. The rectenna is 37% smaller than two standard patch antennas located on the same substrate without a decoupling structure. In addition, it is able to fully charge a standard 4.8 V battery in 5 hours over a distance of 23 cm. However, few results are presented the rectenna RF to DC conversion efficiency.

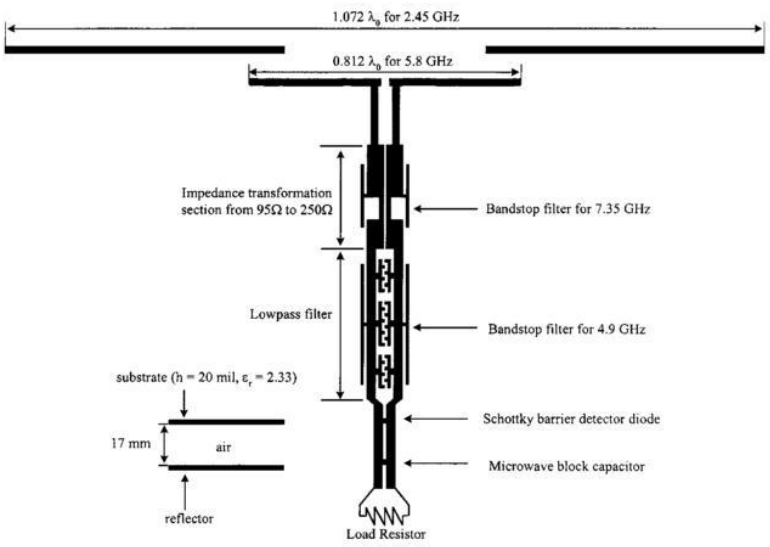

Fig. 2.6: The dual-frequency rectenna for 2.45 and 5.8 GHz wireless power transmission [16]

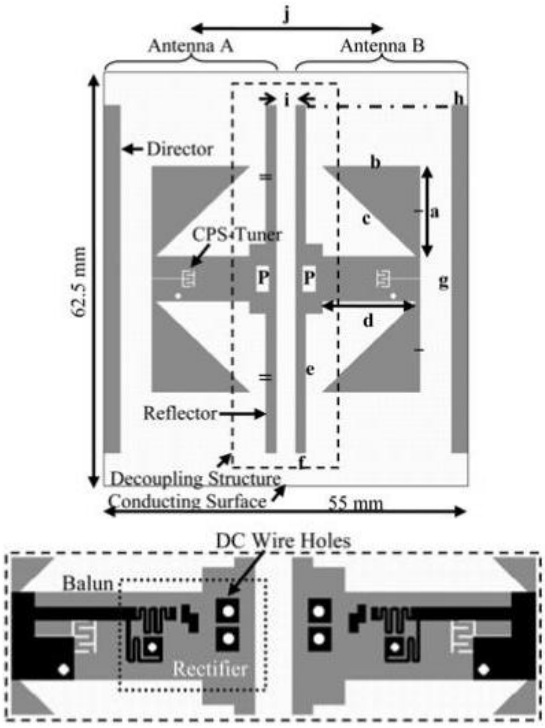

Fig. 2.7: The decoupling dual-dipole rectennas [21]

In [44], a high efficiency 2.45 GHz rectenna that can harvest low power input RF power effectively was investigated which is shown in Fig. 2.8. The antenna with a simple structure and high gain of 8.6 dBi was proposed for the rectenna. The antenna was designed to directly match the

rectifying circuit at 2.45 GHz and mismatch it at the second and third harmonics so that the use of band-pass filter between the antenna and rectifying circuit can be eliminated. The rectenna showed a maximum conversion efficiency of 83% with a load of 1400 Ω.

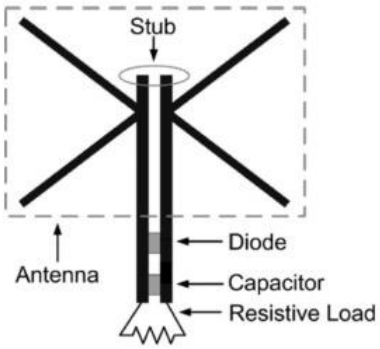

Fig. 2.8: The high efficiency planar dipole rectenna[44]

2.2.2.2 Micro-strip Patch Rectennas

Micro-strip patch rectennas were also proposed and investigated in the past decades. A 2.45 GHz dual polarised circular patch rectenna was designed [28]. The configuration of this rectenna is shown in Fig. 2.9. The dual polarisation was achieved by two orthogonal micro-strip feed lines and rectification is achieved by Schottky diodes located on each feed line. A RF to DC conversion efficiency of 48% was demonstrated.

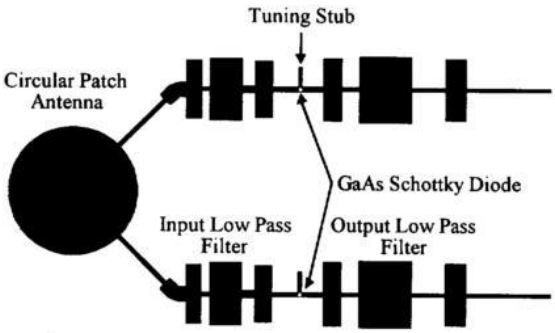

Fig. 2.9: The dual-polarised circular patch rectenna[28]

In [43], a dual polarised patch rectenna array was developed which is shown in Fig. 2.10. The rectenna consists of a coplanar strip-line (CPS) truncated patch antenna and CPS band-pass filter. The design compared single shunt diode rectifier with dual diodes rectifier. It was shown that the single shunt diode works as a half-wave rectifier and the output DC voltage of single shunt diode rectenna only half of that of dual diodes rectenna. The dual-diode rectenna achieved an RF to DC conversion efficiency of 76% at 5.8 GHz. In addition a rectenna array formed by the rectenna element was demonstrated and the investigation for various interconnection methods for a rectenna array was reported.

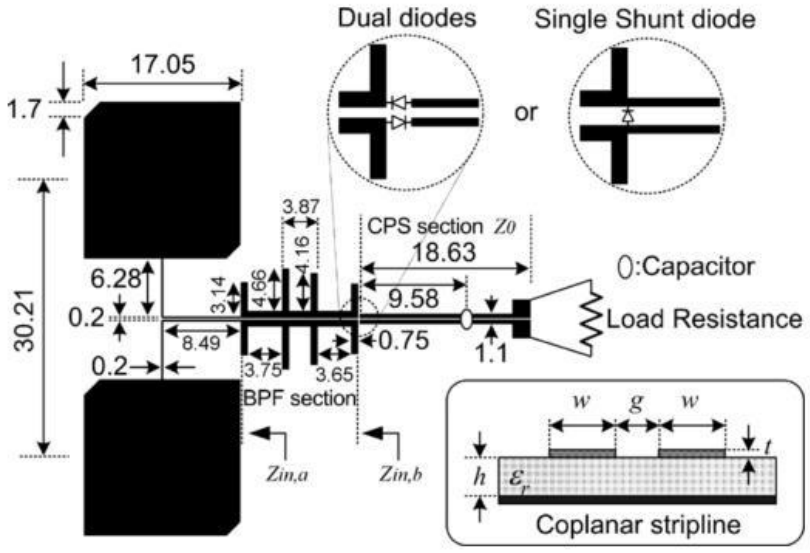

Fig. 2.10: The dual polarised patch rectenna array [43]

An integrated patch rectenna shown in Fig. 2.11 was also designed for wireless power delivery at low incident power densities, from 25 to 200 μW/cm^2. Source-pull nonlinear measurement of the rectifying device is compared to the harmonic-balance simulations. For incident power density range of interest, the rectifying circuit achieved maximum RF to DC conversion efficiency of 63% and the total rectenna conversion efficiency of 54% [24].

Fig. 2.11: A dual polarised rectangular patch rectenna [24]

2.2.2.3 Slot Rectennas

In the past few years, many slot rectennas were also proposed for WPT and RF wireless energy harvesting applications. Because of this attractive features such as low-profile, low-cost, ease of fabrication and omni-directional radiation pattern.

In [25], a X-band planar rectenna was presented and shown in Fig. 2.12. The proposed device consists of a slot antenna and a micro-strip rectifying circuit. A surface mount Schottky diode HSMS8202 was used as the rectifying element. Measurements performed at 9.3 GHz demonstrated that an RF to DC conversion efficiency of about 21% can be obtained with an input power density of 245 μW/cm^2.

In [26], circular polarised retro-directive rectenna arrays were proposed which is plotted in Fig. 2.13. The proximity-coupled micro-strip ring antenna is used as the array element, which can automatically block harmonic signals up to the third order from reradiating by the rectifying circuit. The array can track the incoming power source signals automatically and is less sensitive to the power incident angle variations. The conversion efficiency of the 4element array is around 55% when the power density is 10 mW/cm^2.

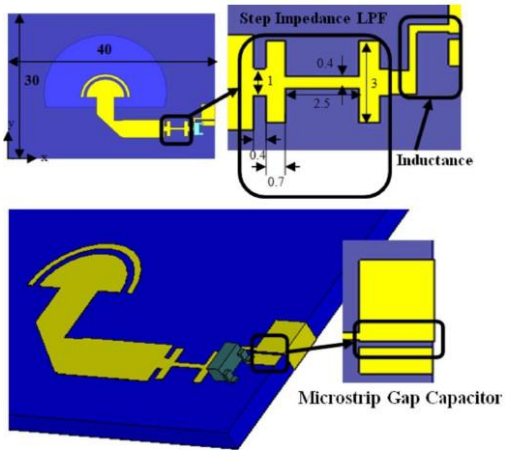

Fig. 2.12 The X-band slot rectenna [25]

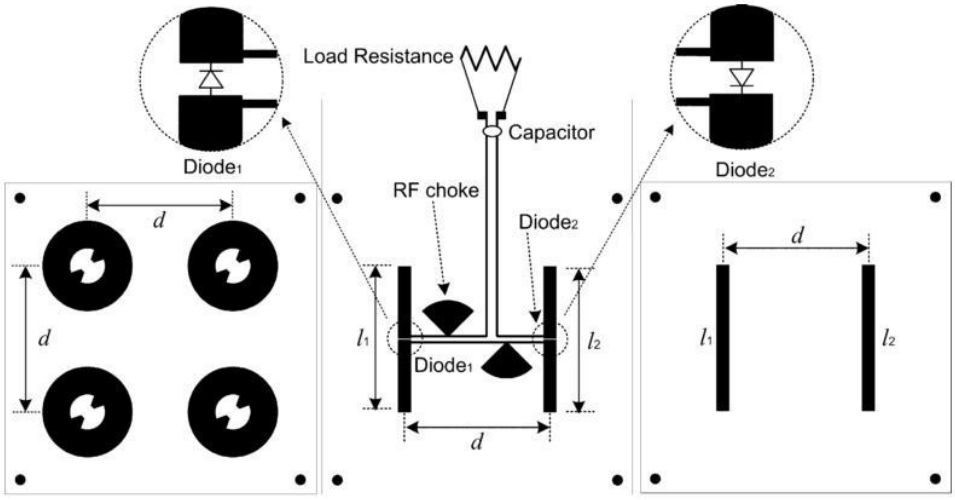

Fig. 2.13: A circular polarised retro-directive rectenna array [26]

In [47], a dual-frequency rectenna operating at 2.45 and 5.8 GHz were presented shown in Fig. 2.14. The rectenna consists of two compact ring slot antennas, a hairpin low-pass filter and a rectifying circuit. The dual-frequency rectenna achieved RF to DC conversion efficiencies of 65 % and 46% at 2.45 and 5.8 GHz, respectively, when the power density is 10 mW/cm^2.

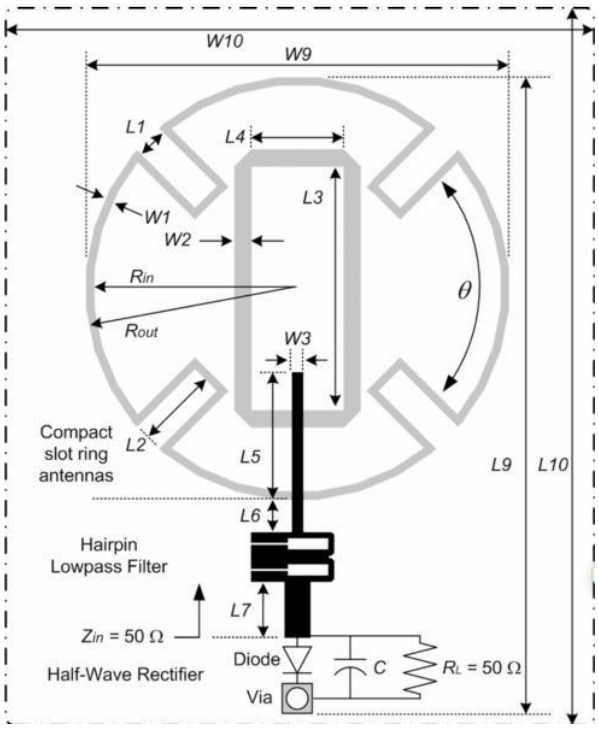

Fig. 2.14: The dual-frequency slot ring rectenna [47]

2.2.2.4 Spiral Rectennas

In [36], a broadband rectenna array using a frequency independent spiral antenna operated between 2 to 18 GHz and incorporated to a diode that did not have a matching circuit was presented. The frequency independent spiral antenna was designed as an Omni-directional broadband antenna, which is shown in Fig. 2.15, to enable recovery of all available signals within the operating frequencies to maximise the DC power harvested. The RF to DC conversion efficiency of 20% was achieved for 8 × 8 element array.

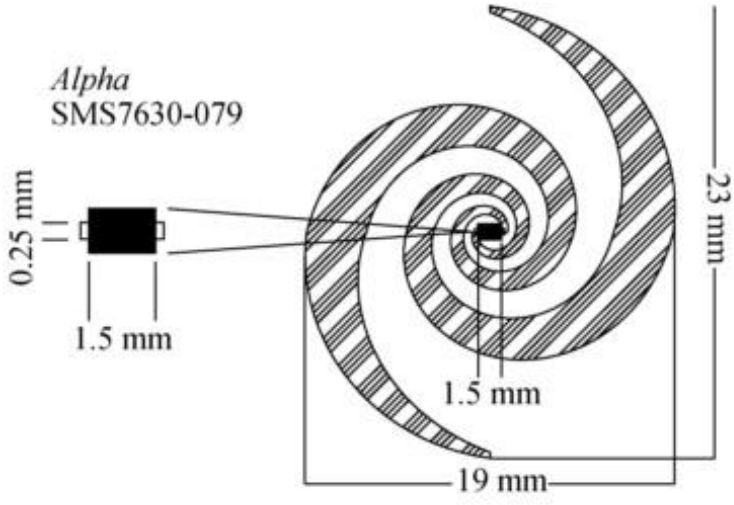

Fig. 2.15: a spiral rectenna element [36].

Moreover, Table 2.1 gives an overview of some of rectennas described in the literature[24]. It is important to note that the efficiencies are listed as reported in the papers, but they cannot be directly compared due to the different power levels and, perhaps more critically, different efficiency definitions. For example, most work does not include the antenna efficiency or coupling efficiency from antenna to the rectifier. The power incident on the rectifier is measured in a circuit with no antenna or estimated from simulation. In some cases, the incident power density is also provided.

In [17, 29, 35, 39, 45] power levels incident on the diode are in 100 mW range with 40% to 82% rectification efficiency. In [39], the rectifier was directly connected to a signal generator without antenna. In [37], the 42% efficiency was measured as the ratio of the DC power and estimated input power to the diode of 0.1 mW for a fairly large antenna area whose total dimensions not given in the paper. In [30], the diode impedance was optimized at the fundamental frequency with harmonic balance non-linear simulations for 1 mW of power incident on the diode. However, when the diode was matched to a 50 Ω antenna. The efficiency calculation was done

by estimating antenna gain when the antenna is not connected to the rectifier. So at least part of the antenna efficiency was taken into account by simulations. [31] reported rectification as well as the overall integrated rectifier antenna efficiency also found from simulated unloaded antenna gain for 10 mW estimated incident power on a 4 diode rectifier. The rectifier was integrated with the antenna on the same substrate and the overall device is compact. In [36], 64 elements formed dual-polarised broadband spirals with diodes direct connected at the feeds were presented for the case of very low incident power density, which only has 20% calculated conversion efficiency.

Table 2.1: Overview of integrated rectifier antennas and rectifiers in the literature

Ref	f (GHz)	$P_{RF,in}$	Antenna	η
[17]	5.8	50 mW	LP dipole omi-dir	82%
[35]	5.8	100 mW	LP dipole omi-dir	67%
[45]	2.45	310 mW	LP 4 element patch array	65%
[29]	2.45	100 mW	LP patch on FR4	40%
[6]	2.45	20 mW (5 uW/cm^2)	48 element LP dipole array	50%
[30]	2.45	1 mW	LP patch	50-80%
[31]	2.45	10 mW (150 uW/cm^2)	LP patch	52%
[37]	2.45	0.1 mW	LP miniaturized patch	42%
[39]	5.8	40 mW	LP printed grounded antenna	59.5%
[36]	2-18	62 uW/cm^2	64 dual CP spiral elements	20%
[24]	2	25-200 uW/cm^2	LP patch	54%

* LP: linear polarized; CP: circular polarized; η : efficiency

The first problem for RF energy harvesting is lacking of wideband rectennas. Currently, it is clear that most of rectenna designs were focused on single frequency or dual-frequency bandwidths which were mainly designed for wireless power transmission. Some of them can provide good performance at low power density levels. However, it is important to note that based on a survey of ambient power density for various wireless PF power resource in London [48], very broadband of wireless energy can be harvest in the air. It is also interesting to note that most of the energy (>10 nW/cm^2) is concentrated in GSM 900, GSM 1800 and 3G (880 MHz - 2.2 GHz) bandwidth. While, Wi-Fi systems only have the lowest power density. Thus, most of current rectenna designs operating at single frequency only harvest a small part of RF energy in the air. It is necessary to design a wideband rectenna specific for RF energy harvesting to capture most of the available RF energy. Although, there are a few wideband rectenna design such as [36, 48], [36] only provided very low conversion efficiency of 20%. Because it is difficult to match antenna with the rectifying circuit over wide bandwidth and [48] use 4 narrowband antennas to harvest the ambient energy at each frequency which is too complicated and incontinent in reality. Thus, a wideband rectenna is desired for RF wireless power harvesting applications.

Table 2.2: Summary of ambient RF power source in London[48]

Band	Frequencies (MHz)	Average S_{BA} (nW/cm^2)	Maximum S_{BA} (nW/cm^2)
DTV (during switch over)	470-610	0.89	460
GSM900 (MTx)	880-915	0.45	39
GSM900 (BTx)	925-960	36	1,930
GSM1800 (MTx)	1710-1785	0.5	20
GSM1800 (BTx)	1805-1880	84	6,390
3G (MTx)	1920-1980	0.46	66
3G (BTx)	2110-2170	12	240
WiFi	2400-2500	0.18	6

The other problem for this project is to obtain higher conversion efficiency for wideband rectenna at low input power levels . As one of core elements of the rectenna, the rectenna conversion efficiency is strongly dependent on the RF to DC conversion efficiency for a diode. Due to the diode characteristic shown in Fig. 2.16, the RF to DC conversion efficiency of a diode depends on the microwave power input intensity and the optimum connected load. When the power or the load is not matched, the efficiency becomes quite low. Furthermore, the diode has its own junction voltage and breakdown voltage. If the input voltage of the diode is lower than the junction voltage or higher than the breakdown voltage the diode does not show a rectifying characteristic. As a result, the RF to DC conversion efficiency drops with a lower or higher input than the optimum. It is shown that a diode becomes a more efficient rectifier at higher input power levels. In [16], the RF to DC conversion efficiency of a diode exceeding 80% for an input power level of 20 dBm (0.1 W) was reported for a rectenna.

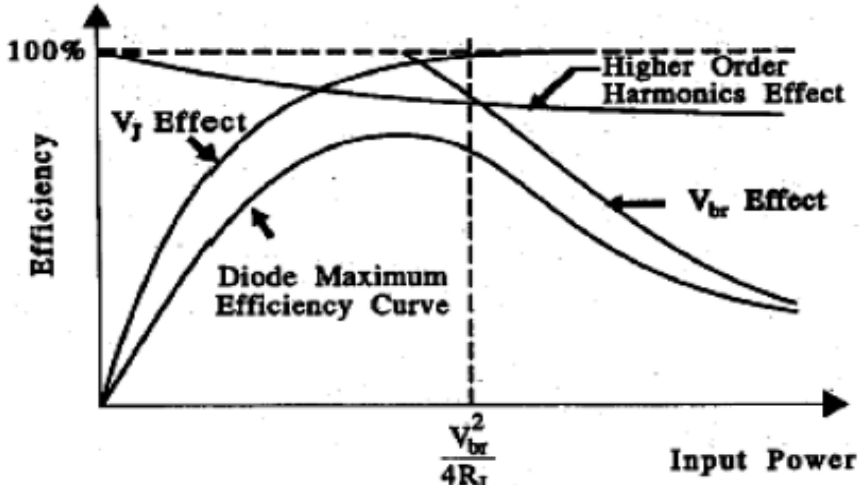

Fig. 2.16: General relationship between microwave to DC power conversion efficiency and input power [46]

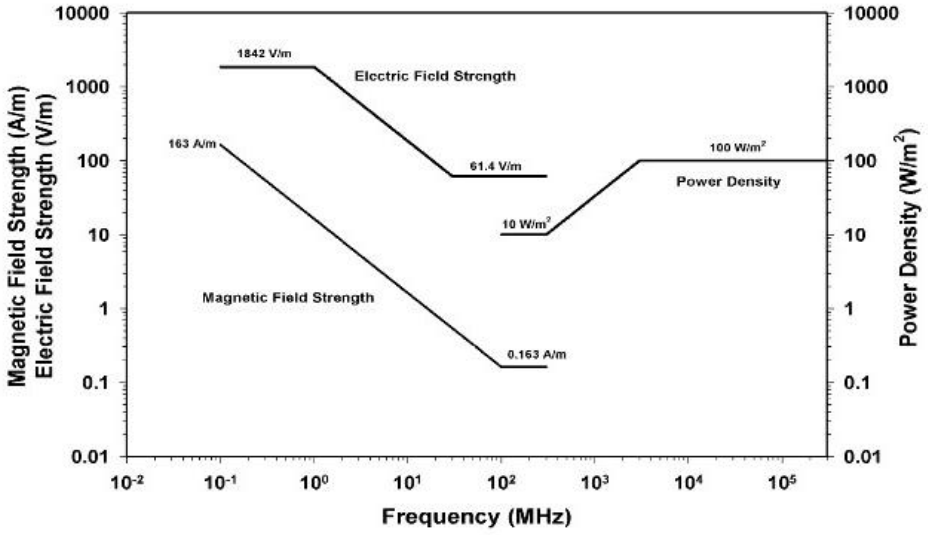

(a) Maximum permissible exposure limits for controlled RF environments

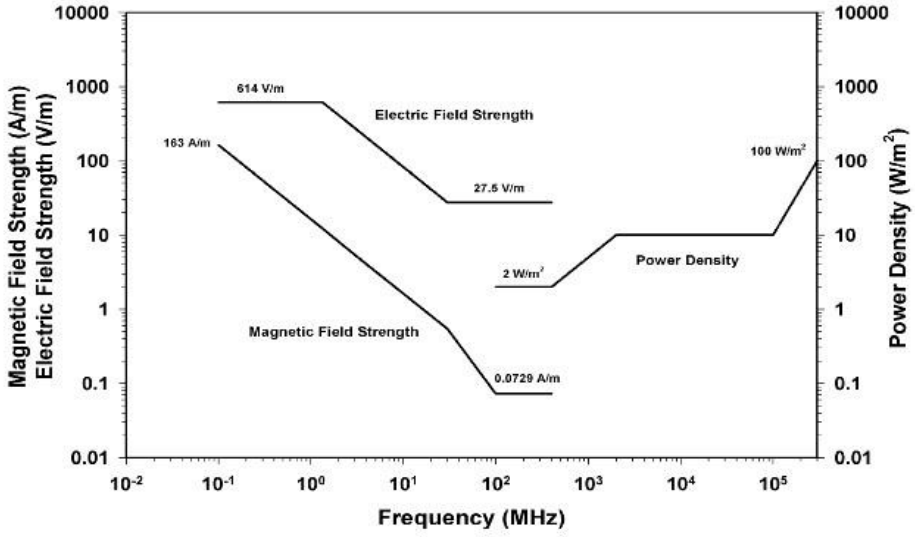

(b) Maximum permissible exposure limits for general public

Fig. 2.17: Graphic representation of the maximum permissible exposure limits (2005) [49]

Thus, the first approach to increase the rectenna conversion efficiency for low input power is to increase the power received by the rectifying diode. However, using transmission-power-restricted RF bands,

we encounter a challenge. Due to the IEEE Standard for Safety Levels with Respect to Human Exposure to Radio Frequency Electromagnetic Fields (3 kHz to 300 GHz) published in 2005 [49, 50], shown in Fig. 2.17, power densities in controlled environment at frequency range over the 0.1 GHz to 10 GHz are 10 mW/m^2-100 mW/m^2 (1mW/cm^2- 10 mW/cm^2). The power densities in general public over the frequency range from 0.1 GHz to 10 GHz are 1 mW/m^2- 10 mW/m^2 (0.1 mW/cm^2- 1mW/cm^2). It is important to note that based on the Friis Equation the input power captured by the antenna is low at low input power level so the rectifier cannot operate effectively. It is strongly affected the rectenna conversion efficiency. As a consequence, the power captured by using 'traditional' antenna is not sufficient. Therefore, a few broadband antennas [23, 36], large antenna arrays [5, 12, 26, 36, 43] and circular polarised or dual polarised antennas [3, 26, 28, 36, 43] were designed and experimented. The broadband antenna enables relatively high RF power to be received from various sources. While the antenna array can increase incident power delivered to the diode by enlarging antenna aperture and antenna gain. However, a trade-off arises between the small size antenna and the high radiation gain. The circularly polarised antenna overcomes the limitations of rectenna orientation. The other approach is to develop a new rectifying circuit to increase the efficiency at a weak microwave input for example, schottky diodes are widely used in rectenna design due to the good performance at low input power and low forward voltage.

2.1 Summary

In this chapter, the literature review of wireless power transmission system has been reviewed. Furthermore, the overview of the rectenna system and some challenges has been also presented. It is shown that quite a few wideband rectennas[36, 48] have been achieved and published in the literature but all of them has very low conversion efficiency or only has high efficiency at single frequency. In addition, only two proposed

narrowband rectennas[24, 44] can achieve high RF to DC conversion efficiency at low input power level. To address the issues identified there is a need to further investigate a wideband rectennas with high RF to DC conversion efficiency at low power density level which is the main objective of this study.

References

[1] William C. Brown, "The technology and application of free-space power transmission by microwave beam," *Proceedings of the IEEE*, vol. 62, pp. 11-25, 1974.

[2] J. O. McSpadden, T. Yoo, and Chang Kai, "Theoretical and experimental investigation of a rectenna element for microwave power transmission," *Microwave Theory and Techniques, IEEE Transactions on*, vol. 40, pp. 2359-2366, 1992.

[3] Hubregt J. Visser, *Approximate Antenna Analysis for CAD*: WILEY, 2009.

[4] Huang Yi, Kevin Boyle, *Antennas: from theory to practice*. UK: Wiley, 2008.

[5] W.C.Brown, "The history of power transmission by radio waves," *IEEE Trans. Microwave Theory Tech.*, vol. MTT-32, pp. 1230-1242, Sept. 1984.

[6] W. C. Brown, "An experimental low power density rectenna," in *Microwave Symposium Digest, 1991., IEEE MTT-S International*, 1991, pp. 197-200 vol.1.

[7] W. C. Brown and J. F. Triner, "Experimental Thin-Film, Etched-Circuit Rectenna," in *Microwave Symposium Digest, 1982 IEEE MTT-S International*, 1982, pp. 185-187.

[8] R. M. Dickinson, "Performance of a High-Power, 2.388-GHz Receiving Array in Wireless Power Transmission Over 1.54 km," in *Microwave Symposium, 1976 IEEE-MTT-S International*, 1976, pp. 139-141.

[9] P.; Cha Koert, J.; Machina, M., "35 and 94 GHz rectifying antenna systems," presented at the SPS 91 - Power from space; Proceedings of the 2nd International Symposium, France, , 1991

[10] S. S. Bharj, R. Camisa, S. Grober, F. Wozniak, and E. Pendleton, "High efficiency C-band 1000 element rectenna array for microwave powered applications," in *Antennas and Propagation Society International Symposium, 1992. AP-S. 1992 Digest. Held in Conjuction with: URSI Radio Science Meeting and Nuclear EMP Meeting., IEEE*, 1992, pp. 123-125 vol.1.

[11] Peter E Glaser, "Power from the Sun: Its Future," *Science*, vol. 162(3856), pp. 857-861, 22 Nov. 1968.

[12] Yoshiyuki FUJINO Takeo ITO Masaharu FUJITA Nobuyuki KAYA Hiroshi MATSUMOTO Kazuaki KAWABATA Hisashi SAWADA Toshihiro ONODERA and "A Driving Test of a Small DC Motor with a Rectenna Array," *IEICE TRANSACTIONS on Communications* vol. E77-B, pp. 526-528, 20/04/1994 1994.

[13] W.C.Brown, "Solar Power Satellite Program Rev.," *Final Proc. conference 800491*, June 1980.

[14] J. A. Hagerty and Z. Popovic, "An experimental and theoretical characterization of a broadband arbitrarily-polarized rectenna array," in *Microwave Symposium Digest, 2001 IEEE MTT-S International*, 2001, pp. 1855-1858 vol.3.

[15] A. Slavova and A. S. Omar, "Wideband rectenna for energy recycling," in *Antennas and Propagation Society International Symposium, 2003. IEEE*, 2003, pp. 954-957 vol.3.

[16] Y Suh and K. Chang, "A high-efficiency dual-frequency rectenna for 2.45- and 5.8-GHz wireless power transmission," *Microwave Theory and Techniques, IEEE Transactions on*, vol. 50, pp. 1784-1789, 2002.

[17] J. O. McSpadden, Fan Lu, and Chang Kai, "Design and experiments of a high-conversion-efficiency 5.8-GHz rectenna," *Microwave Theory and Techniques, IEEE Transactions on*, vol. 46, pp. 2053-2060, 1998.

[18] Tu Wen-Hua, Hsu Shih-Hsun, and Chang Kai, "Compact 5.8-GHz Rectenna Using Stepped-Impedance Dipole Antenna," *Antennas and Wireless Propagation Letters, IEEE*, vol. 6, pp. 282-284, 2007.

[19] Zhang Fang, Nam Hee, and Lee Jong-Chul, "A novel compact folded dipole architecture for 2.45 GHz rectenna application," in *Microwave Conference, 2009. APMC 2009. Asia Pacific*, 2009, pp. 2766-2769.

[20] H. J. Visser, "Printed folded dipole antenna design for rectenna and RFID applications," in *Antennas and Propagation (EuCAP), 2013 7th European Conference on*, 2013, pp. 2852-2855.

[21] W. S. Yeoh, W. S. T. Rowe, and K. L. Wong, "Decoupled dual-dipole rectennas on a conducting surface at 2.4 GHz for wireless battery charging," *Microwaves, Antennas & Propagation, IET*, vol. 6, 2012.

[22] Y. J. Ren and K. Chang, "Bow-tie retrodirective rectenna," *Electronics Letters*, vol. 42, pp. 191-192, 2006.

[23] H. Sun, Y. Guo, M. He, and Z. Zhong, "A Dual-Band Rectenna Using Broad-Band Yagi Antenna Array for Ambient RF Power Harvesting," *Antennas and Wireless Propagation Letters, IEEE*, vol. PP, pp. 1-1, 2013.

[24] E Falkenstein, M Roberg, and Z. Popovic, "Low-Power Wireless Power Delivery," *Microwave Theory and Techniques, IEEE Transactions on*, vol. 60, pp. 2277-2286, 2012.

[25] G. Monti, L. Tarricone, and M. Spartano, "X-Band Planar Rectenna," *Antennas and Wireless Propagation Letters, IEEE*, vol. 10, pp. 1116-1119, 2011.

[26] Ren Yu-Jiun and Chang Kai, "New 5.8-GHz circularly polarized retrodirective rectenna arrays for wireless power transmission,"

Microwave Theory and Techniques, IEEE Transactions on, vol. 54, pp. 2970-2976, 2006.

[27] C. H. K. Chin, Q Xue, and C.H Chan, "Design of a 5.8-GHz rectenna incorporating a new patch antenna," *Antennas and Wireless Propagation Letters, IEEE*, vol. 4, pp. 175-178, 2005.

[28] J. O. McSpadden and K. Chang, "A dual polarized circular patch rectifying antenna at 2.45 GHz for microwave power conversion and detection," in *Microwave Symposium Digest, 1994., IEEE MTT-S International*, 1994, pp. 1749-1752 vol.3.

[29] J. A. G. Akkermans, M. C. van Beurden, G. J. N. Doodeman, and H. J. Visser, "Analytical models for low-power rectenna design," *Antennas and Wireless Propagation Letters, IEEE*, vol. 4, pp. 187-190, 2005.

[30] J. Heikkinen, P. Salonen, and M. Kivikoski, "Planar rectennas for 2.45 GHz wireless power transfer," in *Radio and Wireless Conference, 2000. RAWCON 2000. 2000 IEEE*, 2000, pp. 63-66.

[31] H. Takhedmit, B. Merabet, L. Cirio, B. Allard, F. Costa, C. Vollaire, *et al.*, "A 2.45-GHz low cost and efficient rectenna," in *Antennas and Propagation (EuCAP), 2010 Proceedings of the Fourth European Conference on*, 2010, pp. 1-5.

[32] T. Yoo, J. McSpadden, and K. Chang, "35 GHz rectenna implemented with a patch and a microstrip dipole antenna," in *Microwave Symposium Digest, 1992., IEEE MTT-S International*, 1992, pp. 345-348 vol.1.

[33] Zhao Yun, Hong Jing-song, Zhang Guang-Min, and Wang Bing-Zhong, "A harmonic-rejecting monopole antenna with SIR ground for rectenna," in *Signals Systems and Electronics (ISSSE), 2010 International Symposium on*, 2010, pp. 1-3.

[34] A. Georgiadis, A. Collado, S. Via, and C. Meneses, "Flexible hybrid solar/EM energy harvester for autonomous sensors," in *Microwave Symposium Digest (MTT), 2011 IEEE MTT-S International*, 2011, pp. 1-4.

[35] B. Strassner and Chang Kai, "5.8 GHz circular polarized rectenna for microwave power transmission," in *Energy Conversion Engineering Conference and Exhibit, 2000. (IECEC) 35th Intersociety*, 2000, pp. 1458-1468 vol.2.

[36] J. A. Hagerty, F. B. Helmbrecht, W. H. McCalpin, R. Zane, and Z. B. Popovic, "Recycling ambient microwave energy with broad-band rectenna arrays," *Microwave Theory and Techniques, IEEE Transactions on*, vol. 52, pp. 1014-1024, 2004.

[37] G. Andia Vera, A. Georgiadis, A. Collado, and S. Via, "Design of a 2.45 GHz rectenna for electromagnetic (EM) energy scavenging," in *Radio and Wireless Symposium (RWS), 2010 IEEE*, 2010, pp. 61-64.

[38] Pham Binh, J. C. S. Chieh, and Pham Anh-Vu, "A wideband composite right/left hand rectenna for UHF energy harvesting

applications," in *Antennas and Propagation Society International Symposium (APSURSI), 2012 IEEE*, 2012, pp. 1-2.

[39] Y. Hiramatsu, T. Yamamoto, K. Fujimori, M. Sanagi, and S. Nogi, "The design of mW-class compact size rectenna using sharp directional antenna," in *Microwave Conference, 2009. EuMC 2009. European*, 2009, pp. 1243-1246.

[40] Hung Jui, Chou, Lin Ding-Bing, Weng Kuo-Lin, and Li Hsueh-Jyh, "Novel T-shape slot couple feed dual circular polarized rectenna," in *Antennas and Propagation (ISAP), 2012 International Symposium on*, 2012, pp. 178-181.

[41] J. Heikkinen and M. Kivikoski, "A novel dual-frequency circularly polarized rectenna," *Antennas and Wireless Propagation Letters, IEEE*, vol. 2, pp. 330-333, 2003.

[42] Suh Young-Ho and Chang Kai, "A novel dual frequency rectenna for high efficiency wireless power transmission at 2.45 and 5.8 GHz," in *Microwave Symposium Digest, 2002 IEEE MTT-S International*, 2002, pp. 1297-1300 vol.2.

[43] Ren Yu-Jiun and Chang Kai, "5.8-GHz circularly polarized dual-diode rectenna and rectenna array for microwave power transmission," *Microwave Theory and Techniques, IEEE Transactions on*, vol. 54, pp. 1495-1502, 2006.

[44] H Sun, Y. Guo, M He, and Z. Zhong, "Design of a High-Efficiency 2.45-GHz Rectenna for Low-Input-Power Energy Harvesting," *Antennas and Wireless Propagation Letters, IEEE*, vol. 11, pp. 929-932, 2012.

[45] J. Zbitou, M. Latrach, and Serge Toutain, "Hybrid rectenna and monolithic integrated zero-bias microwave rectifier," *Microwave Theory and Techniques, IEEE Transactions on*, vol. 54, pp. 147-152, 2006.

[46] T. W. Yoo and Chang Kai, "Theoretical and experimental development of 10 and 35 GHz rectennas," *Microwave Theory and Techniques, IEEE Transactions on*, vol. 40, pp. 1259-1266, 1992.

[47] Ren Yu-Jiun, M. F. Farooqui, and Chang Kai, "A Compact Dual-Frequency Rectifying Antenna With High-Orders Harmonic-Rejection," *Antennas and Propagation, IEEE Transactions on*, vol. 55, pp. 2110-2113, 2007.

[48] M. Pinuela, P. D. Mitcheson, and S. Lucyszyn, "Ambient RF Energy Harvesting in Urban and Semi-Urban Environments," *Microwave Theory and Techniques, IEEE Transactions on*, vol. 61, pp. 2715-2726, 2013.

[49] "IEEE Standard for Safety Levels with Respect to Human Exposure to Radio Frequency Electromagnetic Fields, 3 kHz to 300 GHz," *IEEE Standard for Safety Levels with Respect to Human Exposure to Radio Frequency Electromagnetic Fields, 3 kHz to 300 GHz*.

[50] "IEEE Standard for Safety Levels with Respect to Human Exposure to Radio Frequency Electromagnetic Fields, 3 kHz to 300 GHz in 1999," *IEEE Standard for Safety Levels with Respect to Human Exposure to Radio Frequency Electromagnetic Fields, 3 kHz to 300 GHz*.

CHAPTER 3

PLANAR RECTENNA DESIGNS AND INVESTIGATIONS

3.1 Introduction

In this chapter, planar broadband antennas with unidirectional radiation patterns are investigated and designed for wireless applications [1, 2]. Moreover, based on the knowledge gained, a new broadband dipole antenna on top of a conducting ground plane (a reflector) is proposed and investigated. The antenna is optimised by changing the dipole shape, diameter, feed gap and the spacing between antenna and the ground plane. This aim is to understand the behaviour and guide of the planar dipole antenna design. In addition, a new simple circular dipole rectenna and rectenna arrays are investigated, fabricated and measured and described in the later part of the chapter.

3.2 Dipole Antennas with Unidirectional Radiation Pattern

With the rapid development of various wireless systems, there is a need to have a broadband rectenna for wireless power transmission/ collection. The desired rectenna should be of a wide frequency bandwidth and dual polarisation [3, 4]. Since the available RF wireless power source and their power densities in urban was reported in Chapter 2 which covers over a broad bandwidth from 470 MHz to 2.5 GHz. A wideband rectenna is more convenient to harvest the available ambient electromagnetic power in the air than the single frequency rectenna. In addition, using dual-polarised rectenna can maximise the reception of the wireless energy because the incident wave can be any polarisation. The radiation pattern should be unidirectional which means the antenna has high gain and broad bandwidth over the frequency range of interest since antenna can be insensitive to the direction.

Ultra-wide band (UWB) wireless system is another hot research topic in recent years, since it is aimed to provide ultra-fast high data rate communication using licence-free UWB spectrum (from 3.1 to 10.6 GHz). A great number of broadband antennas have been developed. Most of them are planar monopole type with micro-strip feed-line [2, 5, 6]. But in some applications the dipole type antenna with a balanced feed-line is preferred [7-11].

Commonly, an UWB signal was defined as a signal with a fractional bandwidth larger than 20% or an absolute bandwidth at least 500 MHz when the centre frequency is above 6 GHz. The definitions of the fractional bandwidth and absolute bandwidth are given by

$$BW_{factional} = \frac{2(f_H - f_L)}{f_H + f_L} \tag{3.1}$$

$$BW_{abs} = f_H - f_L \tag{3.2}$$

where f_H and f_L are the highest and lowest cutoff frequency (-3 dB) respectively

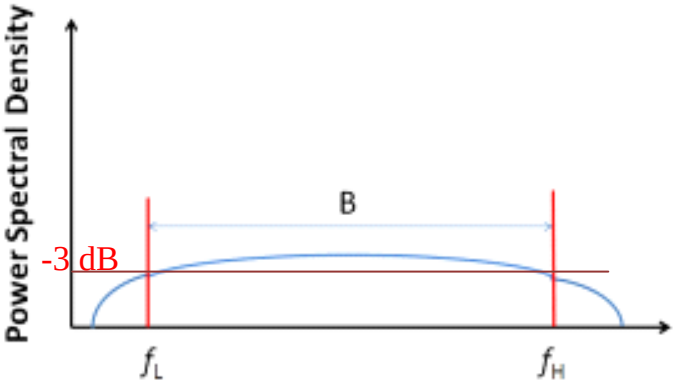

Fig. 3.1: Illustration of a UWB signal with its power spectral density in the frequency domain

3.2.1 Broadband Dipole Antenna

The dipole is a well-known classic antenna with an omni-directional radiation pattern. The planar broadband dipole antennas such as circular, square and hexagonal dipoles are derivative of the wire dipole but with a wider frequency bandwidth. At the beginning of this research, these antennas are optimized by changing the shape, the feed gap and the dimension of conventional dipole antennas to cover part of the frequency band from 2.4 GHz to 10.6 GHz which covers a large number of the current and emerging wireless systems (such as Bluetooth, wireless LAN, 3G, UWB, LTE and Wi-Fi).

The geometry and major parameters of proposed dipole antenna are illustrated in Fig. 3.2. This antenna is built on a low-cost FR4 substrate with relative permittivity ε_r = 4.4 and a thickness of 1.5 mm. The gap between the two arms and poles of the dipole is *G* which is a variable to be optimised. The diameter of the circular poles is set to be another variable *W*. In addition, a 50 Ω lumped feed-line is assumed to feed the dipole antenna.

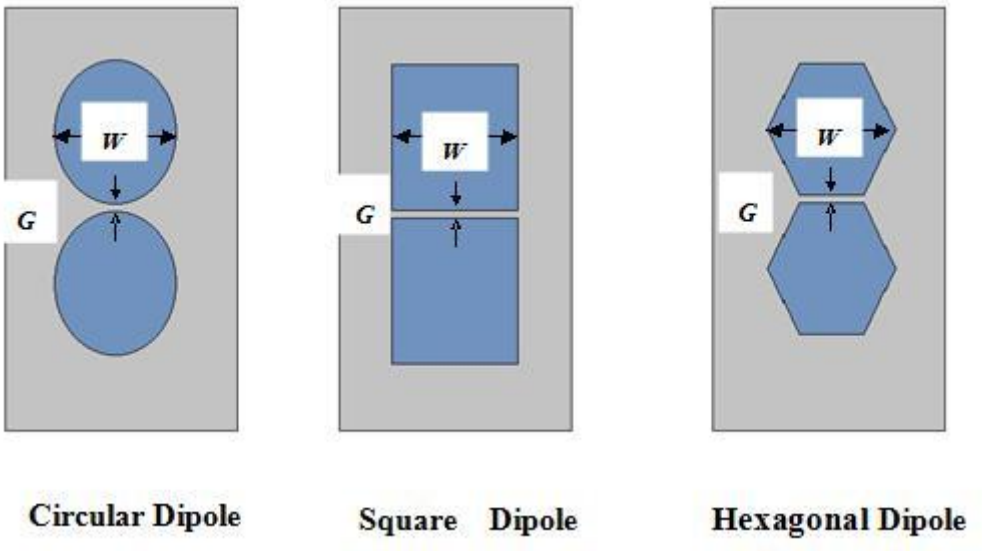

Fig. 3.2: Geometry of the broadband dipoles

3.2.1.1 Effects of Feed Gap and Diameter

Computer software packages, Ansoft HFSS and CST Microwave Studio [12], are employed to aid the antenna design and analysis. All other parameters of the dipole antennas are kept the same; except the feed gap which is varied to tune the impedance matching. The dipole simulated with different shapes (only circular, square and hexagonal shapes are reported here). From the simulation results the lowest usable frequency (f_L), the highest usable frequency (f_H) and the bandwidth of the antenna for S11<-10 dB are recorded and shown in Tables 3.1-3.3. It is quite clear that frequency bandwidth for S11<-10 dB generally decreases with the increase of the gap *G* for the circular dipole. However, the bandwidth is increased for the square dipole. While the hexagonal gets the peak bandwidth at feed gap of 1.5 mm.

Table 3.1: Feed gap of dipoles = 1 mm

Diameter (mm)		f_L (GHz)	f_H (GHz)	Bandwidth (GHz)
16	Circular	2.8	4.1	1.3
	Square	2.8	4.2	1.4
	Hexagonal	3.2	>12	**>8.8**
20	Circular	2.4	3.5	1.1
	Square	2.5	3.5	1
	Hexagonal	2.7	9.5	**6.8**
24	Circular	2	3	1
	Square	2.2	3	0.8
	Hexagonal	2.2	7.8	**5.4**

Table 3.2: Feed gap of dipoles = 1.5 mm

Diameter (mm)		f_L (GHz)	f_H (GHz)	Bandwidth (GHz)
16	Circular	2.7	3.8	1.1
	Square	2.7	4.9	2.2
	Hexagonal	3	>12	**>9**
20	Circular	2.3	3.4	0.9
	Square	2.4	4	1.5
	Hexagonal	2.6	9.3	**6.7**
24	Circular	2	2.8	0.8
	Square	2.1	3.5	1.4
	Hexagonal	2.3	8.3	**6**

Table 3.3: Feed gap of dipoles = 2 mm

Diameter (mm)		f_L (GHz)	f_H (GHz)	Bandwidth (GHz)
16	Circular	2.6	3.5	0.9
	Square	2.6	5.5	2.9
	Hexagonal	3	>12	**>9**
20	Circular	2.3	3.1	0.8
	Square	2.2	4.5	2.3
	Hexagonal	2.5	9.7	**6.2**
24	Circular	1.9	2.6	0.7
	Square	2	3.7	1.7
	Hexagonal	2.2	8.3	**6.1**

Consequently, the feed gap serves as an impedance matching circuit and also tunes the resonant frequency for these dipole antennas. Take the circular dipole as an example; the simulated input impedance of the dipole is illustrated in Fig. 3.3. It is important to note that with the increase of feed gap length, the real part and imaginary part of the circular dipole impedance are increased and the 1st resonance frequency of these dipoles is shifted downwards.

It also can be seen from Fig. 3.3 that as frequency varies, the impedance of the circular dipole changes in the vicinity of 50 Ohms, with small values of reactance. This gives rise to a small reflection coefficient across a broad frequency range around the resonance frequency of each mode. As a result, the antenna has a low reflection coefficient over a wide frequency bandwidth, which therefore becomes a wide band antenna.

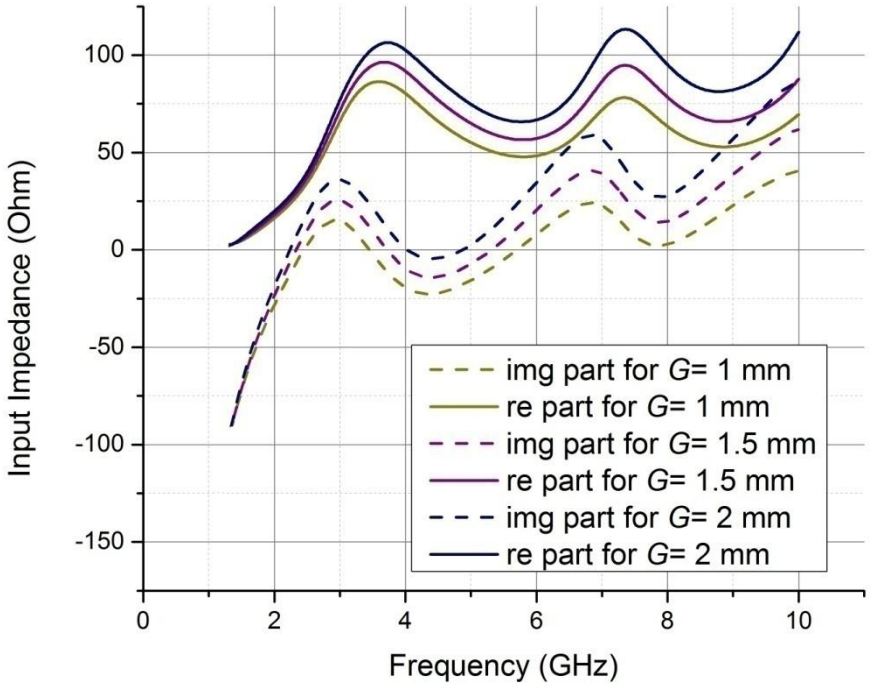

Fig. 3.3: Simulated input impedance for circular dipoles

In addition, we have also investigated the impact of various diameters of these dipole antennas. Tables 3.1-3.3 also show the simulated

results for the antenna with diameters of W=16 mm, 20 mm and 24 mm, respectively. It is seen that the optimum designs can be obtained for the diameter of 16 mm since all the different shaped antennas reach the widest frequency bandwidths at this diameter. Therefore, the diameter at 16 mm is considered as the best in this case. Moreover, from the bandwidth point of view, the hexagonal dipole gives the widest bandwidth (at least from 3 to 12 GHz or higher) than the other antennas investigated in this chapter.

The simulated surface current distribution of the circular dipole at selected resonance frequencies is plotted in Fig. 3.4. It is shown that the planar dipole has the same sinusoidal current distribution as the wire dipole. The current for mode 1 at 2.6 GHz shows a quarter-wavelength distribution on one circular arm without null and peak at the feed point, giving a total of half-wavelength distribution on the whole antenna. As the frequency increases, nulls start to appear at the edge of the structure where the current will travel in opposite direction. There is only one null at mode 2 and the number of nulls increases to two at mode 3. The dipole shows a three-wavelength distribution and five-wavelength distribution on the whole antenna at 5.8 and 8 GHz, respectively.

Furthermore, the optimal feed gaps are found to be 1 mm, 1.5 mm and 2 mm for circular dipole, hexagonal dipole and square dipole respectively. The optimal S11 results are shown in Fig. 3.5. It is shown that hexagonal dipole offers the widest bandwidth. In practice, we have to take other practical facts such as the actual feeding and power handling capacity of the antenna into account.

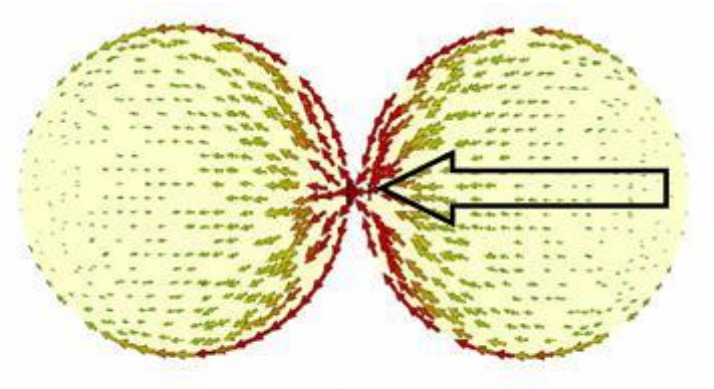

2.6 GHz Mode 1

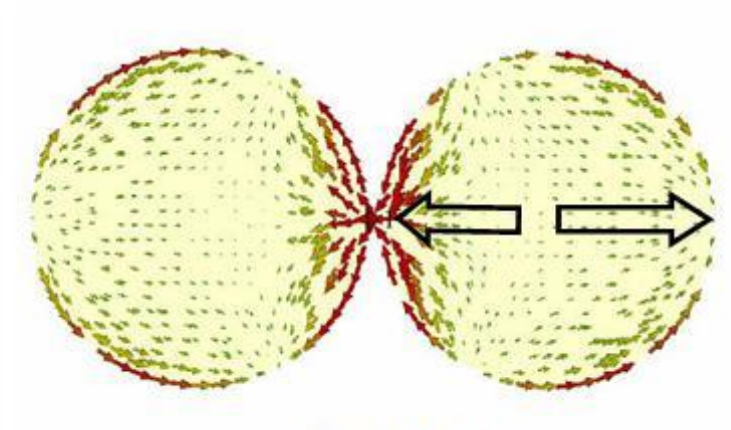

5.8 GHz Mode 2

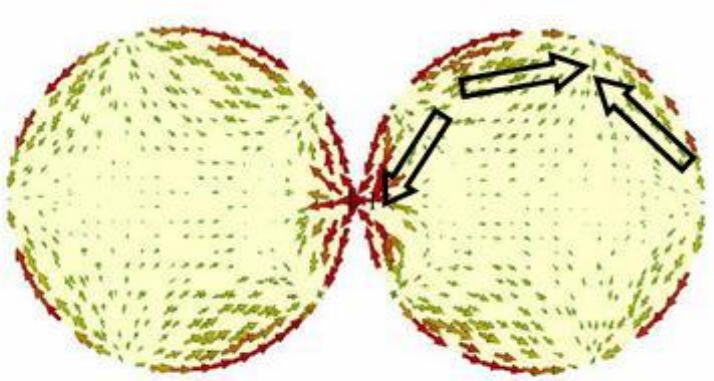

8 GHz Mode 3

Fig. 3.4: Modes at resonant frequencies for the circular dipole with *G* of 1 mm

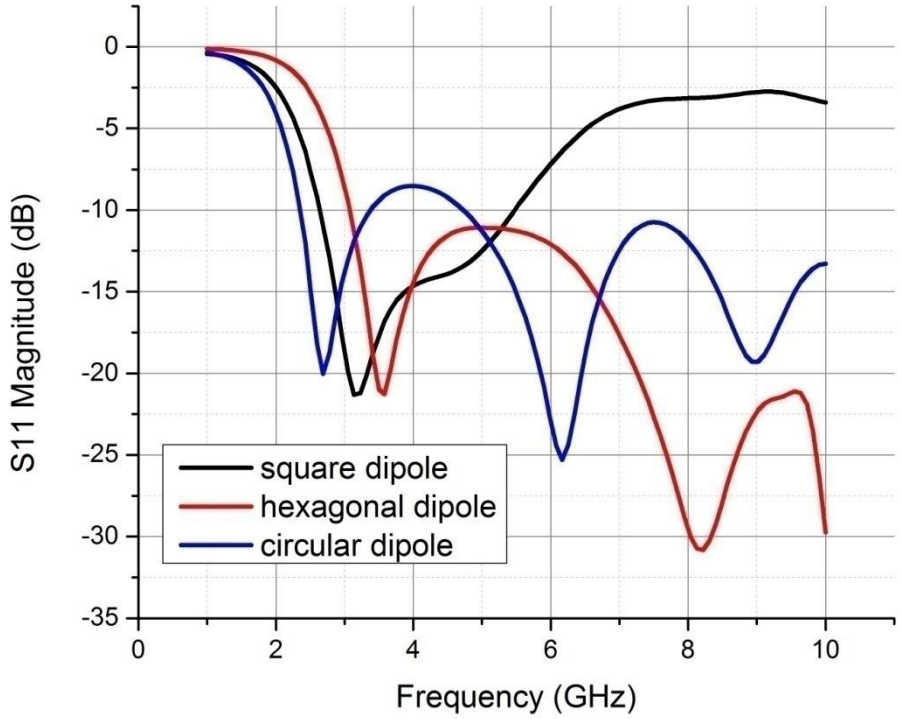

Fig. 3.5: Simulated reflection coefficients of three shapes of dipole

3.2.1.2 Experimental Results and Discussion

The measurement for a circular dipole shown in Fig. 3.6 (b) was carried using facilities in the department of Electrical Engineering and Electronics in University of Liverpool. An Anritsu 37369A vector network analyzer (VNA) and an anechoic chamber were used to obtain the reflection coefficient of the prototype.

For a dipole antenna to operate properly, the currents on both arms of the dipole should be equal in magnitude. However, in practice, an unbalanced SMA connector is connected to the dipole for our measurement. In this case, some of the current may travel down the outside the connector, affecting the measurement results. In order to compare the simulated result with the measured result properly, a circular dipole with a 50 Ω SMA connector model was designed which is shown in Fig. 3.6 (a).In addition, the simulated and measured reflection

coefficients are plotted in Fig. 3.7. It is illustrated that they are generally in good agreement. The differences between simulated and measured results are believed due to the fabrication errors. It is also demonstrated that, the dipole antenna is very sensitive to the feed configuration.

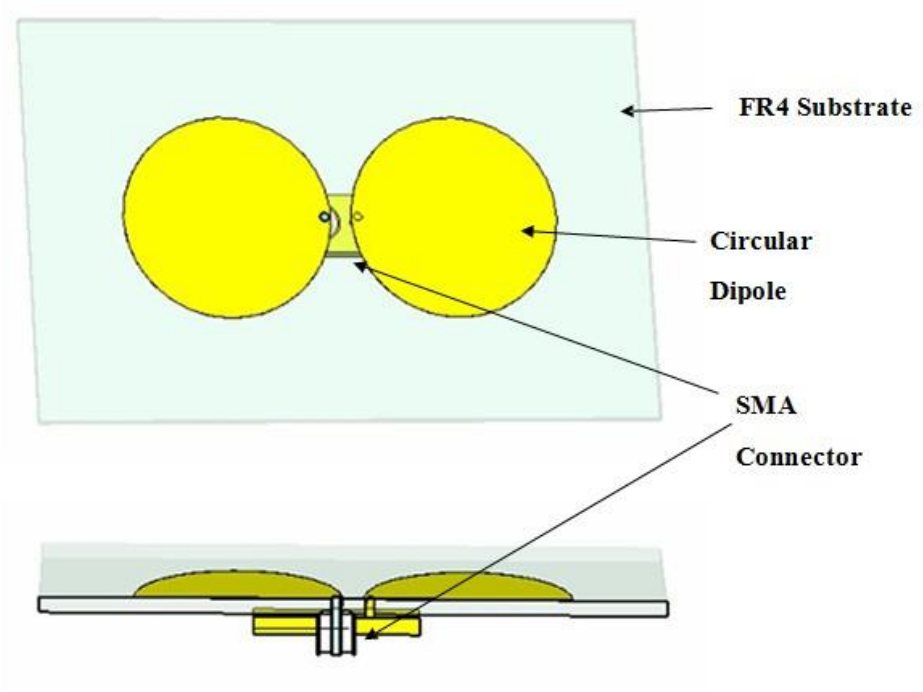

(a): Geometry of the circular dipole antenna

(b): The photo of the circular dipole

Fig. 3.6: Geometry and photo of the circular dipole with a SMA connector

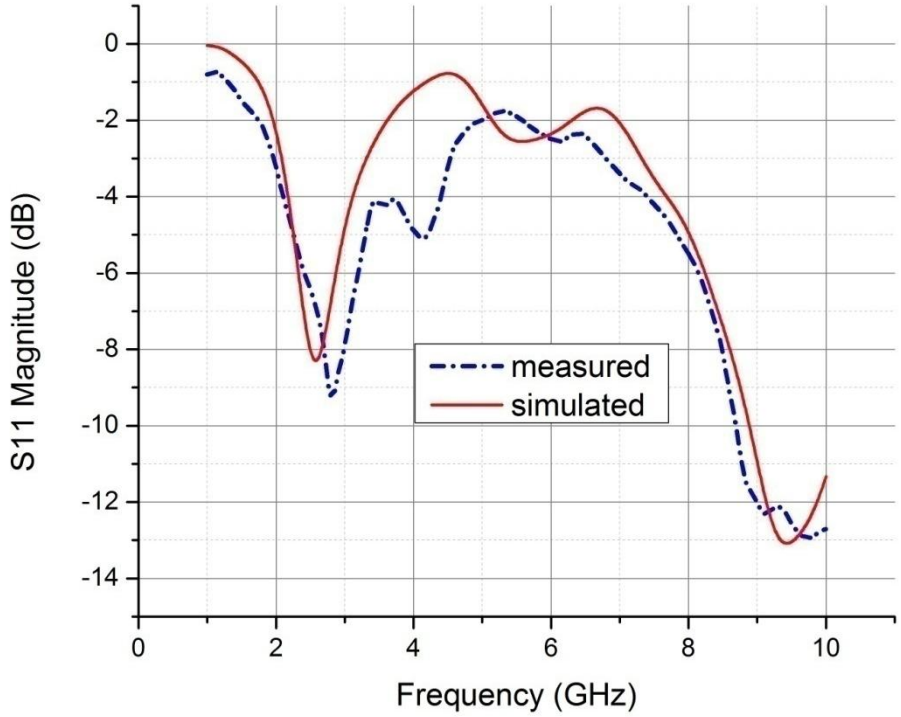

Fig. 3.7: The simulated and measured reflection coefficients of the dipole with a SMA connector

3.1.1 Ground Plane Effect for Broadband Dipoles

With the rapid development of wireless communications such as third-generation (3G), Wi-Fi, and UWB system, the high demand of wideband and low-profile unidirectional antennas that can accommodate several wireless communication systems with excellent electrical characterises such as wide impedance bandwidth, low back radiation and symmetrical radiation pattern over the operating band is desired. In addition, a unidirectional antenna also can be a good candidate for a rectenna device since normally the unidirectional antenna has high radiation gain and it can capture higher incident power than a low gain rectenna due to the Friis Equation.

Several studies have been focus on wideband unidirectional antennas [13-15].A unidirectional antenna can be realised by placing a dipole above a finite ground plane [14]. When the antenna is placed on top of a conducting ground plane, it will interact with the ground plane and result in changes on the antenna properties. This include the antenna impedance and radiation pattern as suggested by the imaging theory.

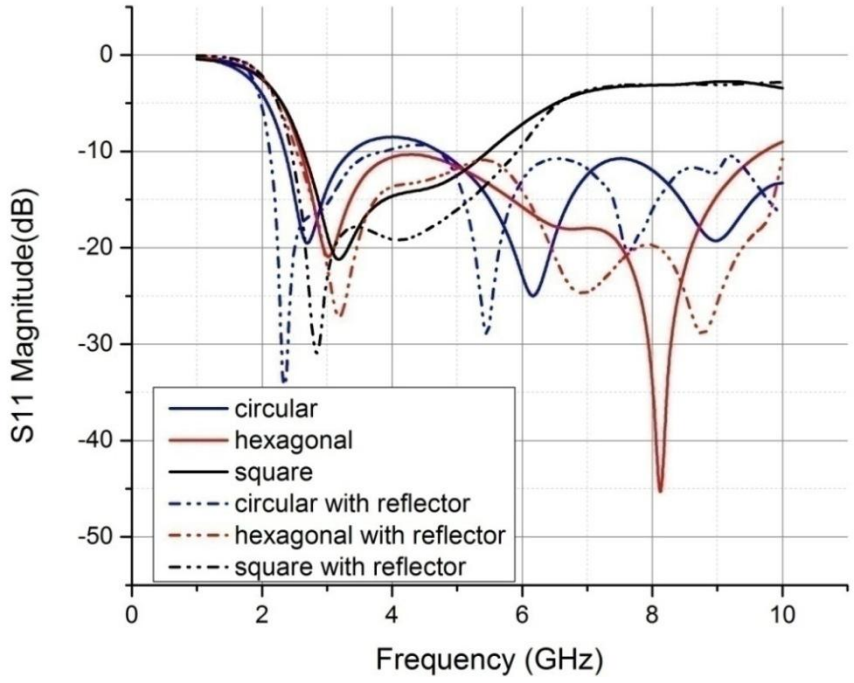

Fig. 3.8: The simulated reflection coefficients of dipoles with (dashed lines) and without reflector (solid lines)

A circular ground plane (reflector) is placed below the antenna to keep the oversize of the antenna compact. Considering the diffraction at the edge of reflector, the size of the antenna is chosen to be a diameter of 120 mm which is comparable with the wavelength of 2.5 GHz which is the lowest operating frequency of the antenna. A comparison between the reflection coefficient of the antenna with and without the reflector is represented in Fig. 3.8. It is clearly that the reflector slightly increases the bandwidth for all dipoles. This is due to the electromagnetic interaction between the antenna and the reflector, which gives rise to an image impedance and changes the overall input impedance of the antenna to

values close to 50 Ohms over the frequency range, particularly at the lower frequency end.

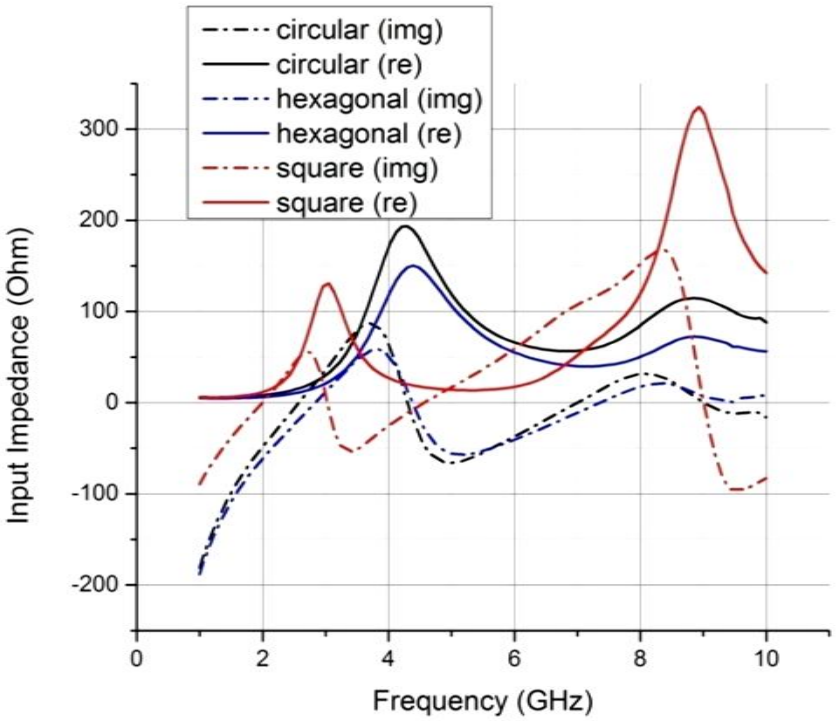

(a): Input impedance for the dipoles with reflector of 10 mm

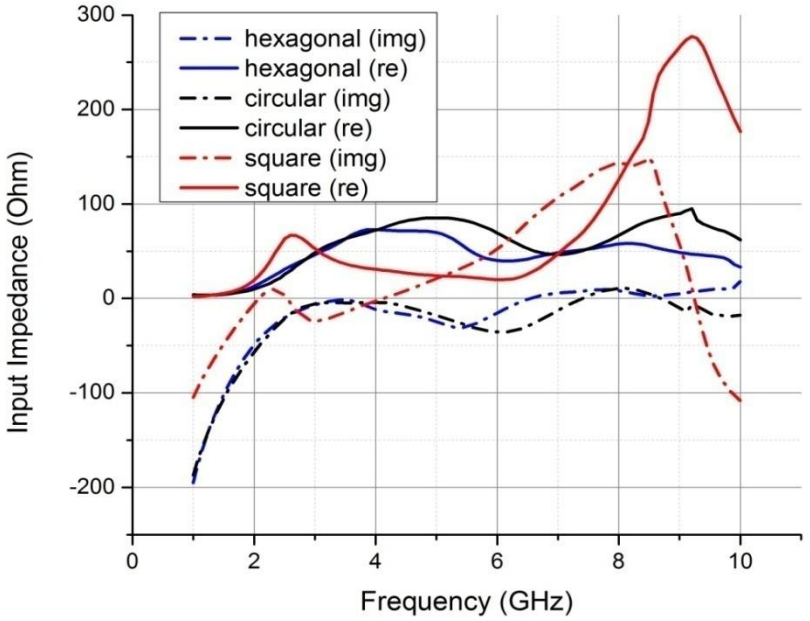

(b): Input impedance for the dipoles with reflector of 30 mm

Fig. 3.9: Input impedance for circular, hexagonal and square dipole with reflector

A parametric study is undertaken by varying the spacing from 10 mm to 40 mm significant changes are observed. Fig. 3.9 (a) and (b) show the impedance for L=10 mm and 30 mm respectively. L is the space between the antenna and the reflector. It is obvious that when L is 10 mm the 1st resonance frequency is between 2 to 3 GHz for these three types of antennas and resistance peaks are near 200 Ω for hexagonal and circular dipoles. When the spacing L is increased to 30 mm, we can see that the 1st resonance frequency is shifted downwards and the impedance variation is reduced and the peak of resistance is shifted downwards to approximately 100 Ω for circular and hexagonal dipoles. Most part of the reactance is between -50 Ω to 50 Ω for the circular and hexagonal dipoles, but not for the square dipole. It is observed that comparing the S11 of the dipole with reflector with the S11 of the dipole without reflector, the reflection coefficient is further improved as shown in Fig. 3.8 and Fig. 3.5.With a reflector the bandwidth can now cover from 2.8 to 12 GHz for S11 <-10 dB for both optimised circular and hexagonal dipoles. In addition, the simulated 3D radiation patterns are shown in Fig. 3.10 and the effect of the reflector on the radiation pattern is investigated and the results for circular dipole are shown in Fig. 3.11. As expected, an unidirectional radiation pattern is obtained for low frequency band because when the space L is much larger than quarter wavelength the dipole does not generate unidirectional radiation patterns. The discrepancy between the measured and simulated results may be due to the finite size of the reflector used in the measurement which is different from the simulation.

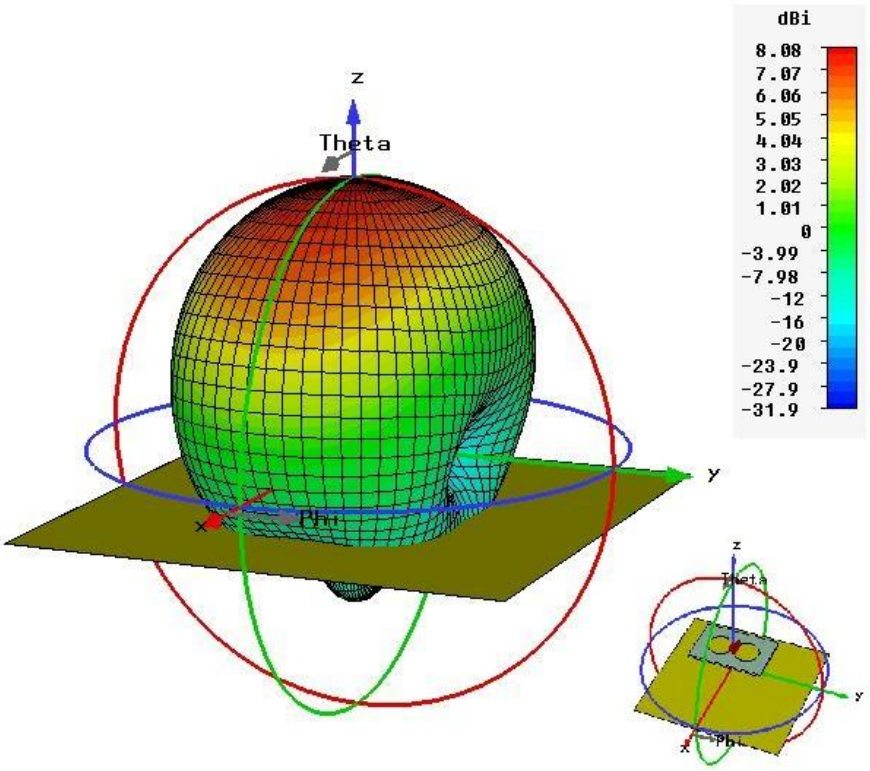

3 GHz

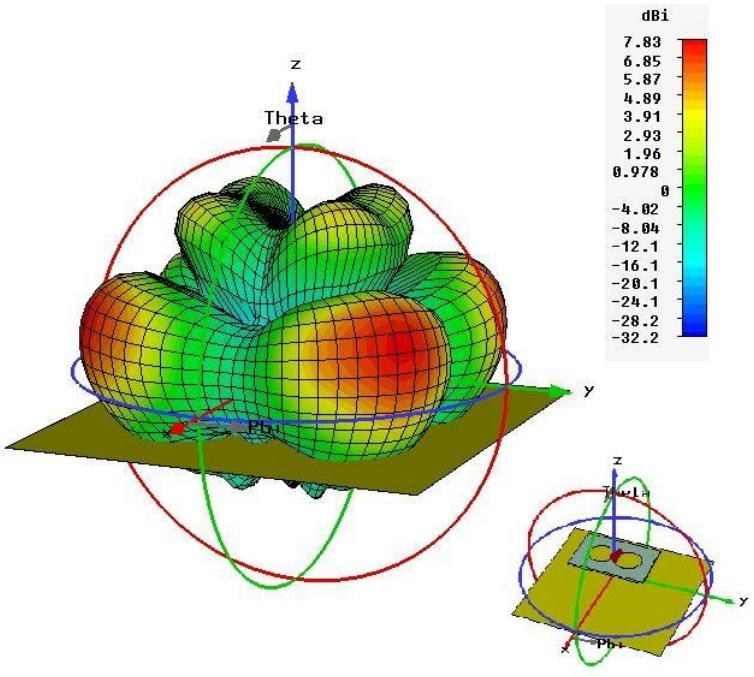

8 GHz

Fig. 3.10: The simulated 3D radiation pattern circular dipole antenna with a reflector at 3 GHz and 8 GHz, respectively

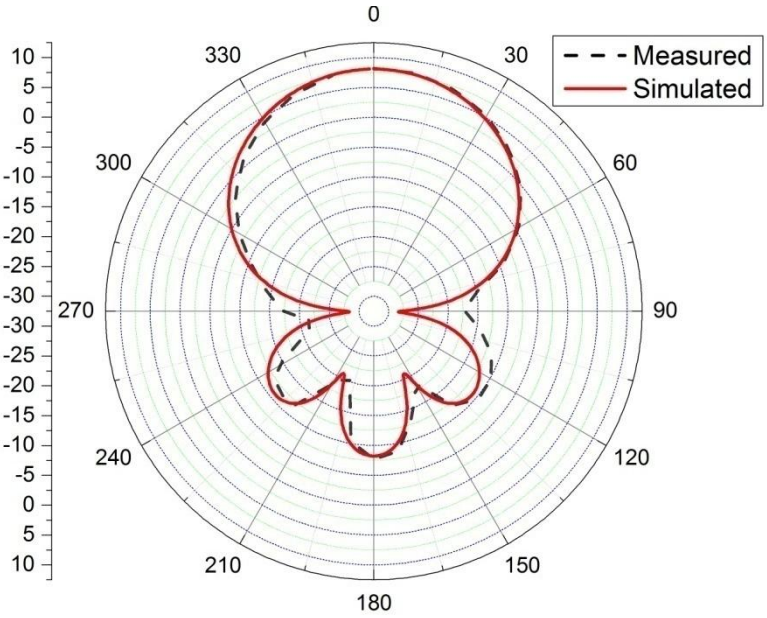

(a) XOZ plane at 3 GHz

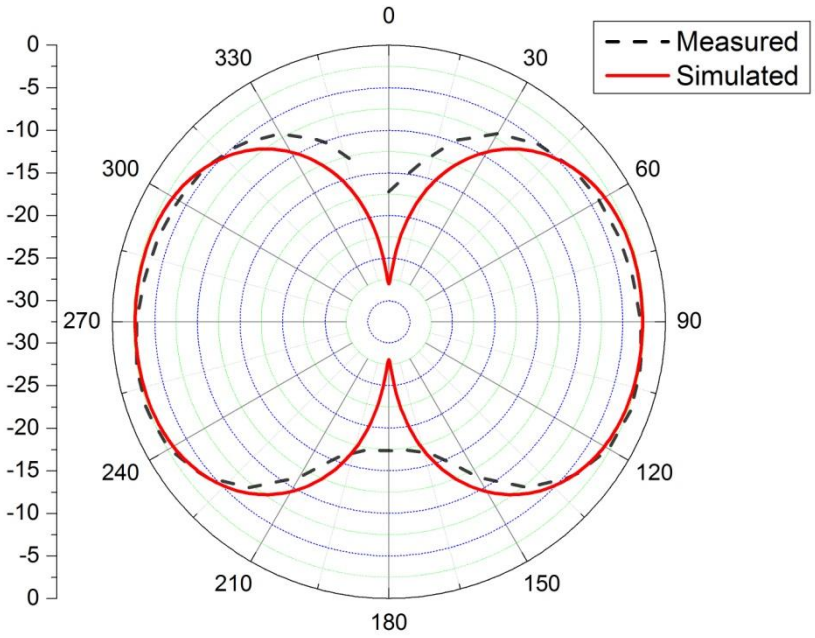

(b) XOY plane at 3 GHz

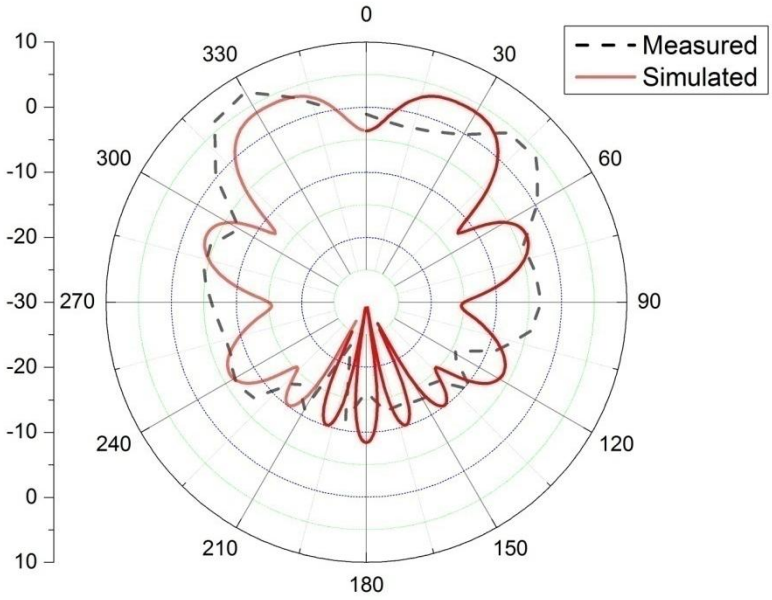

(c) XOZ plane at 8 GHz

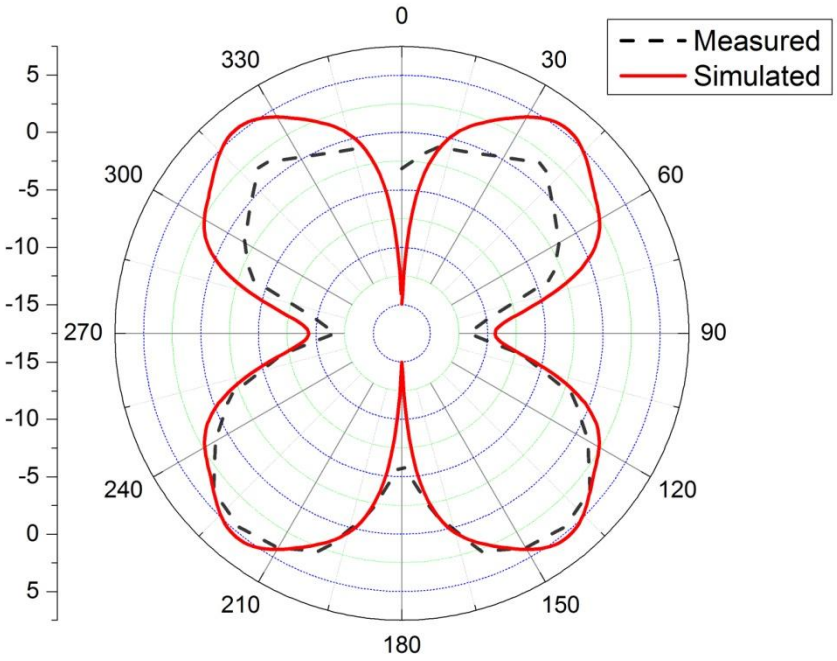

(d) XOY plane at 8 GHz

Fig. 3.11: Measured (dash line) and simulated (solid line) results for circular dipole with reflector in dB

3.3 A Simple Planar Dipole Rectenna

Wireless power transmission (WPT) is a promising technology. There are several potential areas of application. Among these, WPT can be used to power battery-less sensors for monitoring systems or power smart material actuator for applications in vehicle systems. The core device of WPT system is the rectifying antenna (rectenna). A schematic representation of a rectenna has been demonstrated in Chapter 2. The basic architecture consists of three essential components: the antenna, the rectifier and the load. In order to capture the ambient power in the air, it is necessary to have a broadband rectenna with dual-polarisation to maximise the reception of the power energy since the available incoming wave can be of any polarization and various frequencies.

In the recent rectenna development, the most of designs are complicated and linear polarized. In this section, we are going to study a simple broadband dipole rectenna array with dual polarization, using both theoretical and experimental approaches. The array is aimed to harvest the RF energy in the frequency from 2.4 to 6.6 GHz which covers a number of the current and emerging wireless systems (Wi-Fi. Bluetooth and wireless LAN).

The dipole antenna is a famous classic antenna with an omni-directional radiation pattern. Recently, various planar dipole antennas have been investigated to get broadband performance which is presented in Section 3.2. It is concluded that the circular dipole is a suitable element antenna for our rectenna array. A number of rectenna arrays formed by circular dipole antennas and diodes are developed and measured. It shows that, as we expected, rectification is obtained and the output of the rectenna array is proportional to the number of the elements in the array.

3.3.1 Single Rectenna Element

The new simple rectenna consists of a circular dipole and a diode for RF to DC conversion is discussed in this section- this is a step towards the development of a broadband rectenna. As seen in the previous section 3.2, the optimisation of circular dipole antenna has been discussed. For maximal power transfer, the antenna impedance should match with the diode impedance in the case without using a matching circuit between them. However, as the first step of developing a simple planar rectenna, the mismatching between antenna and the rectifying diode is not properly taken into account. The circular dipole is chosen for its broad bandwidth and convenient feeding where a diode can be connected. In addition, it is easier to build as a duel-polarised rectenna array. A circular dipole with dimensions is shown in Fig. 3.12. The circular dipole antenna is made on a FR4 substrate with relative permittivity of 4.4 and the thickness of 1.5 mm. The diameter of the dipole element is 20 mm and the gap is 2 mm between two arms which is limited by the diode size (in practice this gap size is a little bit larger in order to place the diode package). The conductor thickness is 1-oz copper whose metal thickness is 0.035 mm. The simulated and measured S11 result for this circular dipole antenna with a SMA connector has been shown in the previous section Fig. 3.7 and the simulated S11 result for this circular dipole antenna result are shown in Fig. 3.13. Due to the limitation of the diode size, the feed gap of the circular dipole is not the optimum value. Thus the circular dipole for our rectenna has a bandwidth from 2.2 GHz to 2.9 GHz for S11 <-10 dB.

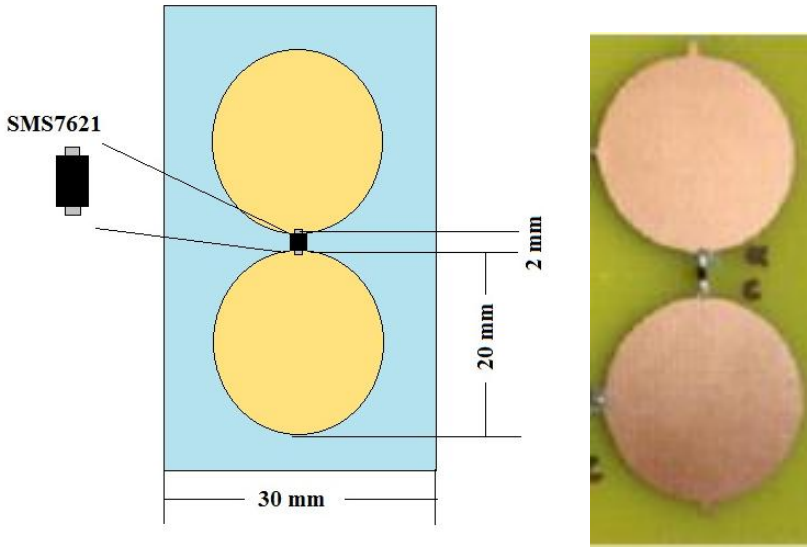

Fig. 3.12: Geometry of the circular dipole antenna element with a package schottky diode connected direct at the feed gap (left) and the photo of single rectenna.

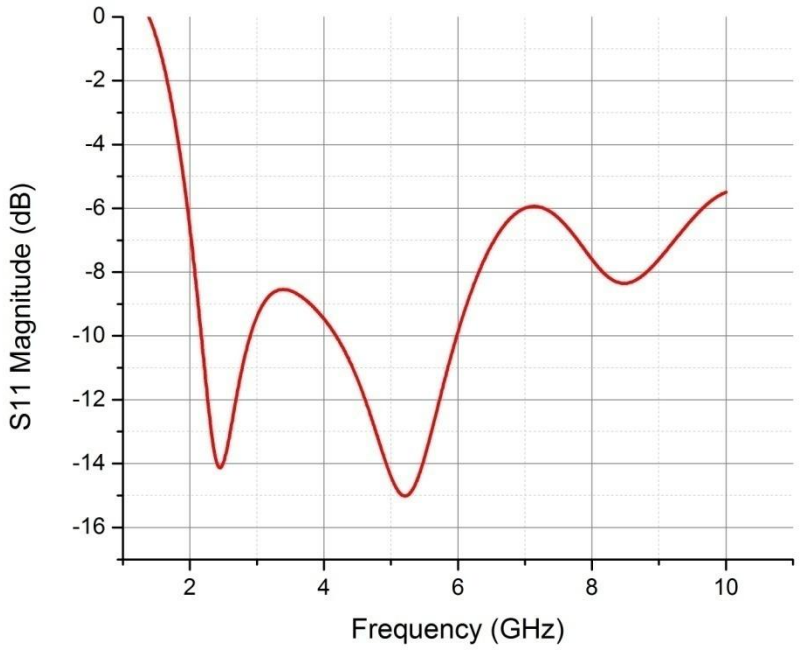

Fig. 3.13: The simulated S11 for the circular dipole antenna with feed gap of 2 mm without a SMA connector

3.3.2 Rectifier Investigations

The diode is an element in the rectifier. Time domain analysis was used in [16, 17] to analyse the diode. The equivalent circuit of the diode and output load is shown in Fig. 3.14.

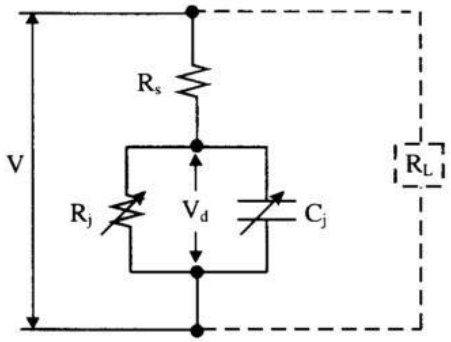

Fig. 3.14: The equivalent circuit of the diode and output load [17]

Assuming input voltage waveform V across the diode terminals, as well as the voltage V_d resulting from the interaction with the nonlinear elements of the diode model shown in Fig. 3.14. The resulting V_d is a clipped sinusoid at the forward bias V_f and follows the input wave during the reverse bias period from θ_{off} to (2π-θ_{off}) as shown in Fig. 3.15. θ_{off} is a dynamic variable dependent on the diode input power. Since the input is connected to the same node as the diode and DC load, the signals added and the input sinusoid is offset by the DC voltage value [16].

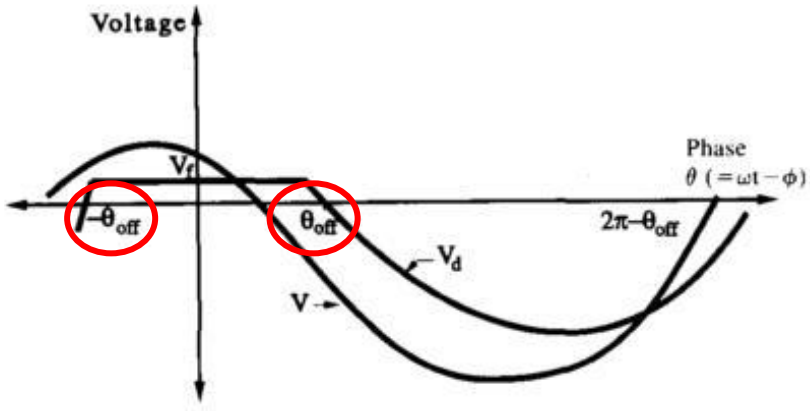

Fig. 3.15: Simplified time domain waveform of voltage V_d [17]

Assuming there are no reflections, the total power is the sum of diode loss and the power on the DC load. The voltage waveform of V and V_d are expressed by

$$V = V_1 cos(\varpi t) - V_0 \tag{3.3}$$

$$V_d = \begin{cases} V_{d1}\, cos(\varpi t - \phi) - V_{d0} & off \\ V_f & on \end{cases} \tag{3.4}$$

Where V_1 is the peak voltage of incident microwave power and V_0 is the bias voltage across the load R_L which offset the input sinusoid. Similar to the mixer, the rectenna is a self-bias circuit. In Equation (3.3), the former one describes when diode is off and the latter one describes when diode is on. In addition, V_{d1} and V_{d0} are the fundamental voltage of the diode junction voltage V_d and DC components of the diode junction voltage.

The diode efficiency can be expressed as

$$\eta = \frac{P_{DC}}{P_{Loss} + P_{DC}} \tag{3.5}$$

Where P_{Loss} is the power dissipated by the diode and P_{DC} is the DC output across the load. They are obtained by

$$P_{DC} = \frac{V_0^2}{R_L}$$

$$P_{Loss} = P_{Loss,diode\ on} + P_{Loss,diode\ off} + P_{Loss,Rs\ on} + P_{Loss,Rs\ off}$$

$$P_{Loss,diode\ on} = \frac{1}{2\pi}\int_{\theta_{off}}^{\theta_{off}} \frac{(V - V_f)V_f}{Rs}\, d\theta$$

$$P_{Loss,diode\ off} = \frac{1}{2\pi}\int_{\theta_{off}}^{2\pi-\theta_{off}} \frac{(V - V_d)V_d}{Rs}\, d\theta$$

$$P_{Loss,Rs\ on} = \frac{1}{2\pi}\int_{-\theta_{off}}^{\theta_{off}} \frac{(V - V_f)^2}{Rs}\, d\theta$$

$$P_{Loss,Rs\ off} = \frac{1}{2\pi}\int_{\theta_{off}}^{2\pi-\theta_{off}} \frac{(V-V_d)^2}{Rs}\, d\theta \tag{3.6}$$

where θ is $(\omega t - \phi)$; θ_{off} is the phrase shift angle when the diode is turn off shown in Fig. 3.15

A ideal diode is simulated at 2 GHz by using ADS software which is shown in Fig. 3.16. It is apparent that the single diode works as a half-wave rectifier and is plotted in Fig. 3.17. A smoothing capacitor is used in the one diode rectifier which is shown in Fig. 3.18. The smoothing capacitor can make the output single more constant and steady and a result of the output signal with and without a smoothing capacitor is given in Fig. 3.19. Then two types of silicon Schottky diode with parameters shown in Table 3.4 were compared by using ADS software. The circuit of the ADS simulation is shown in Fig. 3.20. In addition, Fig. 3.21 and Fig. 3.22 are taken from the RF to DC conversion efficiency and the output DC voltage for a half-wave one diode rectifier. From the results it is apparent that the SMS7621 has better performance around 0 dBm. Thus, the diode used in this rectenna is the GaAs Schottky barrier diodes (SMS7621) from Skyworks COM.[18].

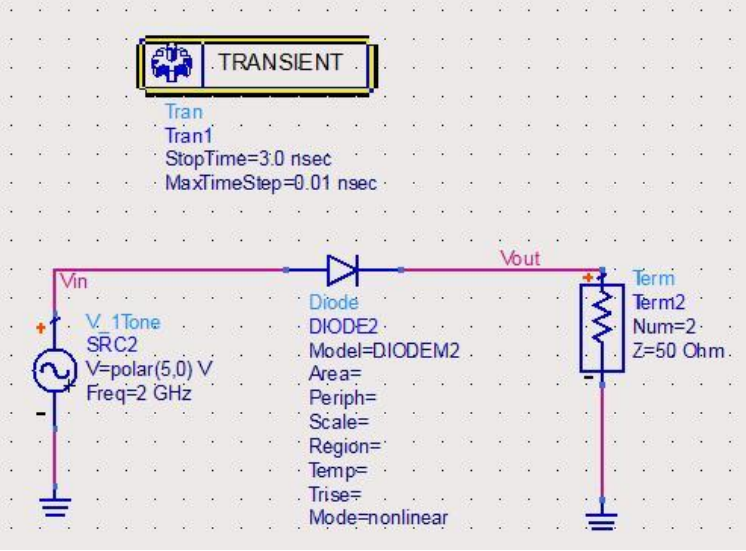

Fig. 3.16: The circuit of ideal diode

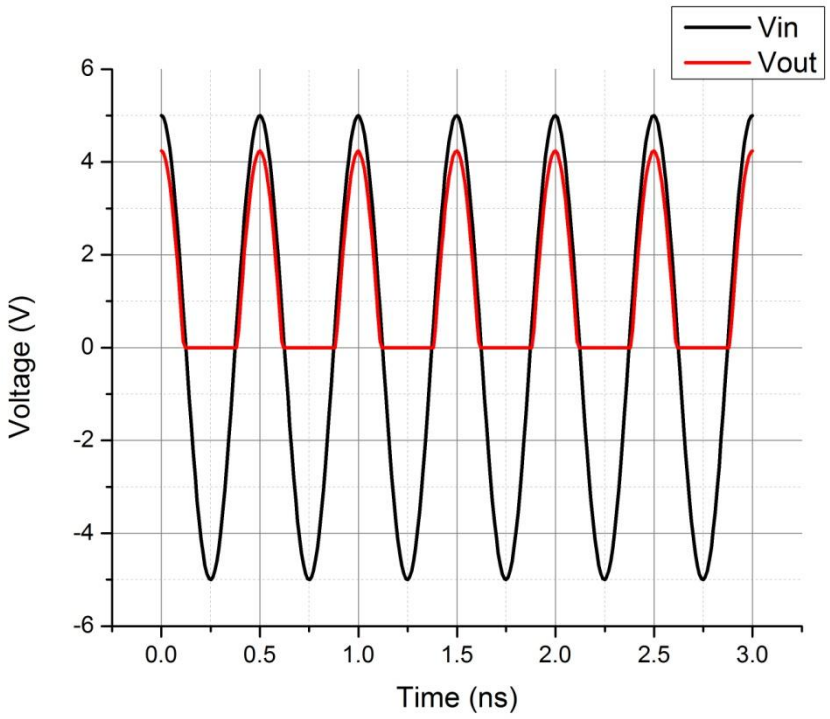

Fig. 3.17: The waveform of incident signal and output signal as a function of time

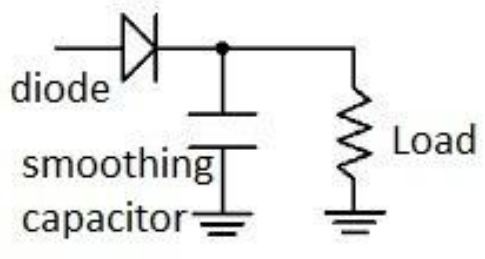

Fig. 3.18: one diode half-wave rectifier

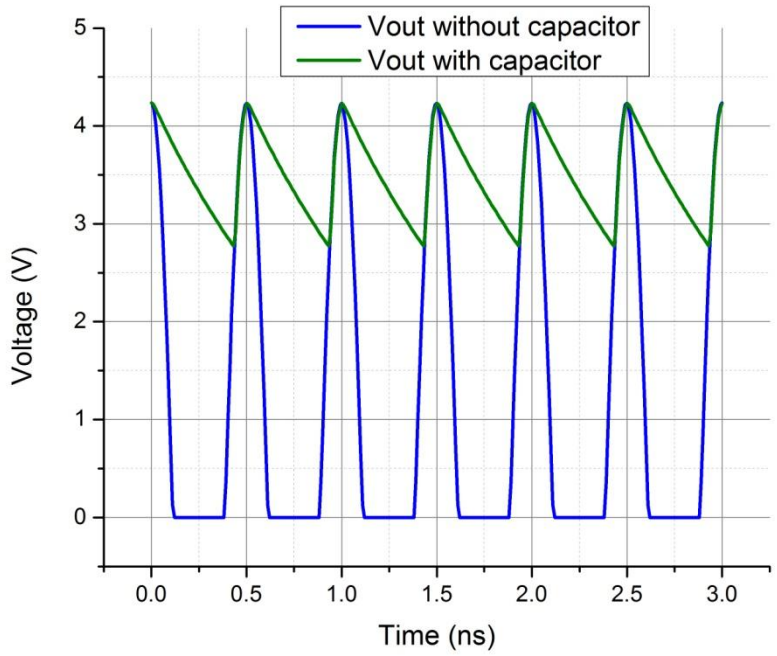

Fig. 3.19: output voltage for single diode rectifier with and without smoothing capacitor.

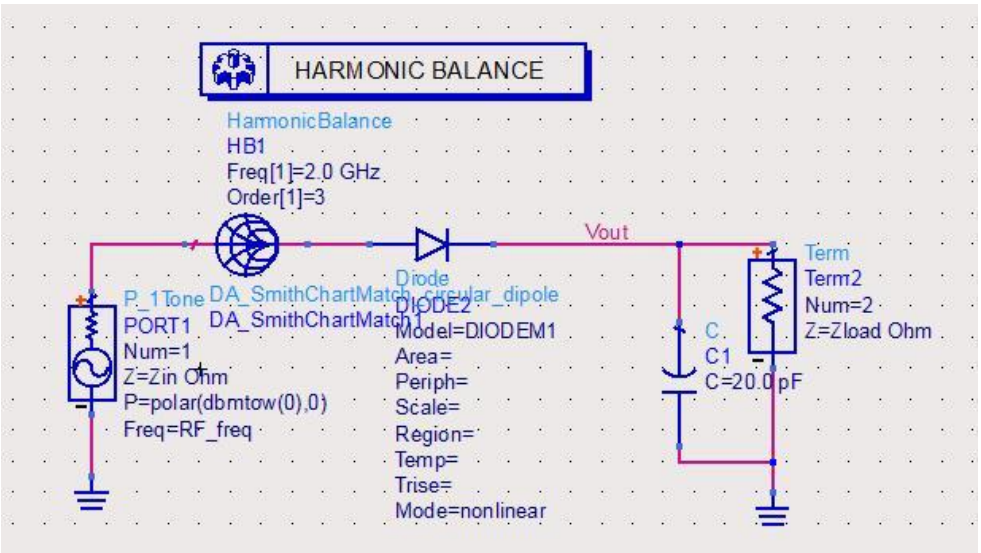

Fig. 3.20: The ADS circuit of comparing two types of diodes

Table 3.4: Diode parameters given by manufacture

Parameter	SMS7621	MA4E2054
I_s (A)	4E-8	3E-8
R_s (Ω)	12	11
N	1.05	1.05
TT	1E-11	0
C_{j0} (pF)	0.1	0.1
V_j(V)	0.51	0.40
M	0.35	0.50
E_g	0.69	0.69
XTI	2	-
F_c	0.5	-
B_v (V)	3	5
I_{BV} (A)	1E-5	1E-5

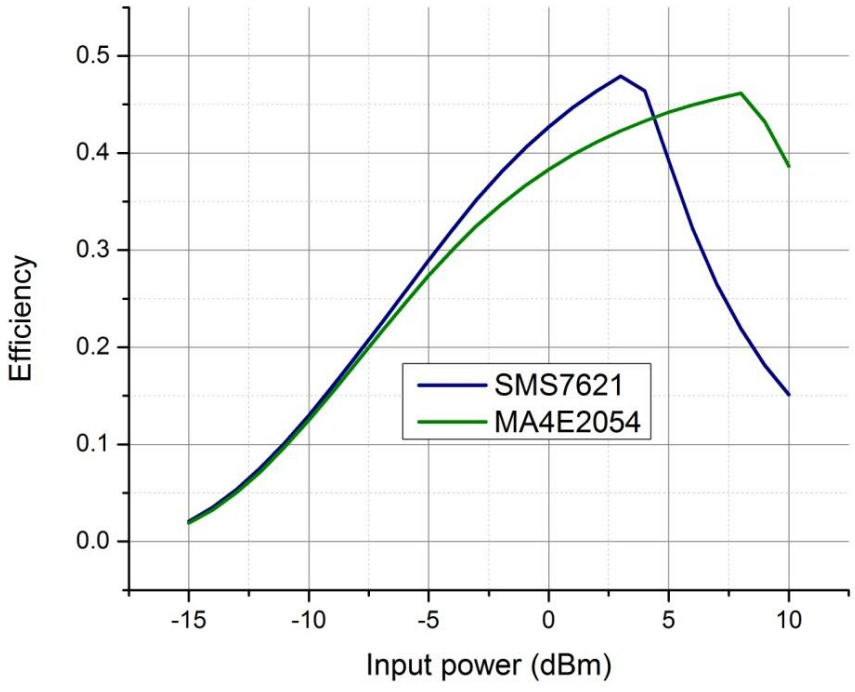

Fig. 3.21: Diode RF to DC conversion efficiency for one diode rectifier

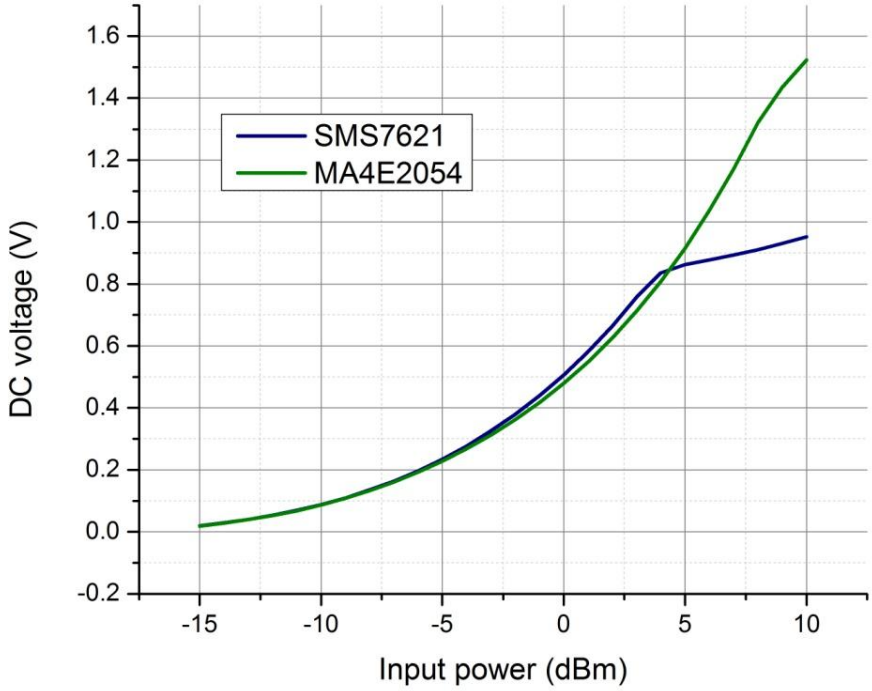

Fig. 3.22: DC output voltage for one diode rectifier

3.3.3 Rectenna Measurement

The measurement method for the rectenna has been studied in [19]. The equipment setup is shown in Fig. 3.23. In this system a transmitting horn antenna is connected to a digital transmitter with a variable frequency. The rectenna is placed near the transmitting antennas and the performance of the rectenna was verified by measuring the output DC voltage using a voltage meter. The transmitting antenna is a Vivaldi horn antenna with a gain around 5 dB over the frequency of interest. Measurements were performed by placing the proposed rectenna at a distance of 40 cm away from the horn antenna. The definition of the RF to DC conversion efficiency of a rectenna is mentioned in Equation 2.3.

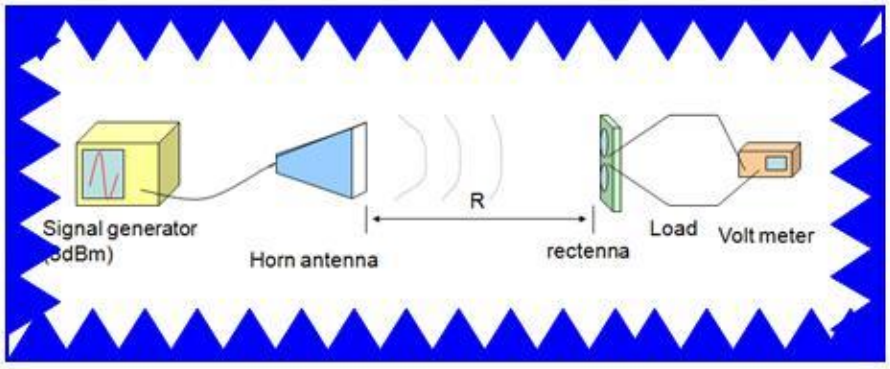

Fig. 3.23: rectenna measurement system

The power density is calculated by using Equation 2.5. In the equation, the power transmitted to the horn antenna was measured by using a spectrum analyser. The gain G_t and efficiency of the reference horn antenna are given on the data sheet. The distance between the horn antenna and the rectenna were fixed. Although the power density used here is a theoretical value it would be quite similar to the measured value. The effective area is also calculated by using the Equation 2.4. The gain G_r of rectenna is the measured gain of the circular dipole antenna.

The rectenna was designed and simulated by using CST MWS and ADS computer software [12]. The input impedance of the antenna was given by using the CST software and then it was imported to the ADS software as the impedance of the power source. A Harmonic balance simulation was made in the ADS to obtain the DC output voltage of the rectifying circuit (the diode and the load). Fig. 3.24 shows the measured and simulated DC output voltage as a function of the frequency with a output load of 100 Ohm and the incident power (P_{RF}) around -3 dBm. Disagreements for simulated and measured results are believed to be caused by three factors. Firstly, the antenna efficiency didn't take into account in the simulation but in practice the antenna radiation efficiency would significantly affect the result. Secondly, the measurement position is another significant factor affected the measurement result because the

planar antenna is a distributed element. Finally, gain of the transmitting horn using in the measurement is very low at the frequency range below 2.5 GHz. It is obvious that this circular dipole rectenna has rectified RF power to the DC electricity around 3.0 GHz. It is important to note that the performance of rectenna as a function of frequency is strongly affected by the antenna bandwidth. In Fig. 3.13, the reflection coefficient of the circular dipole has been demonstrated and the antenna covers the bandwidth from 2.6 to 3 GHz. From the measured result, the bandwidth of rectenna shifted a little bit upwards may result from the fabrication errors and the coupling between antenna and rectifier.

As we mentioned before the rectifier conversion efficiency and the DC output voltage are significantly affected by the input power level. A 30 dB amplifier was added before the horn antenna to increase the input power level of our rectenna measurement. The measured DC output voltage as a function of input power density for various external load resistances at 2.8 GHz is shown in Fig. 3.25. It is clear that with the increases of input power density the DC output voltage for rectenna also increase. The DC output voltage is 100 mV and 320 mV with power density of 0.05 mW/cm^2 for 100 and 1100 Ω, respectively. There is a similar trend for other rectenna: a larger load resistance can achieve a higher DC output voltage.

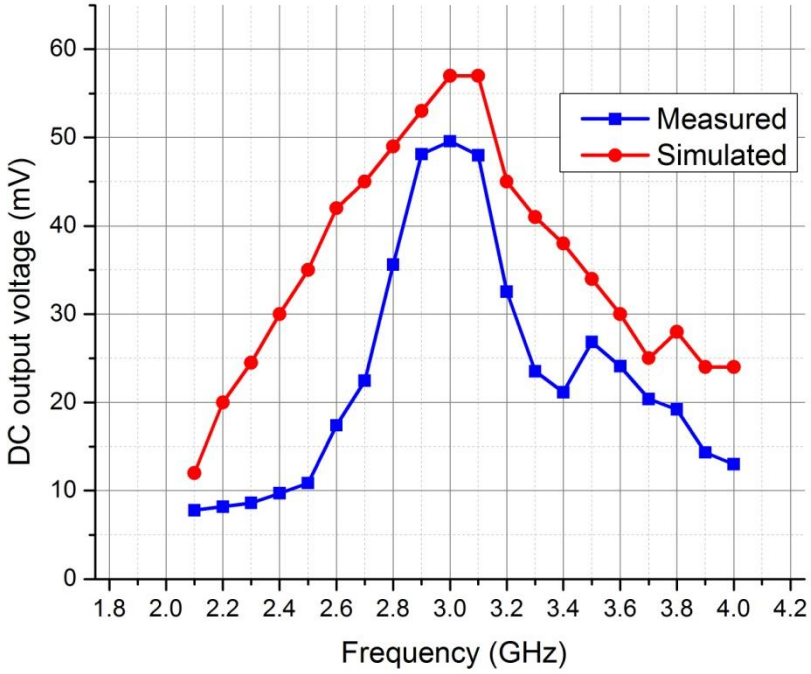

Fig. 3.24: Simulated and measured DC rectified voltage response across a 100 Ω load

Fig. 3.26 shows the RF to DC conversion efficiency as a function of the power density for various loads. The best efficiency, 16.8 %, occurs at a load of1100 Ohm and the DC output voltage is 227 mW. The RF to DC conversion efficiency for using 100 Ohm load is around 16%. It is obvious that the efficiency increases with the increase of power density. Moreover, the efficiency reaches to the peak value and then slightly decreases due to the diode characteristics. There is an optimum input power density level for the rectifying diode.

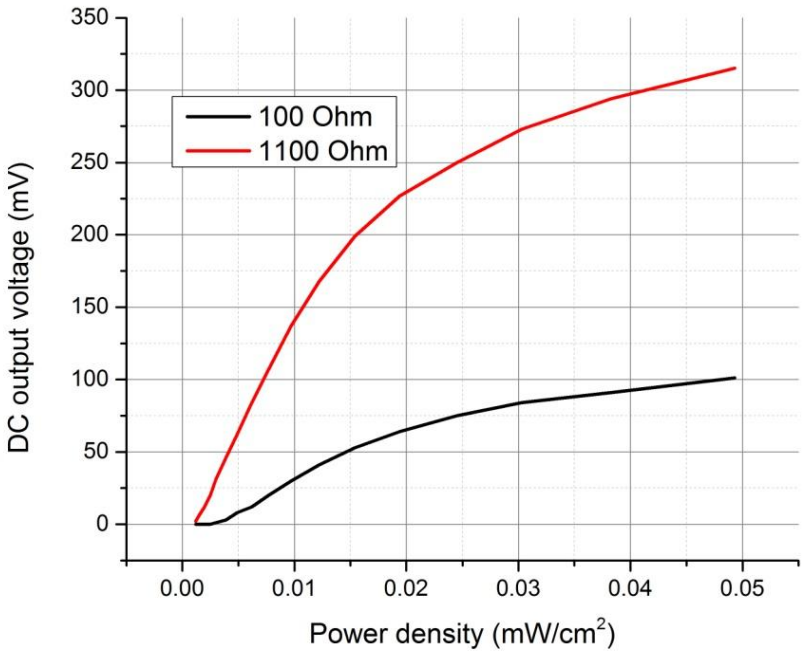

Fig. 3.25: Measured DC voltage as a function of power density at 2.8 GHz

In addition, since the characteristics of the rectifying diode, the conversion efficiency is dependent on the frequency, the incident power level and the output load. Thus, the DC output voltage is also affected by the frequency. The Fig. 3.27 shows the DC output voltage of rectenna on the resonance frequencies with various input power density. Peak output voltages are 200 mV, 325 mV and 375 mV at 2.8 GHz for power density of 0.15, 0.5 and 1.25 mW/cm^2. It is obtained that the working frequency for the rectenna element is around 2.8 GHz. The rectenna bandwidth is narrower than expected. Indeed, the larger gap of the circular dipole, the narrower bandwidth can be achieved. In reality, the gap of the rectenna is much wider than the simulated antenna due to the size limitation of diode package and the fabrication errors. Furthermore, the trend is similar with various input power density and the output voltage gradually increase with the power density.

In addition, the highest conversion efficiency of 16% for the rectenna is much lower than the RF to DC conversion efficiency for other rectenna

designs in the same power density level such as a conversion efficiency of 54% reported in [20]. The first reason is that the rectifying circuit in our rectenna is half-wave rectification and the maximum conversion efficiency can be achieved is only 50%. In addition, since the matching circuit did not take into account in the rectenna design which means the antenna does not match with the rectifier, the conversion efficiency of the rectifying circuit is low. Thus, the total RF to DC conversion efficiency for the rectenna is very low. In order to increase the rectenna conversion efficiency good matching and full-wave rectifier is necessary.

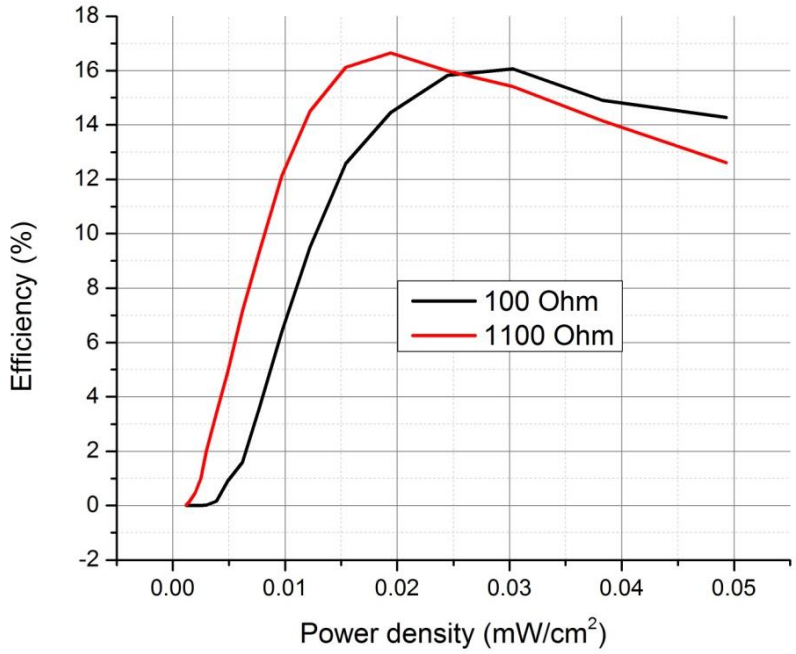

Fig. 3.26: RF to DC conversion efficiency for rectenna with various loads

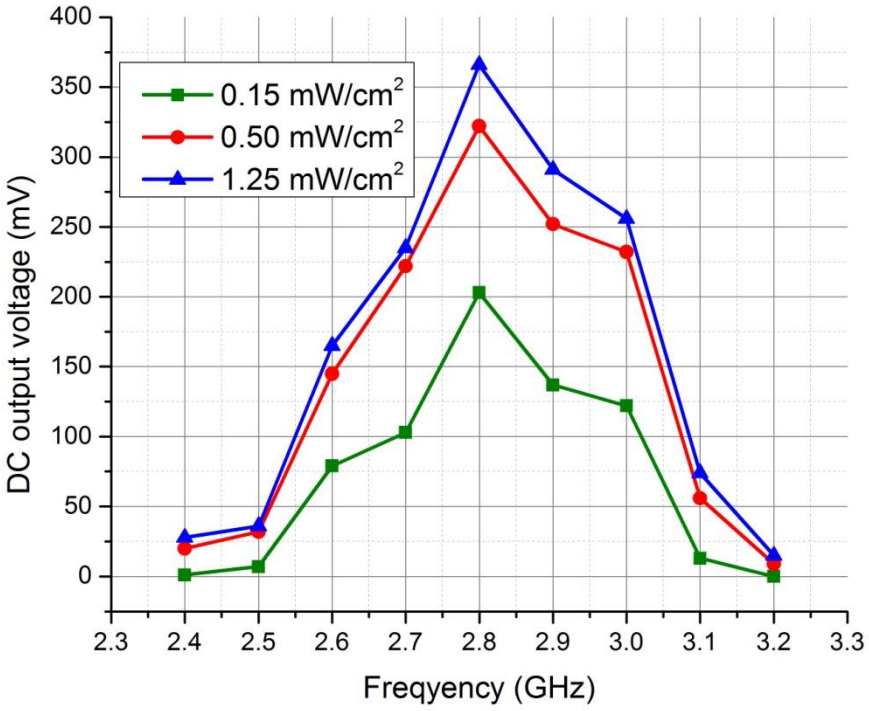

Fig. 3.27 Measured DC output voltage as a function of frequency with various input power density

3.3.4 Planar Dipole Rectenna Array Designs

In most recent rectenna developments, researches were focused on the study of single rectenna element. However, it is necessary to develop a rectenna array when a large DC voltage is desired. Here, the rectenna elements are connected to form a duel-polarised rectenna array to recycle the ambient power in the air.

The RF to DC conversion efficiency of a rectenna is maximised at the optimum input power [17]. The investigation for the method of interconnection of rectenna array has been presented in [4]. It is obtained that the three methods to connect rectenna array are series connection, parallel connection and cascade connection. In these methods, cascade interconnection method can achieve the highest DC output voltage. Thus,

in our rectenna array we use cascade interconnection method to connect our rectenna array.

To achieve higher received power, the circular dipole antenna can extended to become an array by cascade connect more elements shown in Fig, 3.28. Photographs of 2-element array and 3-element array for experiment are shown in Fig. 3.29

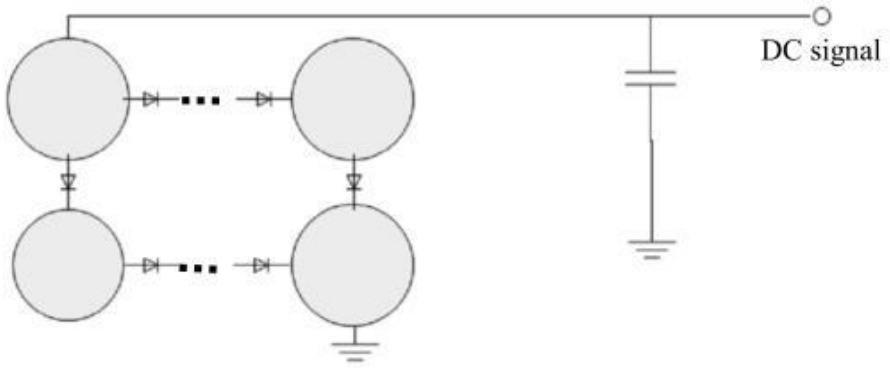

Fig.3.28: The rectenna array scheme

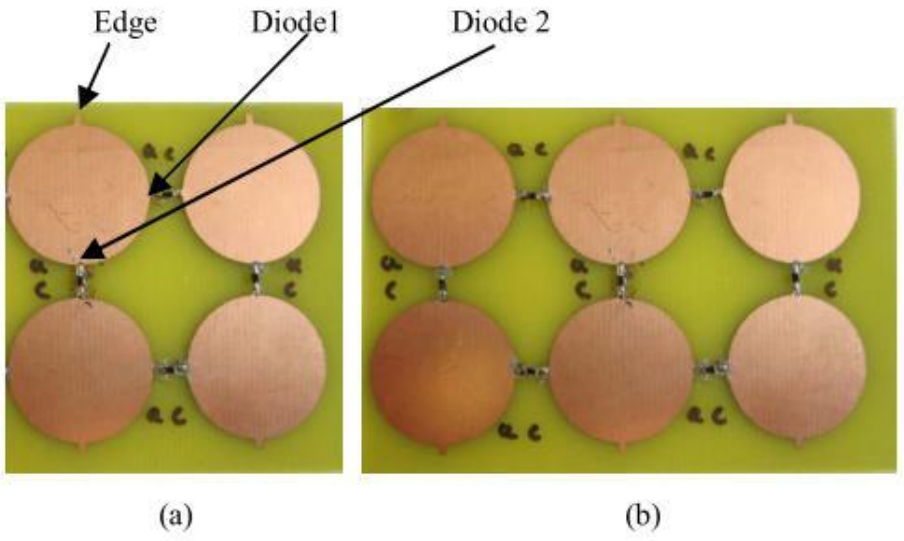

Fig. 3.29: (a) a two-element rectenna array. (b) a three- element rectenna array

The measured DC output voltage of rectenna arrays are shown in Fig. 3.30-3.32. Measured output DC voltages for single rectenna element are also plotted as a comparison. Since the antenna is a distributed element the voltages measured at different positions are different. Therefore we measured three different positions on rectenna arrays (diode 1, diode 2 and edge) as shown in Fig. 3.29.

From the measurement results the DC output from two elements and three elements rectennas are around twice and three times of that of the single element for each position.

The measured output voltage results for single element are given in Fig. 3.30. It can be seen that a maximum output voltage of about 53 mV has been measured when the digital meter probe put on the diode of the element. Measured values of output voltage as a function of the frequency are also illustrated. Since the antenna is a distributed element, the rectenna is very sensitive to measured positions as shown in Fig. 3.30. The load connected to the diode of the single rectenna can receive larger voltage than it is connected to the edge position.

Fig. 3.31 shows the two-element rectenna array which also can be seen as a 2×2 dipole array. These dipole antennas connected in series by diodes. This configuration combines the DC voltage rectified by each dipole rectenna of this array. The measured peak voltage is about 75 mV which is smaller than twice of the peak voltage from a single element ($= 2 \times 55$) which may be resulted from mutual coupling for the antenna elements. Indeed, according to the simulation results shown in Fig.3.33, the single circular dipole element works better than the element of two and three elements arrays from 2.4 to 4 GHz.

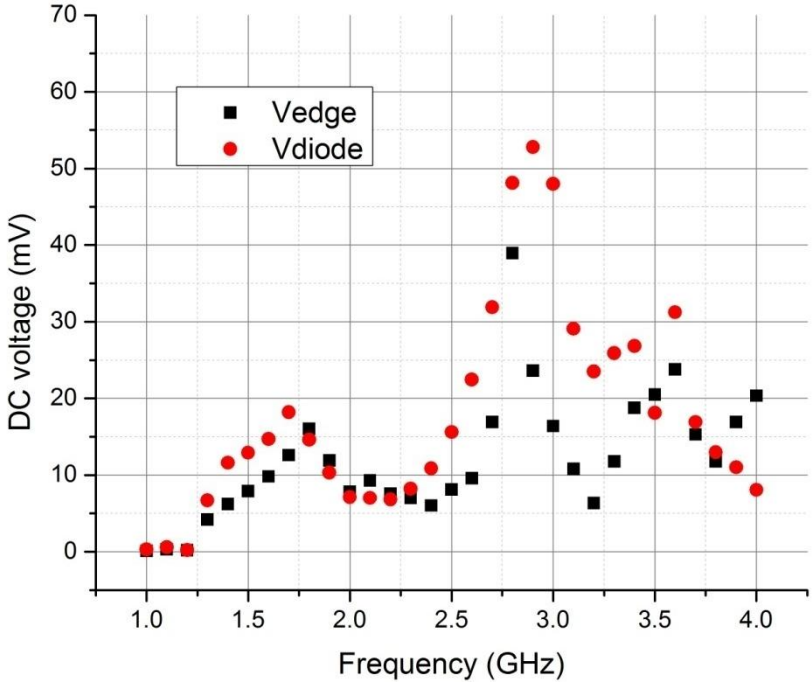

Fig.3.30: Measured DC output voltage for one element rectenna :Curves V_{edge} and V_{diode2} are the DC output voltage measured from the position edge and the position diode 2 respectively which is given in Fig. 3.29.

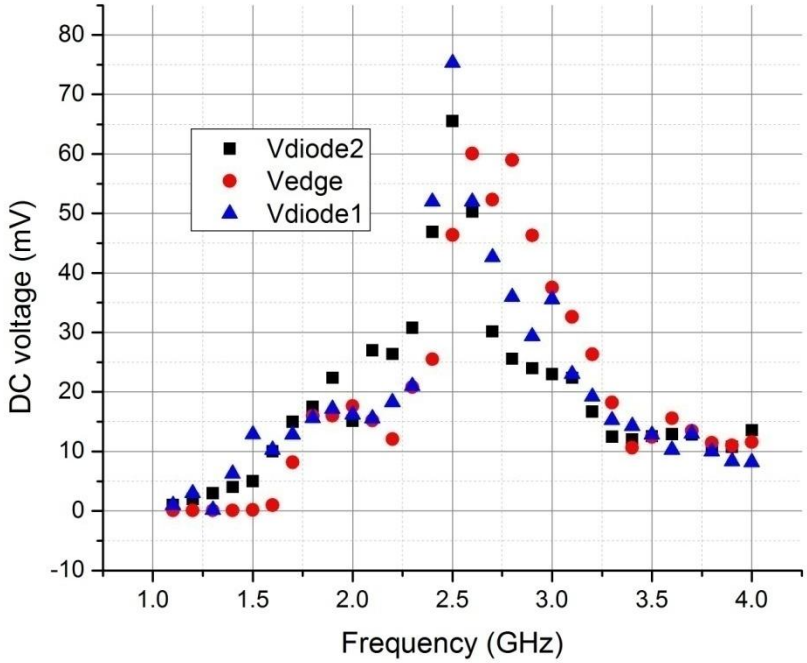

Fig.3.31 : Measured DC output voltage for two elements array

Similarly, Fig.3.32 is the measurement results for three-element rectenna array. As expected, the maximum output voltage is increased to

around 200 mV which is about three times of the voltage from a single rectenna. As mentioned above, the rectenna element was cascade connected together. In this case, the rectenna array becomes very complicated to analyse its operation theory. From the measured results it is concluded that on position diode1 the DC output voltage is higher than the other two positions.

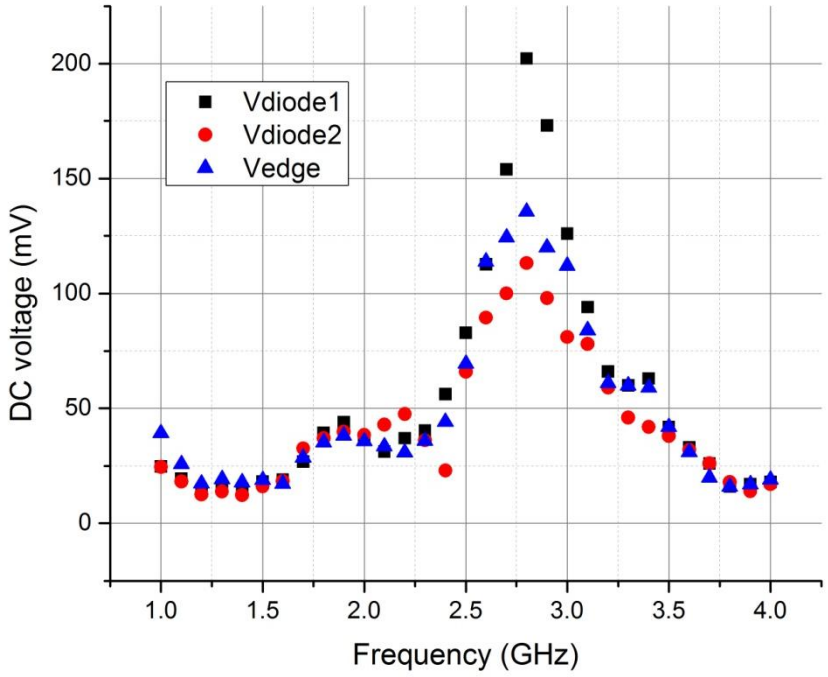

Fig. 3.32: Measured DC output voltage for three elements rectenna array

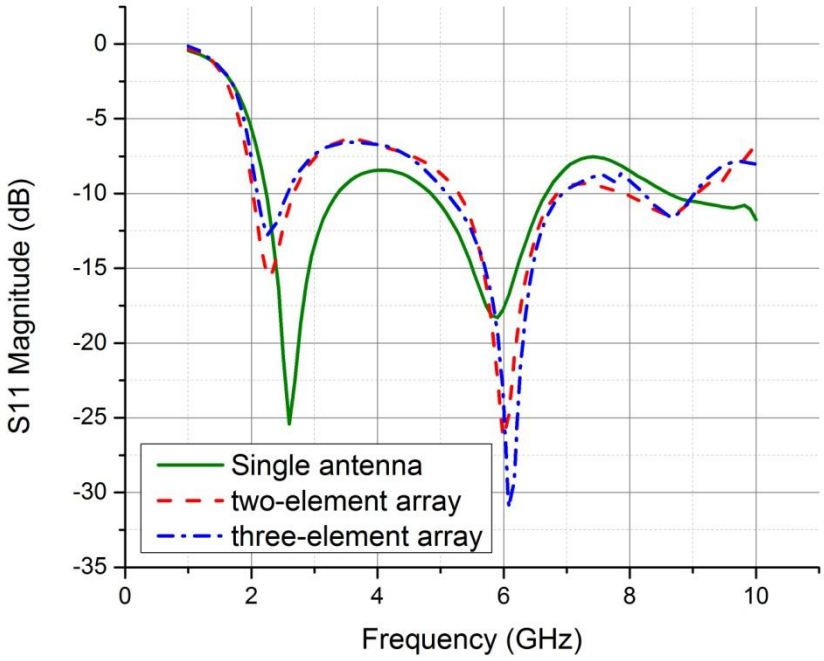

Fig. 3.33: Simulated S11 results for antenna arrays

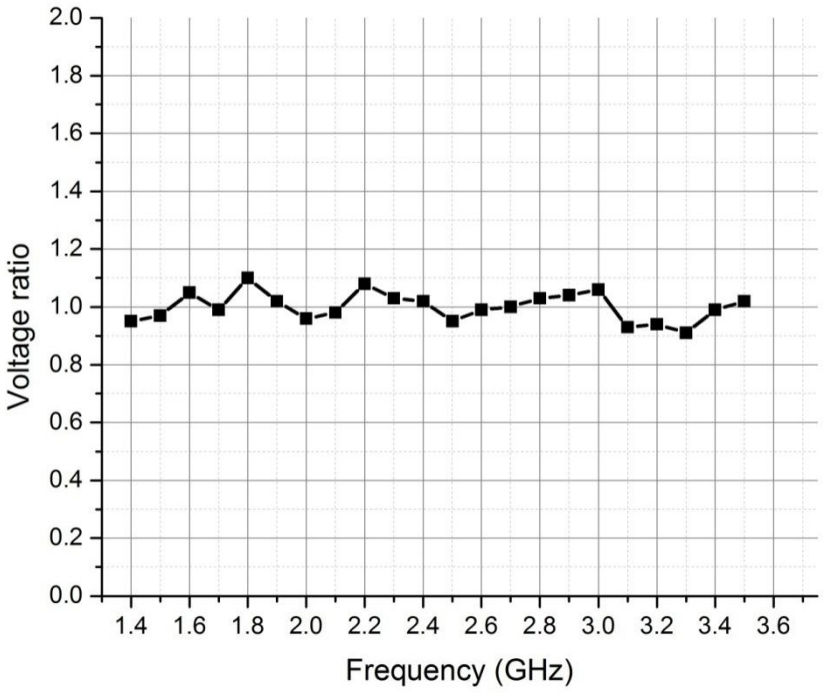

Fig. 3.34: Voltage ratio of the two element rectenna array for two orthogonal polarizations

In addition, because in the chamber measurement the linear polarised transmitting horn antenna is used as the transmitter, the electromagnetic wave generated by the horn is also linear polarised. Thus, we defined the voltage ratio of rectenna output voltage for vertical polarised power to the output voltage for horizontal polarised power.

Voltage Ratio = the rectenna output voltage for vertical polarised power / the rectenna output voltage for horizontal polarised power

The ratio is used to assess the polarisation property of the rectenna. Fig. 3.34 shows the voltage ratio of the two-element rectenna array as a function of the frequency. The voltage ratio is around 1 for the whole frequency range. It is clear that the DC output voltages for orthogonal two polarisations are almost the same because the two element rectenna is a symmetrical structure. Thus, we have demonstrated that the two-element rectenna array is indeed a dual-polarised rectenna array.

3.4 Summary

In this chapter, a broadband planar dipole antennas with an unidirectional radiation pattern which is suitable for wireless energy harvesting applications has been presented. It is clear that the feed gap, the size and the shape of dipoles would significantly affect the antenna performance. In addition, in order to obtain an unidirectional radiation pattern, the dipole is placed above a conducting ground plane. The reflector effect has also been investigated. It is shown that the input impedance of antenna is sensitive to the spacing between antenna and reflector.

Furthermore, a simple circular planar dipole rectenna and dual-polarized rectenna arrays with two and three elements based on the broadband circular dipole have been designed, fabricated and measured. The measurement of the rectenna array is shown that the design has

produced the desired DC power with reasonable efficiency. The rectenna element has achieved a maximum RF to DC conversion efficiency of 16% with a 1100 Ω load at 2.8 GHz with the power density of 0.02 mW/cm^2. Moreover, for the duel-polarized rectenna array with the cascade interconnection, it effectively combine the DC output voltage from each element. Due to the field distribution feature on the rectenna, the current design is sensitive to the position used for the measurement. However, the results have demonstrated that the more elements in the array, the higher the DC voltage (power), that is, the rectenna array concept has been realized in this simple design. Although the rectenna conversion efficiency is not very high, it is the simplest design compared with other rectenna and rectenna array designs [4, 21-23].

References

[1] Zhang Jingwei, Huang Yi, Cao Ping, and H. Chattha, "Broadband unidirectional dipole antennas for wireless applications," in *Antennas and Propagation Conference (LAPC), 2011 Loughborough*, 2011, pp. 1-4.

[2] Cao Ping, Huang Yi, Zhang Jingwei, and Lu Yang, "A comparison of planar monopole antennas for UWB applications," in *Antennas and Propagation Conference (LAPC), 2011 Loughborough*, 2011, pp. 1-4.

[3] J. A. Hagerty, F. B. Helmbrecht, W. H. McCalpin, R. Zane, and Z. B. Popovic, "Recycling ambient microwave energy with broad-band rectenna arrays," *Microwave Theory and Techniques, IEEE Transactions on,* vol. 52, pp. 1014-1024, 2004.

[4] Ren Yu-Jiun and Chang Kai, "5.8-GHz circularly polarized dual-diode rectenna and rectenna array for microwave power transmission," *Microwave Theory and Techniques, IEEE Transactions on,* vol. 54, pp. 1495-1502, 2006.

[5] Cao Ping, Huang Yi, and Zhang Jingwei, "A UWB monopole antenna for GPR application," in *Antennas and Propagation (EUCAP), 2012 6th European Conference on*, 2012, pp. 2837-2840.

[6] Cao Ping, Huang Yi, Zhang Jingwei, and R. Alrawashdeh, "A compact super wideband monopole antenna," in *Antennas and Propagation (EuCAP), 2013 7th European Conference on*, 2013, pp. 3107-3110.

[7] Wu Xuan Hui and Chen Zhi Ning, "Comparison of planar dipoles in UWB applications," *Antennas and Propagation, IEEE Transactions on,* vol. 53, pp. 1973-1983, 2005.

[8] M. Karlsson and Gong Shaofang, "Circular Dipole Antenna for Mode 1 UWB Radio With Integrated Balun Utilizing a Flex-Rigid Structure," *Antennas and Propagation, IEEE Transactions on,* vol. 57, pp. 2967-2971, 2009.

[9] S. M. Nair, V. A. Shameena, R. Dinesh, and P. Mohanan, "Compact semicircular directive dipole antenna for UWB applications," *Electronics Letters,* vol. 47, pp. 1260-1262, 2011.

[10] H. Nazli, E. Bicak, B. Turetken, and M. Sezgin, "An Improved Design of Planar Elliptical Dipole Antenna for UWB Applications," *Antennas and Wireless Propagation Letters, IEEE,* vol. 9, pp. 264-267, 2010.

[11] Low Xue Ni, Chen Zhi Ning, and T. S. P. See, "A UWB Dipole Antenna With Enhanced Impedance and Gain Performance," *Antennas and Propagation, IEEE Transactions on,* vol. 57, pp. 2959-2966, 2009.

[12] CST Microwave Stdio 2011 [Online].

[13] S. Dey, P. Venugopalan, K. A. Jose, C. K. Aanandan, P. Mohanan, and K. G. Nair, "Bandwidth enhancement by flared microstrip dipole antenna," in *Antennas and Propagation Society International Symposium, 1991. AP-S. Digest*, 1991, pp. 342-345 vol.1.

[14] H Sun, Y. Guo, M He, and Z. Zhong, "Design of a High-Efficiency 2.45-GHz Rectenna for Low-Input-Power Energy Harvesting," *Antennas and Wireless Propagation Letters, IEEE,* vol. 11, pp. 929-932, 2012.

[15] S. Barrette, S. K. Podilchak, and Y. M. M. Antar, "Ultrawideband double-sided printed dipole arrays," in *Ultra-Wideband (ICUWB), 2012 IEEE International Conference on*, 2012, pp. 232-235.

[16] J. O. McSpadden, Fan Lu, and Chang Kai, "Design and experiments of a high-conversion-efficiency 5.8-GHz rectenna," *Microwave Theory and Techniques, IEEE Transactions on*, vol. 46, pp. 2053-2060, 1998.

[17] T. W. Yoo and Chang Kai, "Theoretical and experimental development of 10 and 35 GHz rectennas," *Microwave Theory and Techniques, IEEE Transactions on*, vol. 40, pp. 1259-1266, 1992.

[18] skyworks. *Surface_Mount_Schottky_Diodes*. Available: http://www.skyworksinc.com/uploads/documents/Surface_Mount_Schottky_Diodes_200041W.pdf

[19] Y Suh and K. Chang, "A high-efficiency dual-frequency rectenna for 2.45- and 5.8-GHz wireless power transmission," *Microwave Theory and Techniques, IEEE Transactions on*, vol. 50, pp. 1784-1789, 2002.

[20] E Falkenstein, M Roberg, and Z. Popovic, "Low-Power Wireless Power Delivery," *Microwave Theory and Techniques, IEEE Transactions on*, vol. 60, pp. 2277-2286, 2012.

[21] Y. Hiramatsu, T. Yamamoto, K. Fujimori, M. Sanagi, and S. Nogi, "The design of mW-class compact size rectenna using sharp directional antenna," in *Microwave Conference, 2009. EuMC 2009. European*, 2009, pp. 1243-1246.

[22] G. Monti, L. Tarricone, and M. Spartano, "X-Band Planar Rectenna," *Antennas and Wireless Propagation Letters, IEEE,* vol. 10, pp. 1116-1119, 2011.

[23] H. Takhedmit, B. Merabet, L. Cirio, B. Allard, F. Costa, C. Vollaire, *et al.*, "A 2.45-GHz low cost and efficient rectenna," in *Antennas and Propagation (EuCAP), 2010 Proceedings of the Fourth European Conference on*, 2010, pp. 1-5.

CHAPTER 4

WIDEBAND RECTENNA FOR WIRELESS ENERFY HARVESTING

4.1 Introduction

With a rapid development of various wireless systems, there have been many wireless systems developed and installed in our cities. The radio frequency (RF) power in the environment has increased significantly. For example, we can easily receive TV, cellular radio, and Wi-Fi signals, and the RF power density has become quite considerable in many areas. How to recycle or collect these transmitted RF energies has become a subject of increasing interest, there is a need of using a wideband rectenna to recycle these RF powers.

In Chapter 3, a simple rectenna has been investigated. Lacking of a matching circuit and a full-wave rectifier, a low RF to DC conversion efficiency has been reached. In order to increase the RF to DC conversion efficiency over a wide frequency range, a new rectenna is designed. In this

chapter, we are going to study a wideband cross dipole rectenna, using both theoretical and experimental approaches. The rectenna is aimed at harvesting the RF energy in the frequency band from 1.7 to 3GHz which covers a number of the current and emerging wireless systems (Wi-Fi, Bluetooth and 2G/3G/4G cell phone systems) and covers most of the available ambient wireless RF power in urban which is reported in [1].

The double-sided dipole antenna is a famous classic printed antenna with an omni-directional radiation pattern which is first presented by E. Levine in 1988 [2]. Recently, various double-sided planar dipole antennas have been investigated to achieve broadband performance [3-8]. In this chapter, a rectenna formed by a double-sided dipole antennas and a rectifier is proposed and developed. It shows that, as we expected, rectification is obtained that the output voltage of the rectenna is proportional to the power density and the value of load resistance in the structure and conversion efficiency also significantly affected by the power density and the load resistance.

4.2 A Double-Sided Cross Dipole Antenna

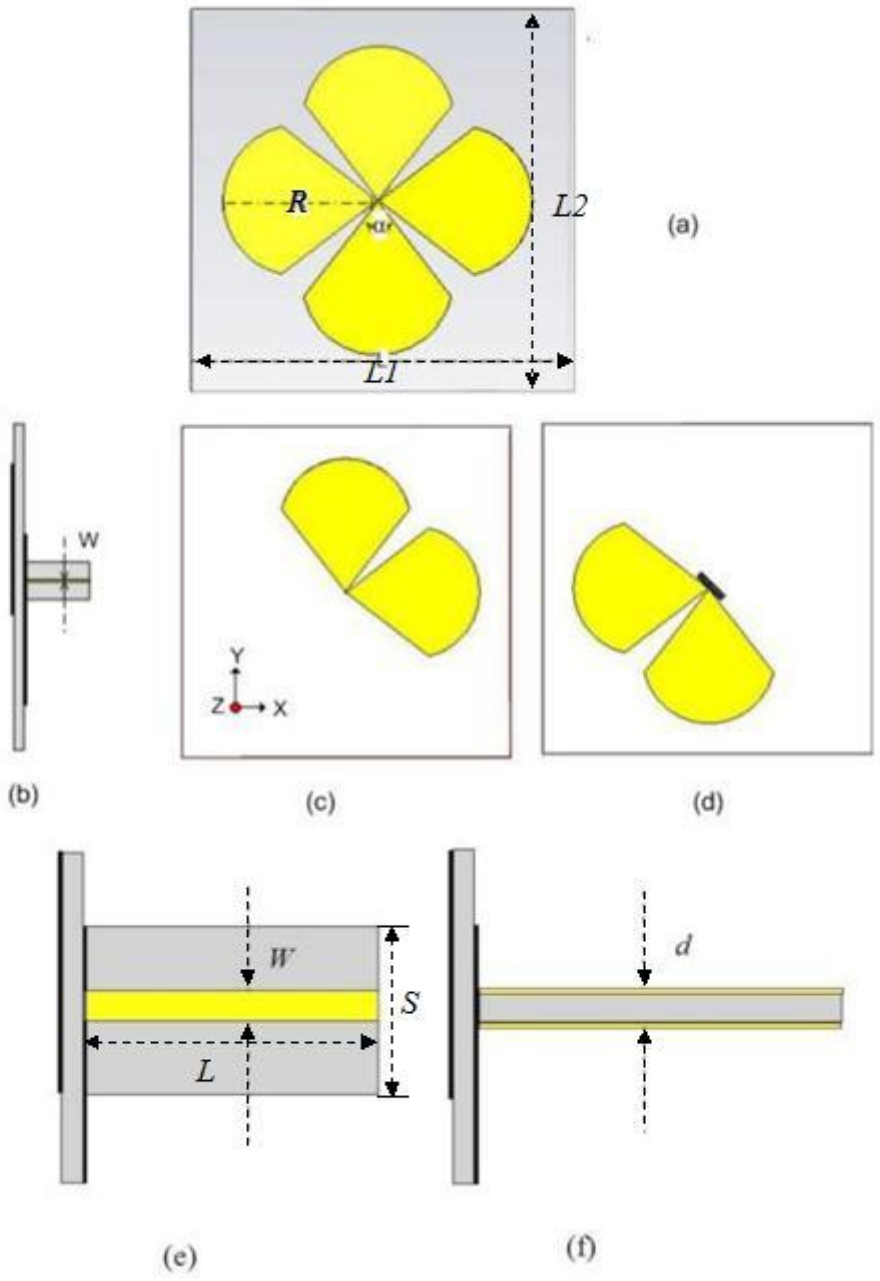

Fig. 4.1: (a) The configuration of the proposed antenna. (b) The side view of antenna structure. (c) The front view of antenna structure. (d) The back view of antenna structure. (e) The front view of parallel strip line. (f) The side view of parallel strip line.

The cross dipole antenna is chosen to be the antenna element of the rectenna. The double-sided cross dipole is better than 'traditional' dipole and there are two main reasons. The first one is that the double-sided cross dipole antenna fed by parallel strip-line not only performs a wide bandwidth but also has potential for integrating a full-wave rectifier structure. The antenna, the low-pass filter and the rectifier can directly connect through transmission line. In addition, the antenna formed by two orthogonal dipoles can achieve dual-polarisation. The layout of the cross dipole antenna presented here is illustrated in Fig. 4.1 (a).

The CST MWS simulation software [9] is used to design the antenna and the rectenna. The cross dipole antenna is designed on an Arlon Cu 217 substrate with a thickness of 0.254 mm and a dielectric constant of 2.17. The very thin substrate is used to reduce the radiation losses in the parallel line [2]. The thickness of the conductor is 0.035 mm (equivalent to 1 oz copper). The antenna is fed by a parallel strip line and formed by two orthogonal double-sided dipole antennas with a vertical feed line which can generate dual-polarisation. Fig.4.1 (b) to (e) show the side view, front view and back view of the antenna, respectively. The substrate length *L1* is 30 mm; the width of parallel strip line *W* is 0.8 mm; the angle α and the length of *R* optimised to cover the required bandwidth by the parametric study. It is important to note that the characteristic impedance Z_0 of a parallel strip line with a thickness of *d* is given by[2]

$$Z_0 = 2Z_{d/2} \qquad (4.1)$$

where $Z_{d/2}$is the characteristic impedance for a micro-strip line with a thickness of *d*/2.

The simulated S11 (reflection coefficient) frequency response of this cross dipole antenna with different dimension and various angle α are shown in Fig. 4.2 and Fig. 4.3. It is found that the angle α can affect the antenna bandwidth. When α is 75 degree the antenna can achieve the

widest bandwidth. In addition, it is obvious that due to the antenna theory the dimension of dipole can affect the centre resonance frequency. From the results, it is clear that the cross dipole antenna covers the frequency range from 1.7 to 3 GHz for S11 < -10 dB when the R = 40 and angle α= 75^{o} that matches with our application requirement.

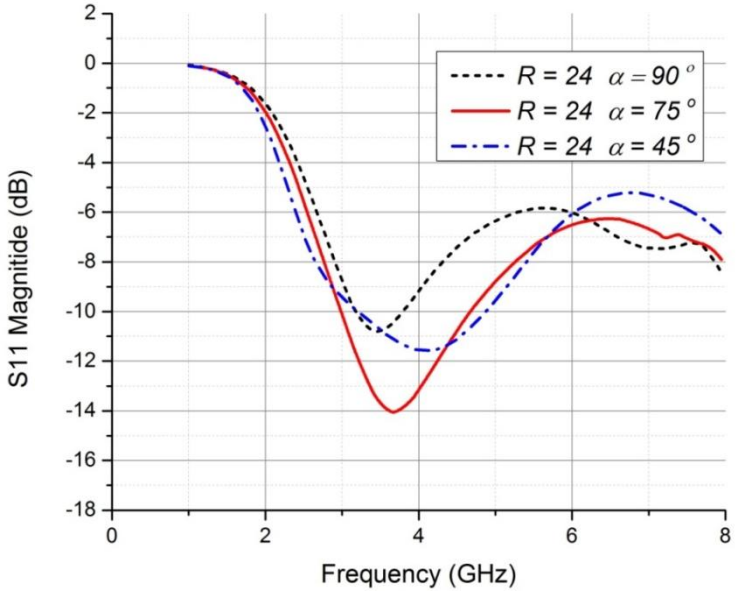

Fig. 4.2: Effect of angle α on reflection coefficient of the cross dipole antenna

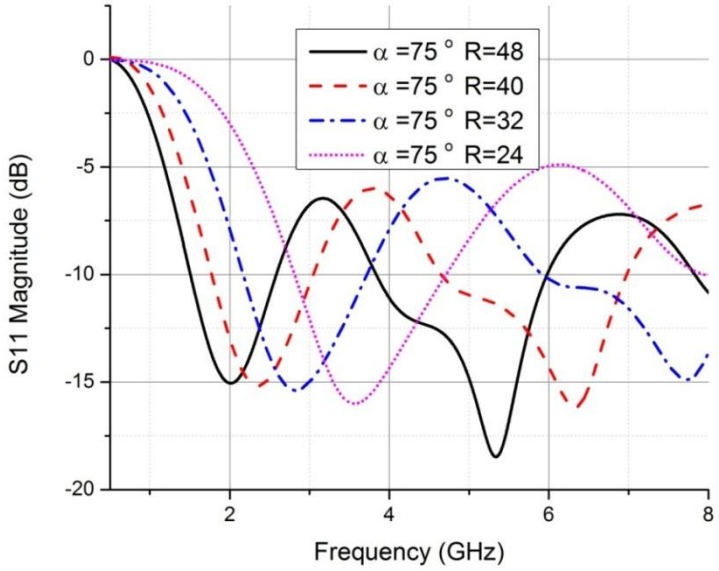

Fig. 4.3: Effect of R length on reflection coefficient of the cross dipole antenna

4.3 Low-Pass Filter Design and Antenna Integration

A major problem in wideband rectenna design is the nature of the antenna and the rectifier frequency-dependent impedance. For the maximum power transfer, the antenna impedance should match with the input impedance of the rectifier circuit over the operational frequencies. In order to increase the RF to DC conversion efficiency of the rectenna a low-pass filter is used before and after the rectifying circuit and the antenna to provide the matching between the antenna and the rectifier. In addition, the low-pass filter also can block higher order harmonics re-radiated back to the antenna.

In practice, this antenna can capture the RF energy from 1.7 to 3 GHz and transmit it into the rectifier. As the main element in a rectifier, diode generates high order harmonics when it rectifies signals due to its non-linear characteristics. Therefore, when the diode works from 1.7 to 3 GHz, the diode generates second order harmonic signals from 3.4 to 6 GHz and third order harmonic from 5.1 to 9 GHz. The antenna will reradiate the signals from 3.4 to 9 GHz which are generated by the diode. This will reduce the RF to DC conversion efficiency of the rectenna. In addition, the mismatching between the rectifying circuit and this antenna also reduces the RF to DC conversion efficiency of the rectenna. Thus, a low-pass filter is necessary to block the high order harmonics and to match the antenna with rectifiers.

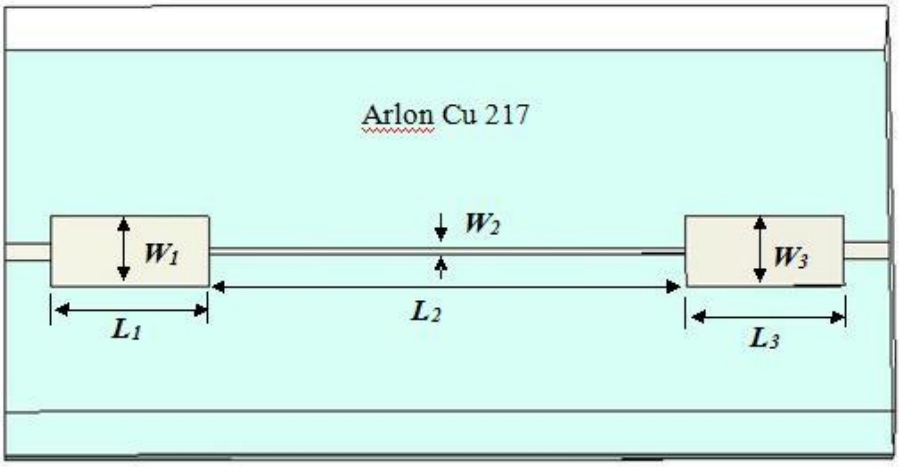

Fig. 4.4: Layout of the LPF on substrate

The next step is to design an antenna and low-pass filter (LPF) integrated structure. It cannot only cover the required frequency range but also reject the higher order harmonics which come back to the antenna and waste the power. As for the LPF, it is a step impedance third-order Butterworth filter shown in Fig. 4.4. It is optimised by using CST MWS in order to have an attenuation coefficient less than 0.1 dB from 1.7 to 3 GHz which is the operating frequency range of the proposed rectenna. The attenuation of the low-pass filter greater than 11 dB after 8 GHz. The corresponding scattering parameters calculated by means of full-wave simulation are illustrated in Fig. 4.5. The parameters of LPF are shown in Table 4.1. In this way, the LPF can block most of the higher order harmonics generated by the rectifier diode.

Before integrating the cross dipole antenna with the LPF, it is necessary to combine the antenna and the LPF. The LPF design as parallel strip line to micro-strip line tuned to match the antenna with the rectifier circuit. Fig. 4.6 shows the frequency response of the reflection coefficient of the antenna with and without the LPF. The result shows that the

reflection coefficient is achieved less than -10 dB over the frequency range from 1.57 to 3 GHz. Theoretically, the diode will generate a second order and a third order harmonics from 3.2 to 8.4. From the result, it is apparently shown that this antenna with an integrated filter structure effectively blocks the higher order harmonics from the diode. Comparing the S11 in Fig.4.6 the slight increase of the structure bandwidth may be result from the coupling between the antenna and the LPF structure. In the resonance frequency band, values of the antenna gain greater than 2.5 dB is obtained by means of full wave simulation which is shown in Fig. 4.7.

Table 4.1 parameters of LPF

$L_1=L_3$	$W_1=W_3$	L_2	W_2
3.44 mm	1.75 mm	10.4 mm	0.14 mm

.

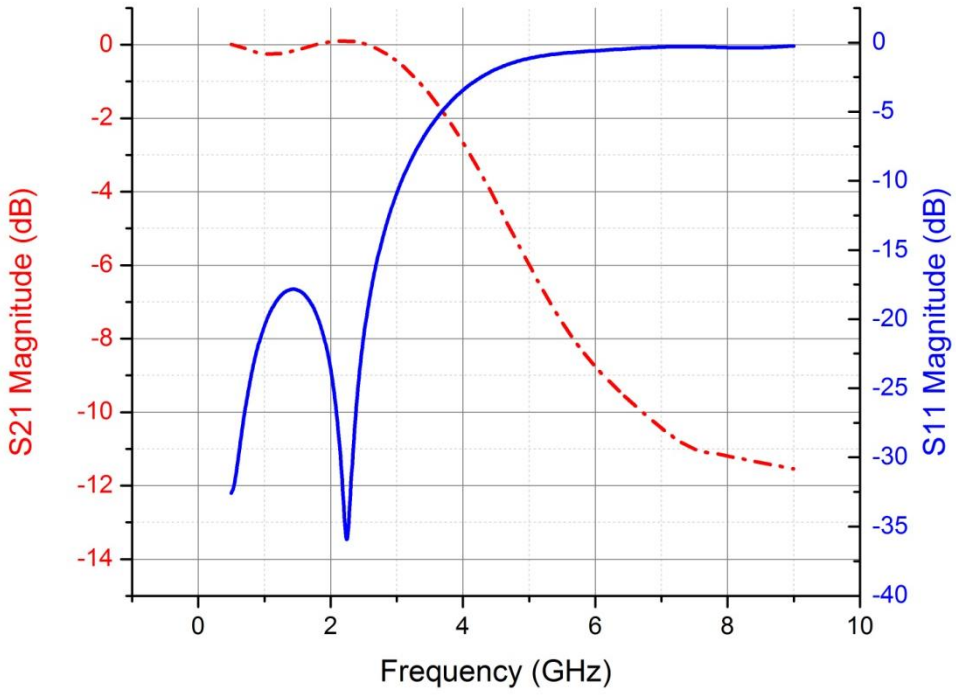

Fig. 4.5: Simulated S21 (dash line) and S11 (solid line) for LPF

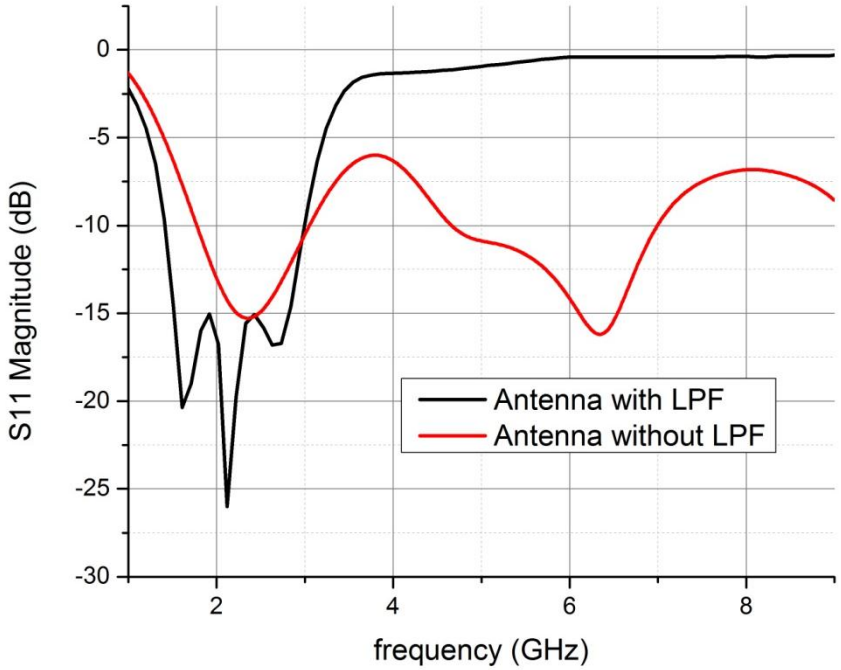

Fig. 4.6: Simulated reflection coefficient for cross dipole antenna with and without the LPF

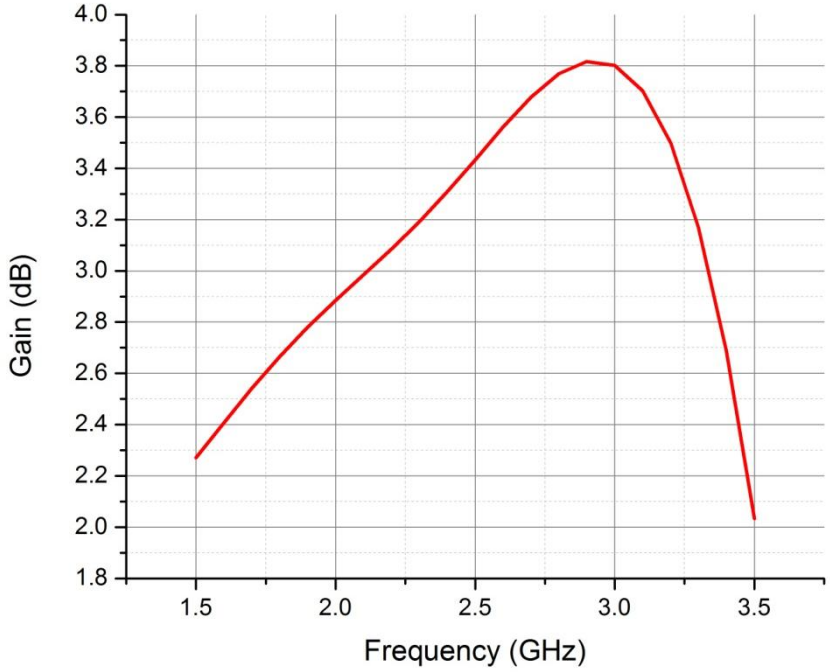

Fig. 4.7: Gain of propose antenna with the LPF

4.4 Rectifier Circuit Investigation

In order to increase DC output voltage and the conversion efficiency we use a voltage doubling circuit for rectifying and the lumped element equivalent circuit is given in Fig. 4.8. The half-wave voltage doubler circuit consists of two sections; each comprises a diode and a capacitor for rectification. It functions as follows. On the negative half cycle of the input voltage, capacitor C1 charges to a voltage. On the positive half-cycle, the input voltage, in series with the voltage of C1 charges capacitor C2 to the desired output voltage. Capacitor C1, which aides in the charging of a capacitor C2, sees alternating current ("AC Cap") while C2 sees only direct current ("DC Cap"). Thus, the voltage on output capacitor is roughly two times the peak voltage of the diode.

Due to the characteristics of the diode the input power level is one of the main factors to affect the diode conversion efficiency [10-12]. The efficiency of the diode is defined by[10]

$$\eta = \frac{P_{DC}}{P_{loss} + P_{DC}} \tag{4.2}$$

$$P_{DC} = \frac{Vout^2}{R} \tag{4.3}$$

Where P_{DC} is calculated by Equation (4.3) and R is the load resistance, P_{DC} is the dc output across R, V_{out} is the DC output voltage and P_{loss} is the loss power. In addition, the equivalent circuit of a Schottky diode is a voltage source in series a junction resistor R_j which is obtained by differentiating the diode voltage-current characteristic and it can be obtained by [13]

$$R_j = \frac{nKT}{q(I_s + I_b)} \tag{4.4}$$

Where n is the diode ideality factor, K is the Boltzmann's constant, q is the electronic charge[14], T is the temperature, $I_s$is the diode saturation current and I_b is the external bias current. At low power levels, $I_s$is very small and for a zero bias diode the external current is zero. Therefore, as presented in Equation (4.4) R_j is much higher than R, for example, R_j for the HSMS2860 diode is approximately 0.57 MΩ at 25^o. Because of the very large R_j the V_{out} across the load resistor is much decreased. As input power increases, some rectified current will result in a drop in the value of R_j, and will increase the value of $V_{out.}$

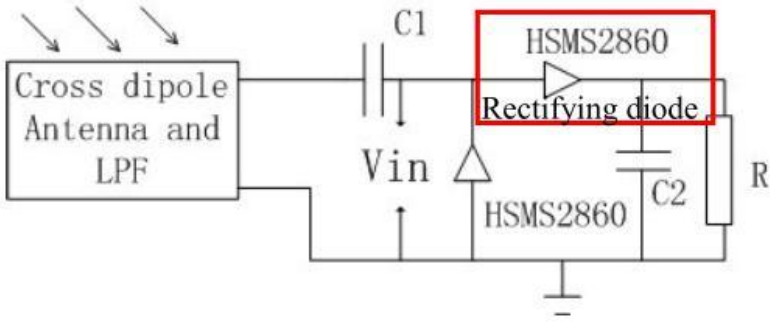

Fig. 4.8: Lumped element equivalent circuit of proposed rectifier circuit

This multiplier rectifier circuit can significantly increase V_{in} by using the first capacitor which charges at the negative half wave and discharges at the positive half wave. The voltage output is twice the input peak voltage minus twice the diode threshold voltage. In addition, the circuit can be extended to n stages, producing even higher output voltage. In this way, the circuit increases the input power level for the rectifying diode and also works as a simple full wave rectifier circuit [14]. Thus, the rectifier can solve the low conversion efficiency problem for the diode working at a low power level.

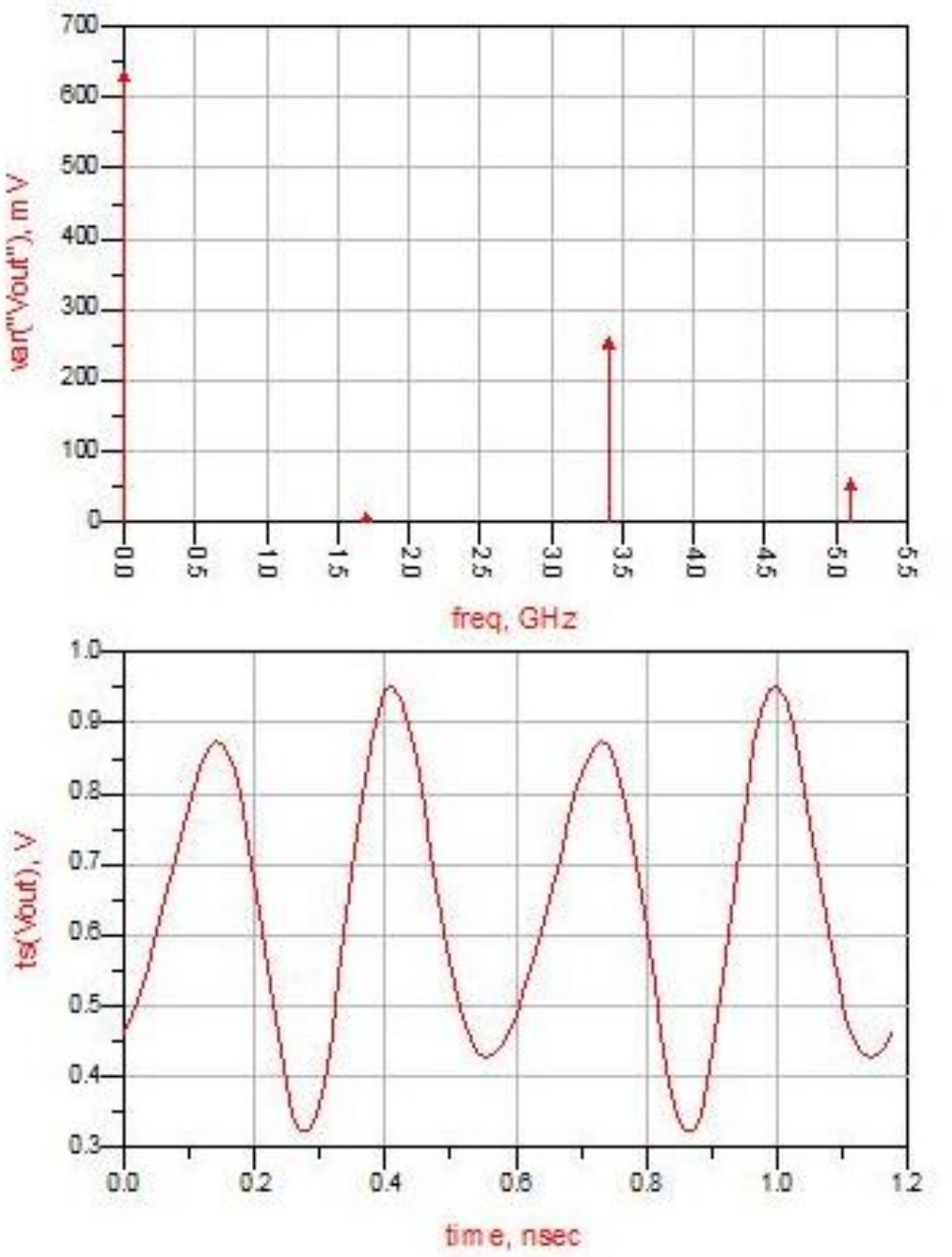

Fig. 4.9: output voltage spectrum and the output waveform of the voltage doubler rectifier

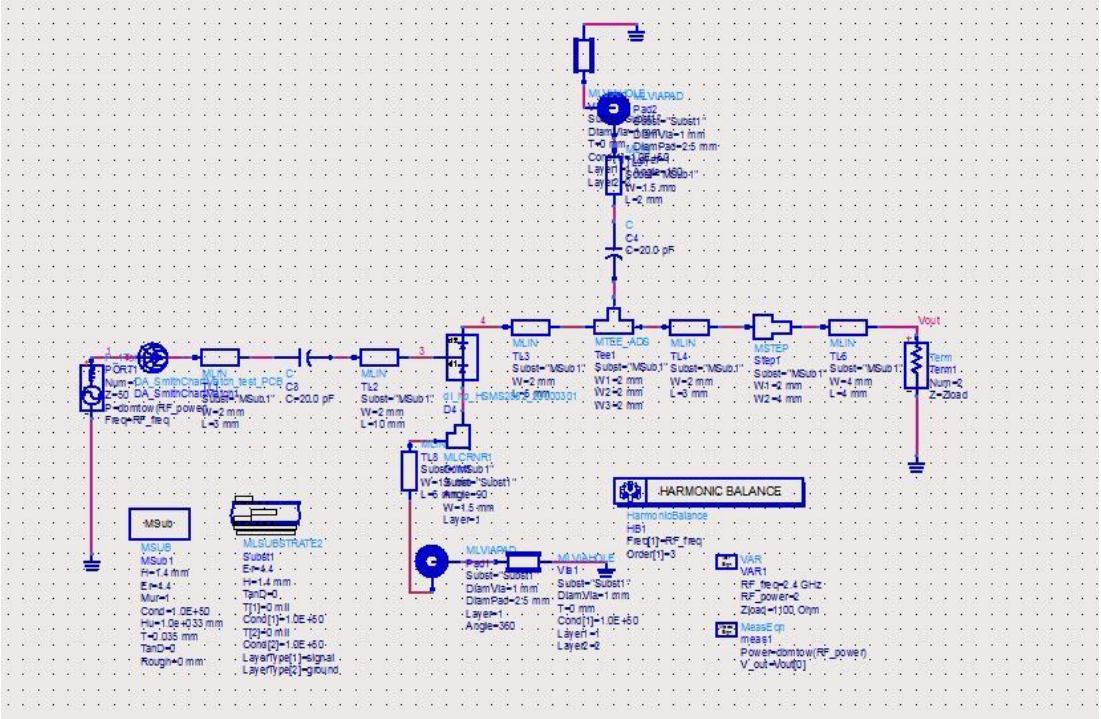

Fig. 4.10: The circuit for ADS simulation

The harmonic balance method of nonlinear circuit analysis is used to simulate and analyse the rectifier. In addition, the harmonic balance (HB) takes into account the energy at DC, the fundamental frequency and a specified number of harmonics in the circuit. The simulated waveform and spectrum are obtained using HB in Agilent ADS shown in Fig. 4.9 and the simulation circuit is plotted in Fig. 4.10. The idealised voltage doubler rectifier is matched at the fundamental frequency for optimal rectification efficiency. It is clear that the output waveform has a 0.6 V offset and the sine waveform is caused by the higher order harmonics. Indeed, the voltage on each frequency can be obtained clearly from the spectrum.

According to the working frequency range reported in data sheet, the HSMS2860 series diode is the best candidate for this application.

4.5 Wideband Cross Dipole Rectenna

Conversion efficiency of rectenna is represented as

$$\eta = \frac{P_{DC}}{P_{recieved}} \times 100\% \quad (4.5)$$

Where P_{DC} is DC power produced at the load resistance R of the rectenna and $P_{receive}$ is power received at the antenna, which can be calculated from the Friis transmission equation.

According to the relationship between RF to DC conversion efficiency and R_{load}, efficiency the η is simulated as a function of input power density with various $R_{load.}$ and results are given in Fig.4.11. It can be noticed that the maximum efficiency of 58.5% has been obtained when the load is 200 Ω at the input power density of 2.15 mW/cm^2 and the corresponding DC output voltage is 2 V. It is clear that the DC output voltage increases with the increasing of load value. However, the efficiency is calculated by using Equation (4.3) and (4.5). In Equation (4.5) the $P_{recieved}$ is a constant when the power density is constant and there is a direct proportion between η and P_{DC}. From Equation (4.3) though the V_{out} is increasing the ratio of V_{out}^2 over R_{load} reaches maximum when load is 200 Ω.

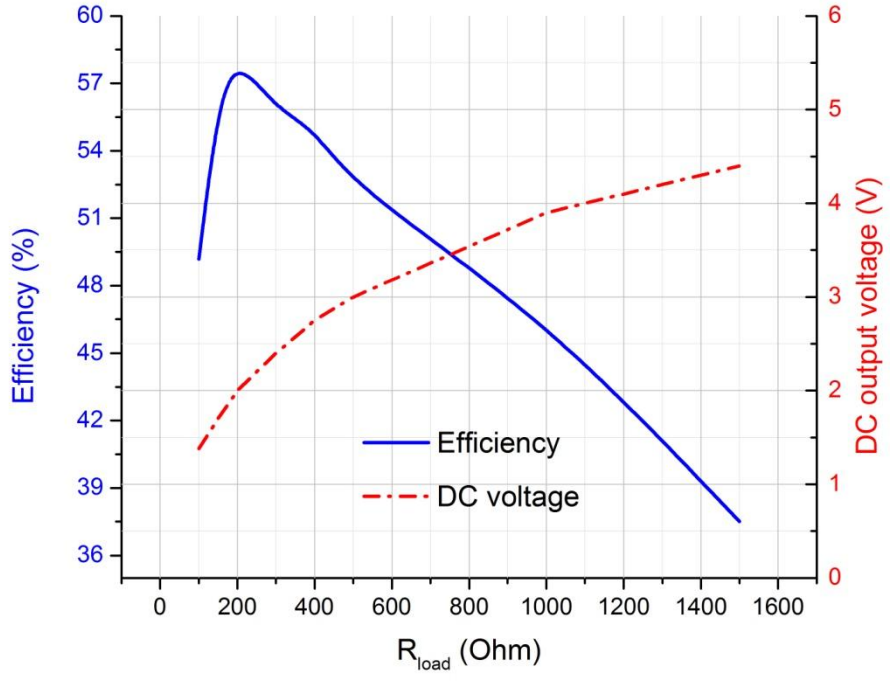

Fig. 4.11:Conversion efficiency as a function of R_{load}(solid line) and DC output voltage as a function of R_{load} (dash line) when the input power density is 2.15 mW/cm^2

The simulated value of RF to DC conversion efficiency η as function of input power density with various R_{load} is demonstrated in Fig. 4.11 It can be seen that the maximum efficiency of about 58% has been achieved when the load is 300Ω with a power density of 2.65 mW/cm^2. In addition, since the input power density level is one of the main factors affecting the diode conversion efficiency, as shown in Fig. 4.12, it is important to understand that a greater value of η is expected when the input power density increases to 7.8 mW/cm^2. According to the simulated results by using CST MWS co-simulation values of η are shapely increased with the increasing of power density. The value of η first increases with the increasing of power density from 0.663 mW/cm^2 to 7.5 mW/cm^2 and then the value drop down. The peak conversion efficiency for a 300 Ω output

load is 74.9% at the power density of 7.5mW/cm^2. The decrease of conversion efficiency is caused by the diode characteristics. With the increasing of power density level the input voltage for the rectifier circuit is increasing. However, when the input voltage is larger than the diode breakdown voltage the diode cannot work effective.

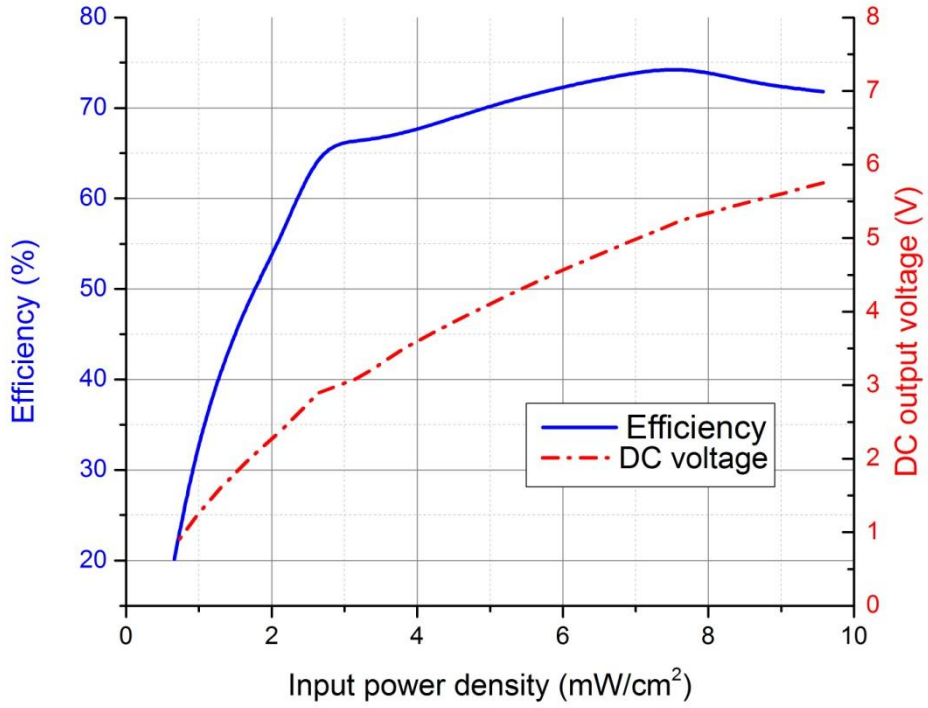

Fig. 4.12: RF to DC conversion efficiency (solid line) and DC output voltage (dashed line) for cross dipole rectenna as a function of input power density

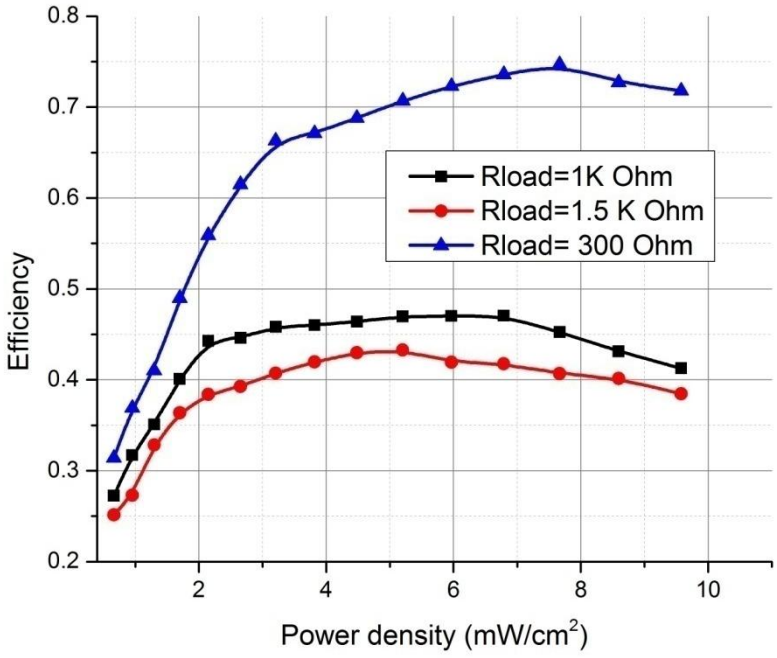

Fig. 4.13 (a): RF to DC conversion efficiency η as function of input power density with various R_{load}

The simulated value of RF to DC conversion efficiency η as a function of the input power density with various R_{load} is demonstrated in Fig. 4.13(a). It can be seen that the maximum efficiency of about 74% has been achieved when the load is 300 Ω with a power density around 7.7 mW/cm^2. In addition, the maximum conversion efficiency of rectennas with 1K Ω and 1.5 K Ω loads are 46% and 42% respectively. Moreover, Fig. 4.13(b) also presents the η and DC output voltage on the load resistance for different input power density. It is clear that with the increase of resistance value the rectenna can generate higher output voltage. It is also worth to highlight that in Fig. 4.13 the results with 300 Ω load has the highest conversion efficiency but the lowest output voltage. The reason is that with a constant input power the efficiency is related to the output power which can be calculated by V^2/R and the relationship between efficiency and output voltage for different load is shown in Fig. 4.11. Thus, the choice of resistance is a trade-off between the output

voltage and the conversion efficiency. It should be mentioned that because of the nonlinear device characteristics the input impedance of the diode is dependent on the frequency and input power density level [15]. Therefore, the antenna and LPF structure may not perfectly match the rectifier circuit and the conversion efficiency η can be affected by the losses between antenna and LPF and rectifier circuit structure.

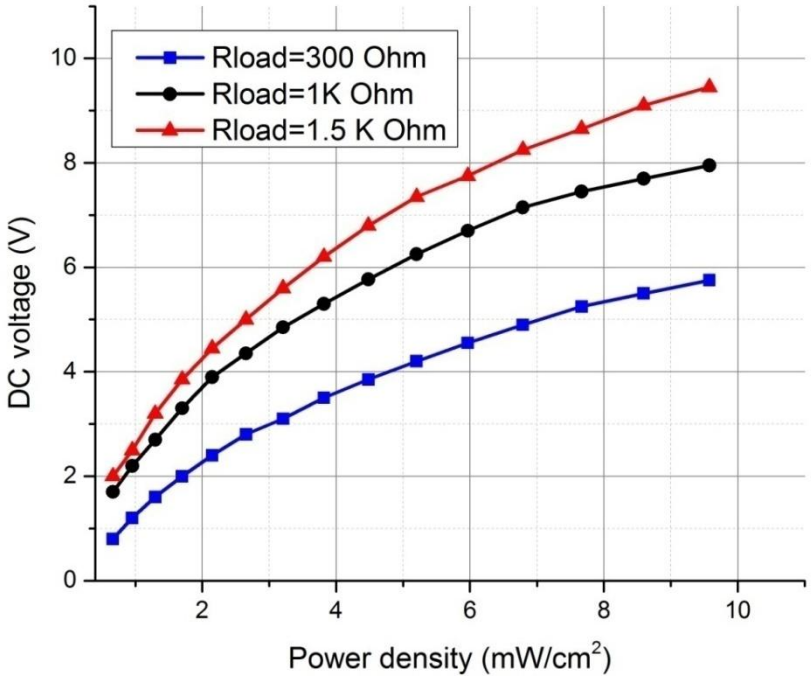

Fig. 4.13(b): Simulated output voltage of rectenna with various resistance

In addition, in practice, the ambient power density is much lower than the optimal power density 7.5 mW/cm^2. It is presented that for the distance ranging from 25 m to 100 m from a GSM base station; the power density level covers the range from 0.1 mW/cm^2 to 3 mW/cm^2. The power density level is roughly 0.01 mW/cm^2 for a WLAN system for a distance of 7 m [16, 17]. Therefore, in this circumstance, our rectenna might not be

as effective as we expect. In order to increase the rectenna conversion efficiency we need further investigation on rectifier circuits.

4.6 Wideband Cross Dipole Rectenna Implement

4.6.1 Antenna and Filter Design

The structure of rectennas is illustrated in Section 2.1. The wideband cross dipole rectenna consists of a receiving wideband dipole antenna, a step-impedance low-pass filter, a voltage doubling rectifier, a microwave block capacitor and a load resistance as we discussed in previous section. The antenna receives the transmitted microwave power at the frequency range from 1.7 GHz to 3 GHz and the input low-pass filters block the higher order harmonics from re-radiation. All microwave signals produced by the nonlinear rectifier, including fundamental and harmonics are confirmed between the low-pass filter and microwave block capacitor. Consequently, the conversion efficiency is improved.

In previous rectenna or wireless battery designs, especially narrowband rectennas, the receiving antenna is connected to the rectifying circuit through an impedance matching network [12, 18-23]. The impedance matching network, which may take the form of a transmission line and a stub, was used to match the 50 Ω antenna impedance with the rectifying circuit. However, since the input impedance for a nonlinear rectifier is a variable with different frequencies and input power levels, in a wideband rectenna design the matching network for specific impedance may not be a good match over the frequency band of interest. Thus low-pass filter is chosen in our design and act as a matching network.

All the circuit simulations including the dipole antenna and the micro-strip line low-pass filter are conducted by using CST MWS software.

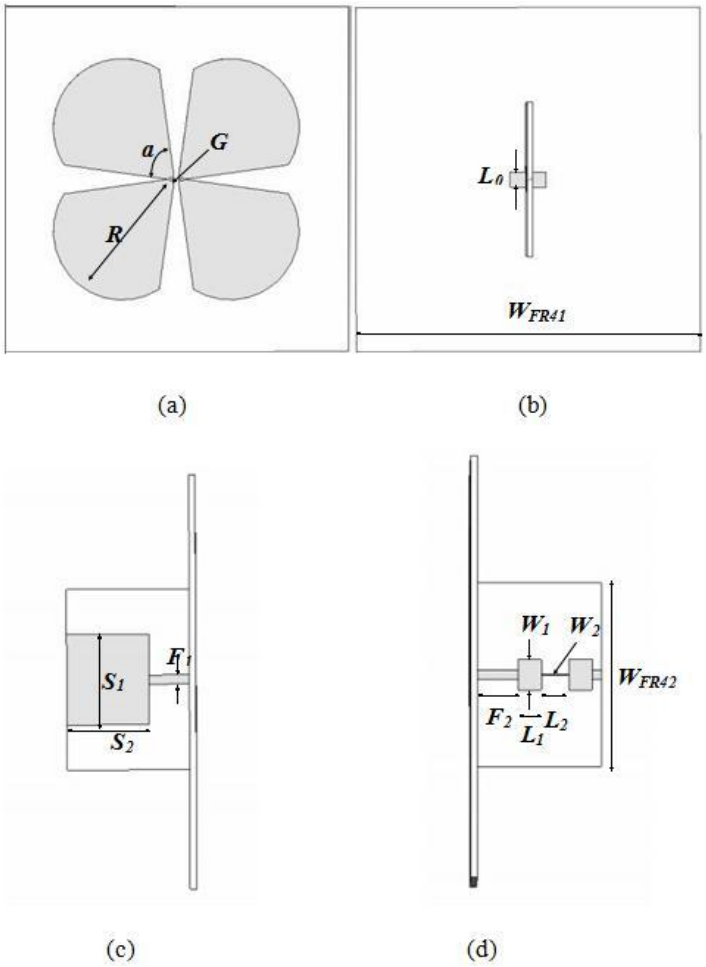

Fig. 4.14: (a) front view, (b) back view (c) and (d) side view of antenna

The configuration of cross dipole antenna with low-pass filter

The cross dipole antenna is designed for 1.7 GHz to 3 GHz is shown in Fig. 4.14. This type cross dipole antenna was introduced in previous section 4.2, the proposed antenna is built on a FR4 substrate and fed by a parallel strip line. The characteristic impedance Z_0 of a parallel strip line with a thickness of d is twice of the characteristic impedance of a micro-strip line with the thickness of $d/2$ [2]. In order to avoid the loss on thick FR4 substrate at high frequencies for a double-side structure, the new

rectenna is designed on one layer of substrate and the antenna is fed by a parallel strip line. The substrate length W_{FR41} is 10 cm; the length of dipole arm R is 40 mm, which is approximately 1/4 wavelength of center frequency , the angle α is 75^{o}, the feed gap of dipole antenna is 1.5 mm, the length parallel strip line F_2 is 10mm and the width of parallel strip line is 0.8 mm.

The measured frequency response of the antenna is shown in Fig. 4.15(a). There is a good agreement between the simulated result and the measured result. It is apparent that the reflection coefficient for this cross dipole antenna covers from 1.8 GHz to 3 GHz for S11<-10 dB, thus the design requirement is roughly met.

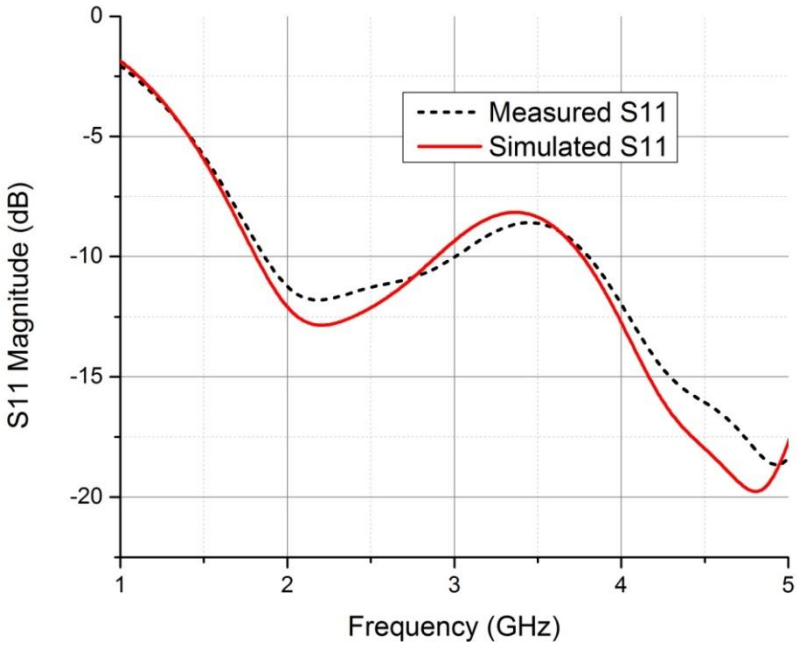

Fig. 4.15(a): Measured reflection coefficient (dashed line) and Simulated refelction coefficient (solid line) of antenna

The total surface current distribution is plotted on Fig. 4.15(b) and it is apparent that only one mode is shown on the radiators: at the resonant frequency it behaves like a traditional half wavelength dipole. There are no nulls in the whole plane and the current on the radiator moves

vertically. In addition, the current is mainly concentrated on the feed area and the external edge of antenna as expected.

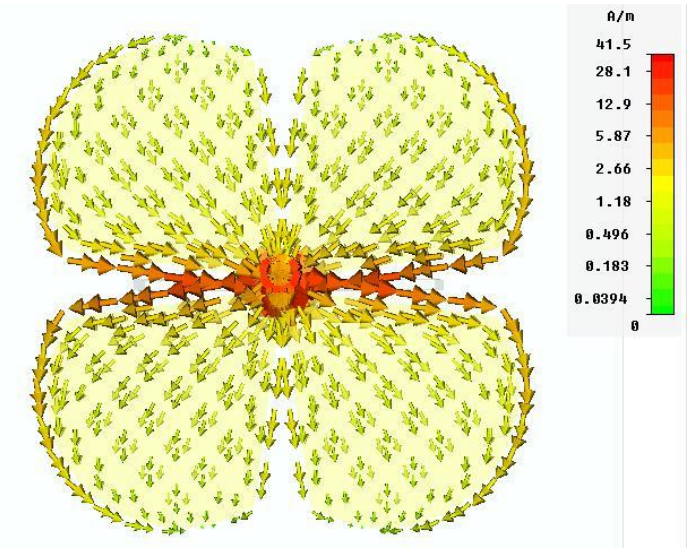

Fig. 4.15(b): The surface current distribution of the cross dipole

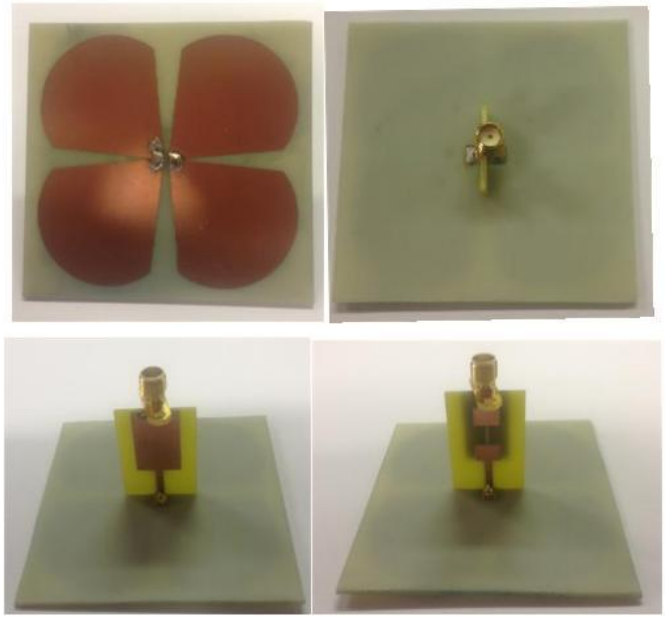

Fig. 4.16: The photographs of cross dipole antenna with the low-pass filter

Some photographs of the realised antenna with low-pass filter are given in Fig. 4.16. More in detail, Fig. 4.14 shows the parameters of this structure. The low-pass filter is then directly connected to the antenna and also acts as a matching circuit. The performance of the ALPF is optimized by using CST software package to make sure that its impedance matches with the rectifier impedance. In addition, a SMA connector is added to the end of the low-pass filter to measure the ALPF performance.

Moreover, corresponding results are shown in Fig. 4.17 and compared to full-wave simulations, a reflection coefficient lower than -8 dB has been measured over the frequency range from 1.7 GHz to 2.5 GHz. The discrepancy may be caused by the inaccuracy of the fabrication and the effects of the connector and cables involved.

The band rejections at the second and the third (3.4GHz to 7.5 GHz) harmonics of the fundamental frequency are larger than -3 dB which shows good low-pass performance for these harmonics. In the same frequency band, the antenna gain greater than 2 dBi has been calculated by means of simulations and the some results are depicted in Fig. 4.18(a). For the antenna with a low-pass filter, the simulated input impedance of the proposed layout is plotted in Fig. 4.18(b). This antenna with a low-pass filter should guarantee a good level of matching with the rectifier over the operation bandwidth and mismatching at second and third harmonics. The 3D simulated radiation pattern is also plotted in Fig. 4.18(c) and the result shows that the proposed antenna with an integrated LPF structure performs an omni-directional radiation pattern and broad beam-width. Thus, the proposed structure is insensitive to the direction.

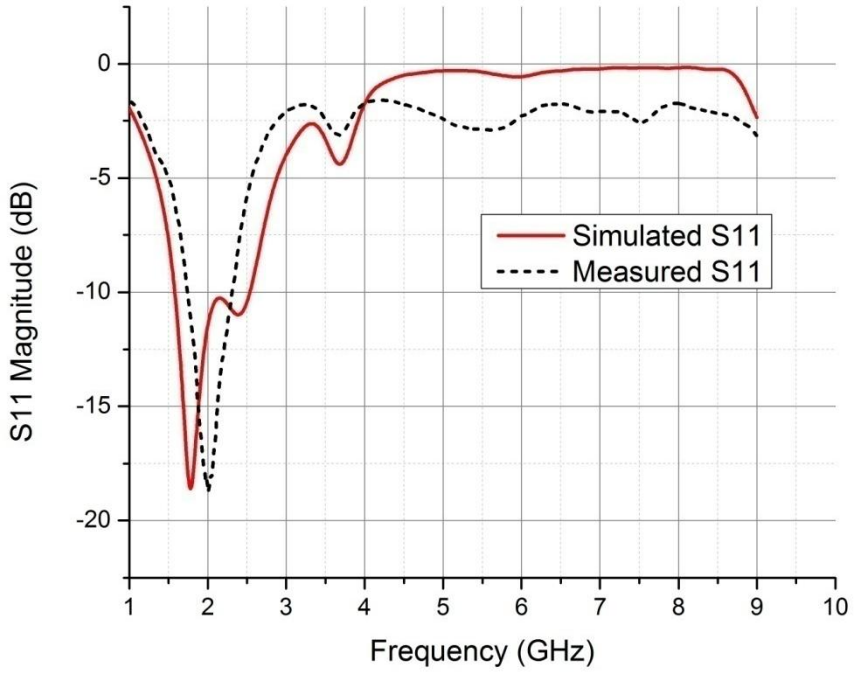

Fig. 4.17: Measured (dashed line) and simulated (solid line) S11 results

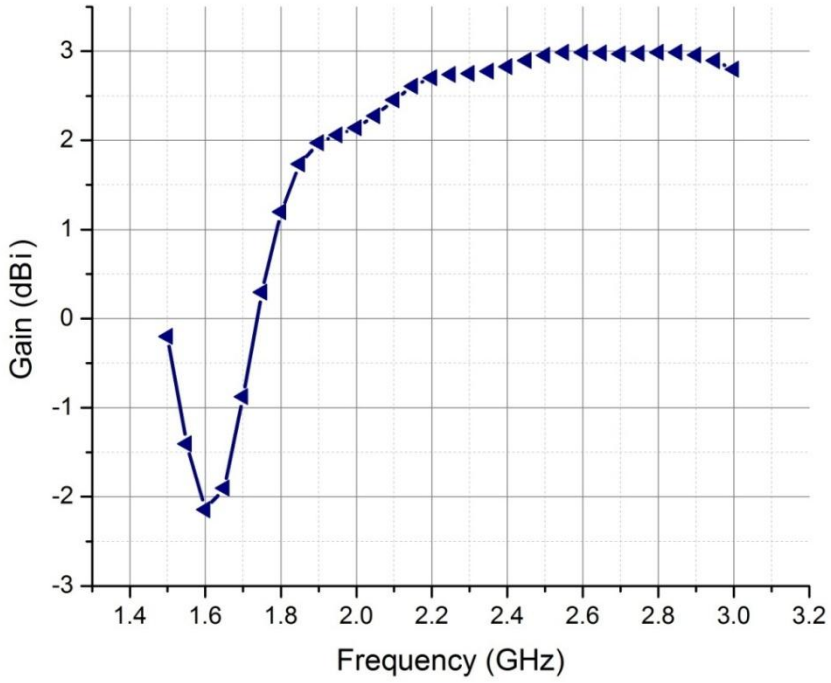

Fig. 4.18 (a): Gain of the proposed antenna with the low-pass filter

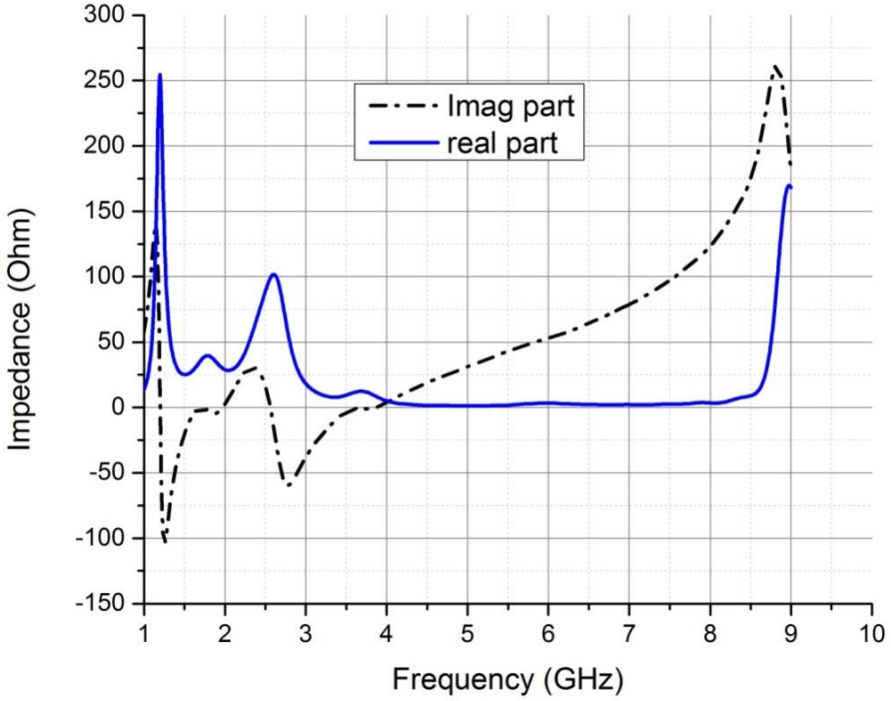

Fig. 4.18 (b): Input impedance of the proposed antenna with the low-pass filter

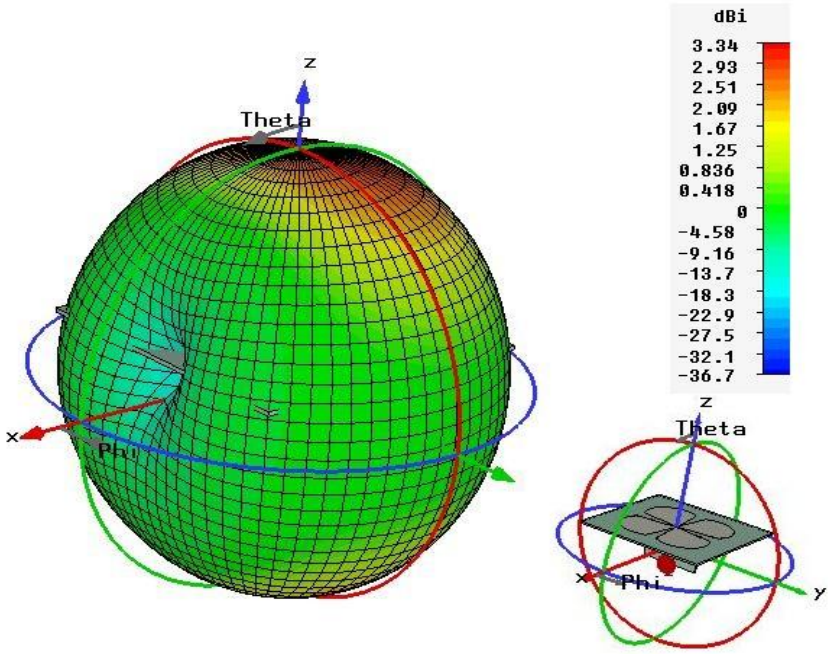

Fig. 4.18 (c): The 3D radiation pattern of the proposed antenna with the low-pass filter at 2.4 GHz

4.6.2 Input Impedance of the Rectifying Circuit

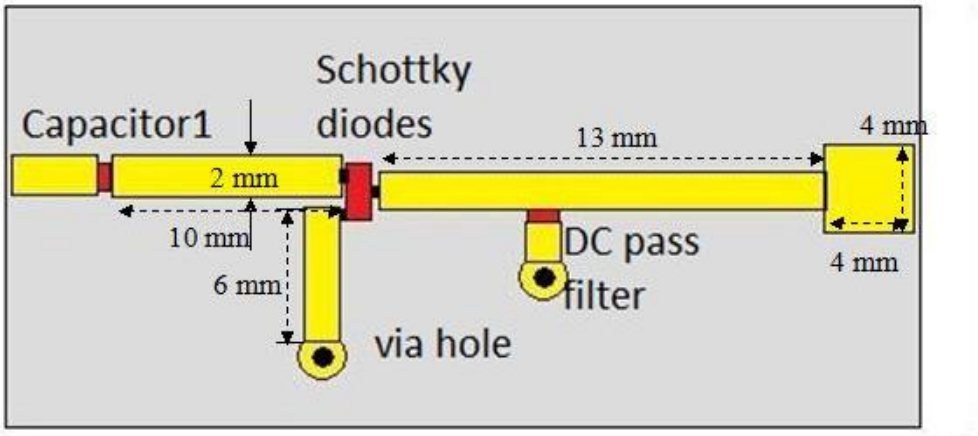

(a) Layout of the proposed rectifier

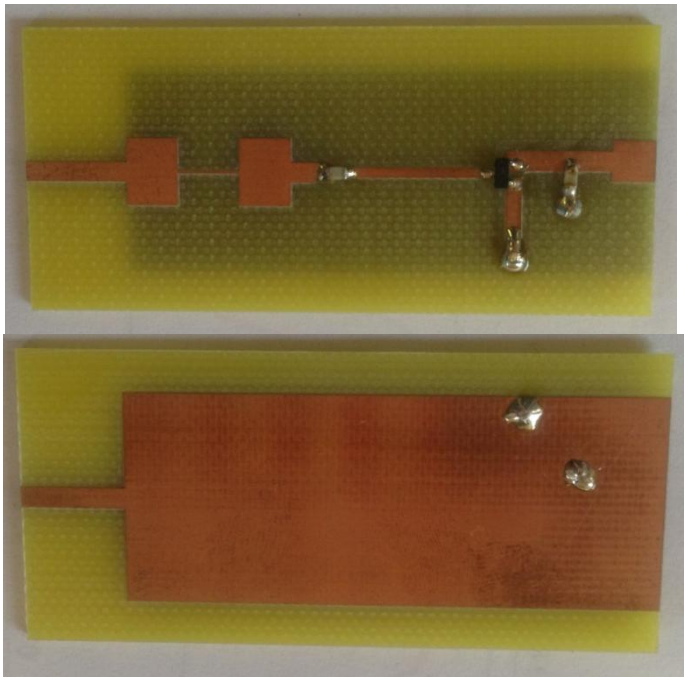

(b) Photographs of the low-pass filter and the rectifier

Fig. 4.19: The configuration of the rectifier

The next step in the design procedure is validation of the integrated rectenna which cinsists a rectifying circuit, a DC pass filter and a resistive

load. The Schottky HSMS 2852 diode is chosen because it has a low built-in voltage with a fast switching response and high cutoff frequency. Components in the rectifying circuit are connected by a micro-strip transmission line as shown in Fig. 4.19. To reduce the size of the rectifier, a capacitor is parallelly connected to the circuit to act as a DC pass filter.

Because of the characteristic of the diode, the input impedance of the rectifying circuit is affected by the frequency, input power level and the output load. The RF to DC conversion efficiency for the rectifying circuit as a function of output load at input power = 6 dBm is shown in Fig. 4.21 at 1.7 GHz, 2.0 GHz and 2.4 GHz, respectively. It is interesting to note that the conversion efficiency reaches the maximum value of 61% when the load is around 1000 Ω at 2.0 and 2.4 GHz. When the output load is 1300 Ω the conversion efficiency has the peak value of 61% at 1.7 GHz. Fig. 4.22 shows the RF to DC conversion efficiency for a rectifying circuit as a function of output load with various input power level at 2.4 GHz. It is obvious that the trend is the same for different power levels and the efficiencies increase with the input power. In order to achieve the highest RF to DC conversion efficiency over the frequency range from 1.7 to 2.5 GHz, the optimum output load is 1100 Ω when the power is around 6 dBm.

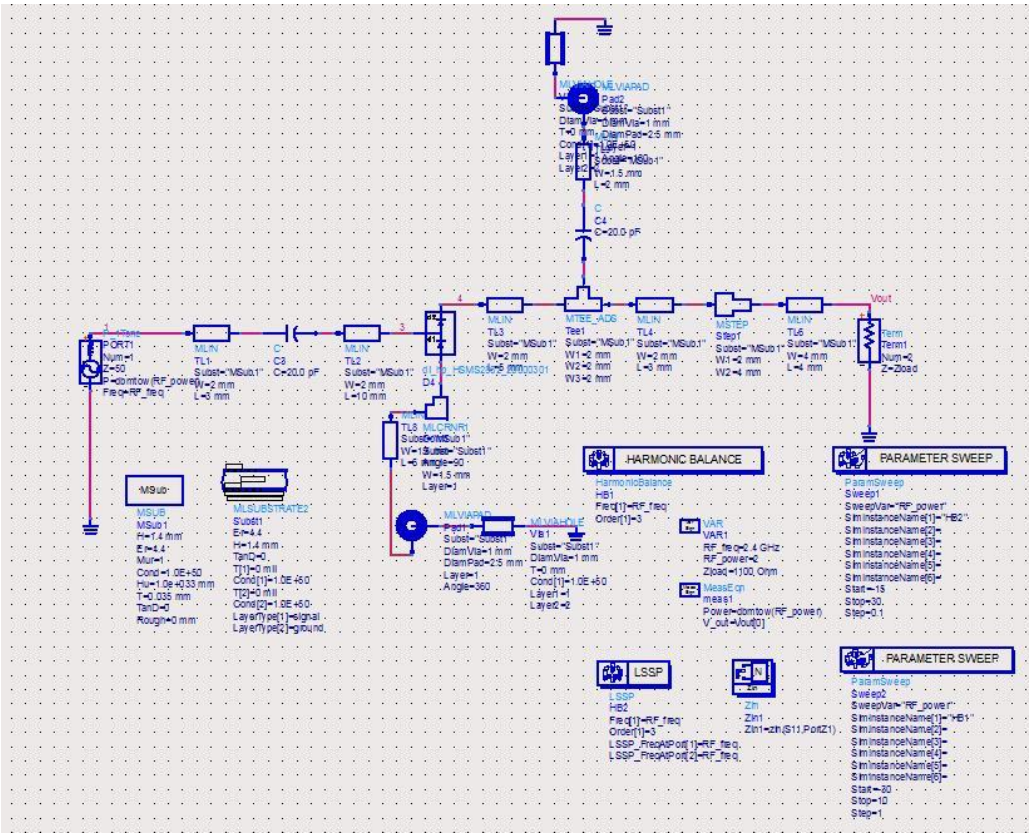

Fig. 4.20: the circuit for ADS simulation

The input impedance of the rectifying circuit as a function of the output load is shown in Fig. 4.23(a). It is obvious that the real part of the input impedance decreases with the increase of the load value but the imaginary part is almost the stable with the increase of the output load resistance.

The input impedance of the rectifying circuit as a function of the input power level is shown in Fig. 4.23(b). It is obvious that in the lower input power level (-15 to 10 dBm), the imaginary part approximately is relatively stable with the increase of the input power while the real part is slightly increased with the input power. In order to match the antenna with a low-pass filter to the rectifying circuit, the performance of the antenna

with a low-pass filter is adjusted based on the input impedance of the rectifier.

The value and the positions of the capacitor and resistor are adjusted to optimize the impedance of the rectifying circuit to directly match the antenna with a low-pass filter. The optimum capacitor is 20 pF.

The next step is to add the DC collection line, without disturbing the fundamental frequency impedance match. The DC line which consists of a micro-strip section and shunt surface mount capacitor act as DC pass filters. The shunt capacitor presents a short circuit which is transformed through the quarter wavelength transformer and presents an open circuit at the fundamental frequency to the diode plane. While not affecting the rectifier impedance, the quarter-wave transformer provides a DC path to the DC load. This configuration is dependent on a combination of a lumped element and distributed circuitry, and is very repeatable in fabrication. The combination of distributed and lumped elements gives a reasonable size circuit which is simple to assemble.

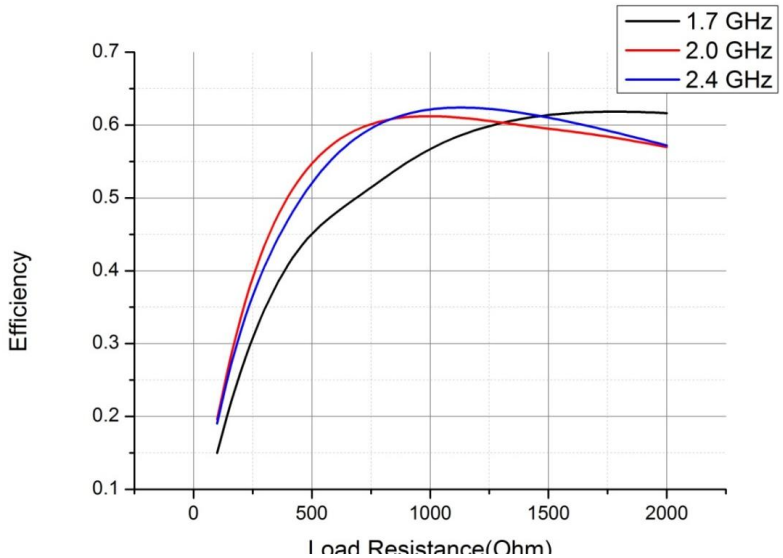

Fig. 4.21: The RF to DC conversion efficiency for the rectifying circuit as a function of the output load resistance.

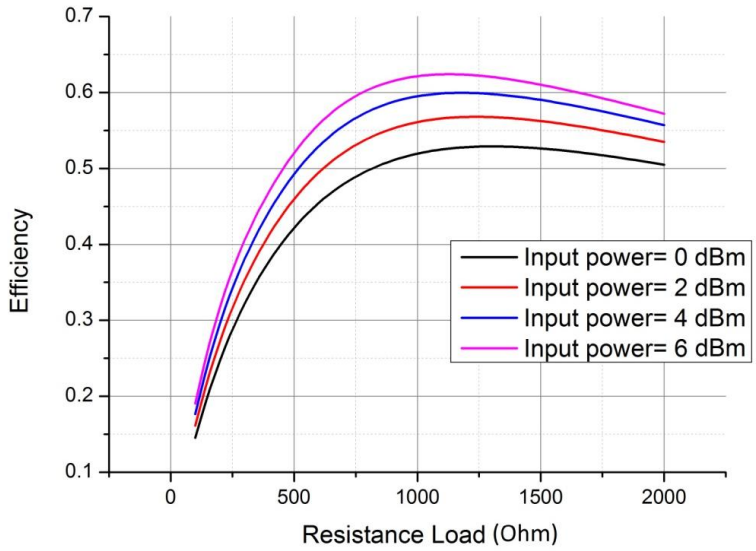

Fig. 4.22: The RF to DC conversion efficiency of the rectifying circuit as a function of output load with different input power at 2.4 GHz

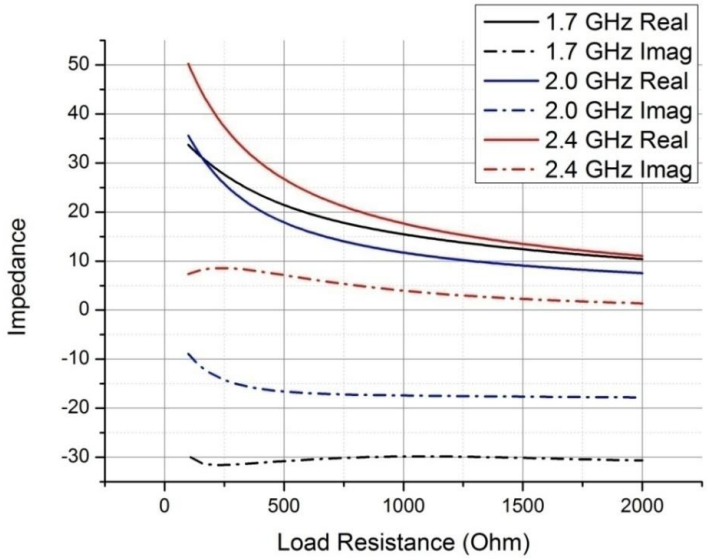

Fig. 4.23(a) Input impedance of rectifying circuit as a function of output load

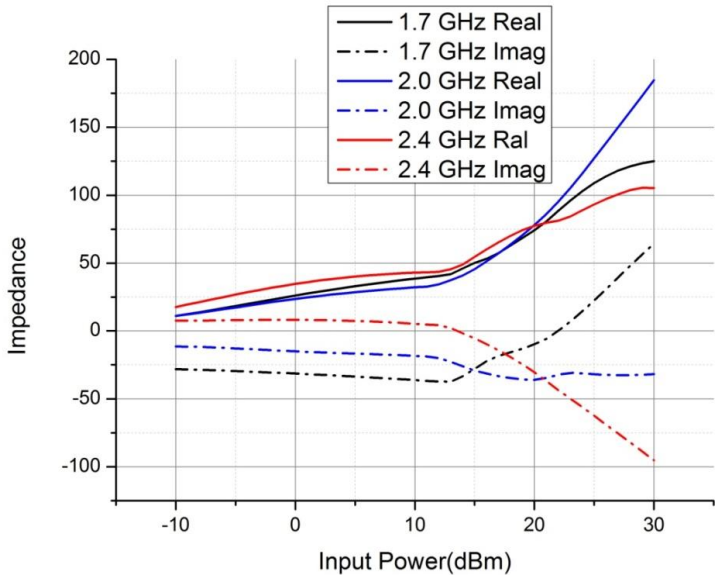

Fig. 4.23(b): Input impedance of proposed rectifying circuit as a function of the input power

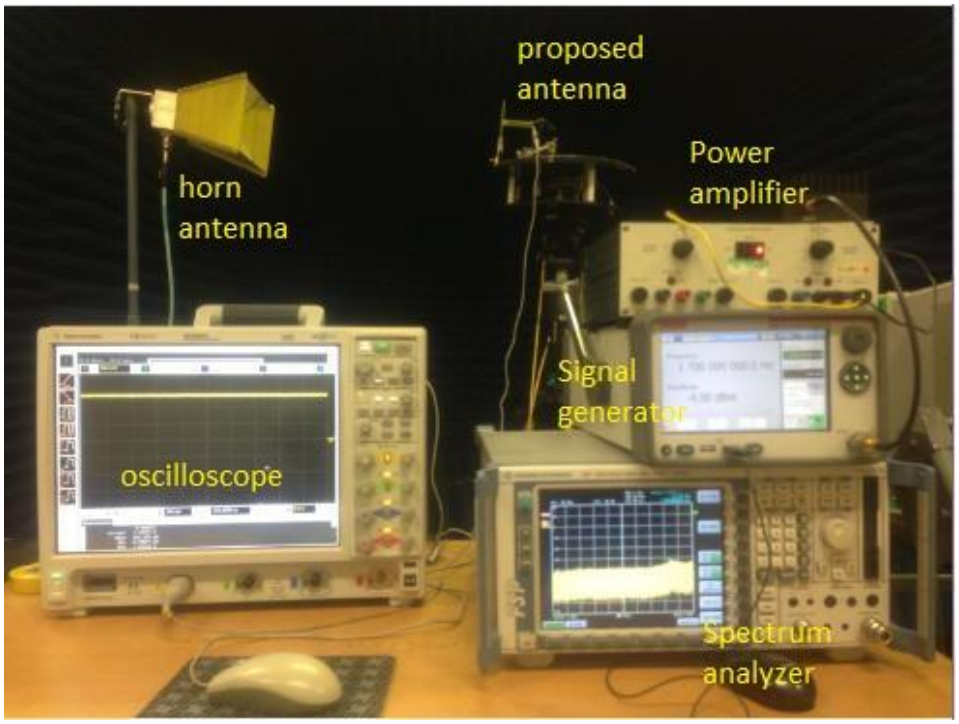

(a) The measurement system in anechoic chamber.

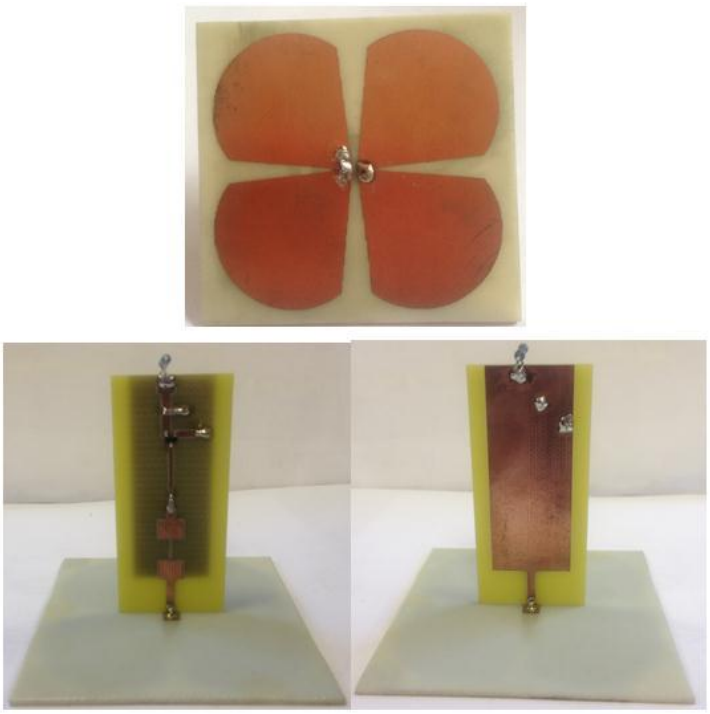

(b) the photographs of proposed rectenna under test

Fig. 4.24: The measurement set-up and photographs of the rectenna under test

4.6.3 Simulation and Experimental Results of A Wideband Cross Dipole Rectenna

The rectenna is tested in an anechoic chamber. The measurement set-up for the rectenna performance is as shown in Fig. 4.24 (a) and rectenna under test is shown in Fig. 4.24 (b). The source is a signal generator connected a 30 dB gain power amplifier, allowing far field measurements to be performed for a range of incident power density in the integrated rectenna at normal incidence. The transmitter antenna is a standard horn antenna (Gain = 8.5 dBi) and the output DC is measured by the oscilloscope. For this measurement the cables and the amplifier that are in the path between the signal generator and the transmission horn were calibrated from 13dBm to 29dBm output power. The generator output

power, corrected by the calibration result by using the spectrum analyser, was then used to calculate the incident power of the rectenna. The conversion efficiency can be obtained using

$$\eta = \frac{V_{dc}^2}{R_L} \times \frac{1}{P_{RF}} \tag{4.6}$$

In the simulation, the input impedance of the antenna with a low-pass filter was imported to ADS for the simulation of the RF to DC conversion efficiency. The simulated conversion efficiency as a function of the input power density is shown in Fig. 4.25. The efficiency obtained using Equation (4.6) gives simulated values for the wideband cross dipole rectenna between 40%- 54% for power densities of 0.02 to 0.6mW/cm^2 at 1.7 GHz as shown in black in Fig 4.25. The conversion efficiency is 40% to 64% for the same power density range at 2.0 GHz. At 2.4 GHz the conversion efficiency is between 23%- 49%. Comparing to the results obtained from 1.7 GHz to 2.4 GHz with the same simulated method. The big different is due to the mismatch between antenna and low-pass filter structure with the rectifying circuit. Since in our design the antenna is self-matching with the rectifying circuit, at 1.7 and 2.0 GHz the antenna has relatively good matching with the rectifying circuit but at 2.4 GHz there is a little bit mismatch between antenna and rectifying circuit which effectively reduce the RF to DC conversion efficiency. In addition, it is important to note that theoretically the conversion efficiency should be increase with the increasing of input power density but in the practice the RF to DC conversion efficiency decreased with higher input power density result from the significantly changes in the input impedance of rectifying circuit at higher power level shown in Fig.4.23 leading the mismatch between the antenna with rectifying circuit.

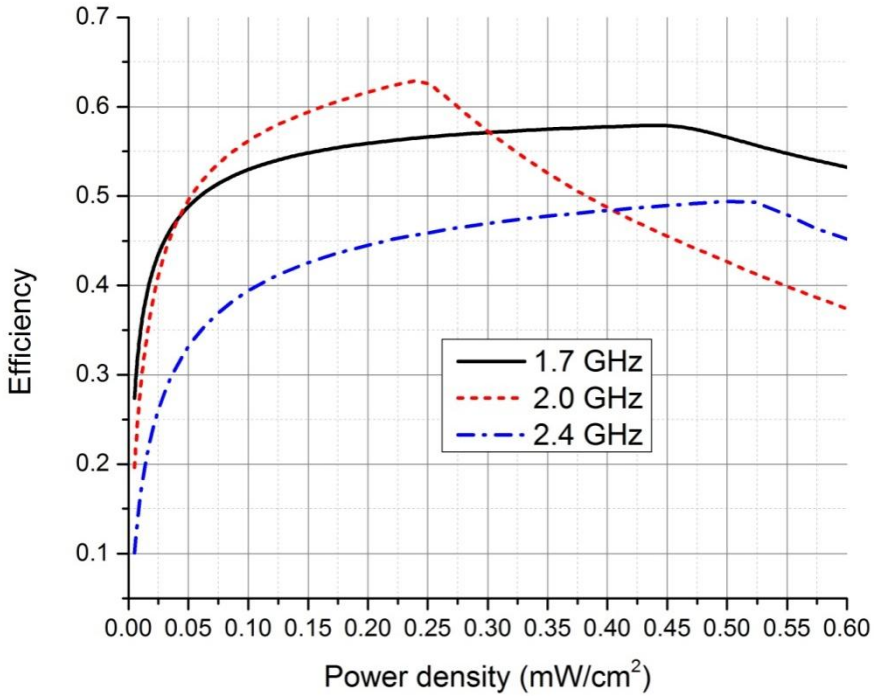

Fig. 4.25: Simulated RF to DC conversion efficiency of the proposed rectenna as a function of the power density

Measured results of the wideband (from 1.7 to 2.5 GHz) integrated cross dipole rectenna are presented in Fig. 4.26. It is clear that the cross dipole rectenna has the conversion efficiency from 28% to 57% with incident power densities varying 5 μW/cm^2 to 0.2 mW/cm^2 at 1.7 GHz. In the same power density range the conversion efficiency changes from 16% to 40% and 5% to 24% at 2.0 and 2.4 GHz, respectively. Because of the equipment limitation, the maximum power density achieved in the measurement was 0.2 mW/cm^2. The measured efficiency was lower than our expectation might be caused by the inaccuracy of the fabrication, the connector and the material (FR4) losses on the rectifier at higher frequencies

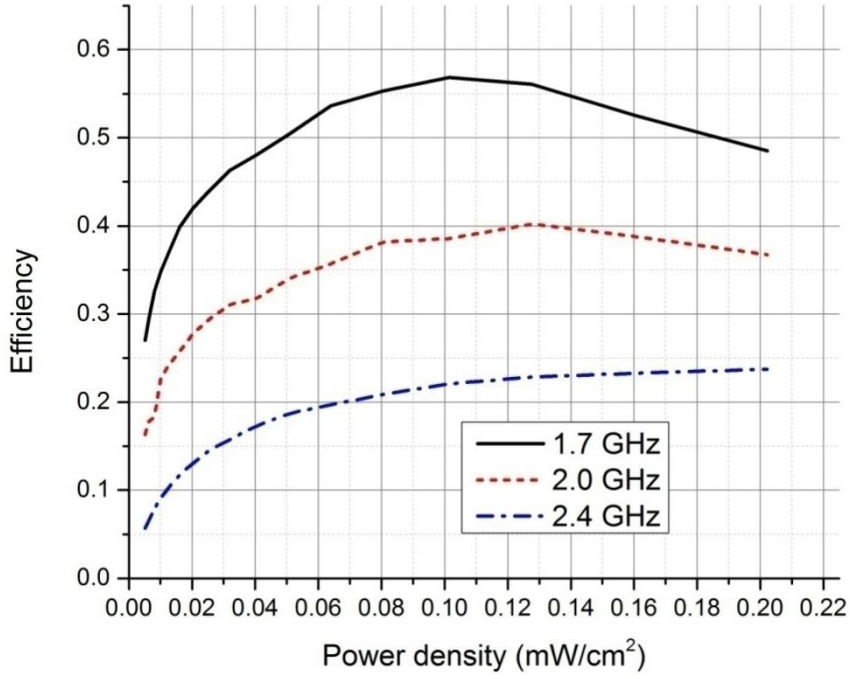

Fig. 4.26: Measured RF to DC conversion efficiency as a function of power density at 1.7, 2.0 and 2.4 GHz respectively.

In the simulation, the conversion efficiency of rectenna at 2.0 GHz is higher than that of at 1.7 GHz but in the measurement, the conversion efficiency of rectenna at 1.7 GHz is higher than that of at 2.0 GHz. It is because the input impedance of the antenna used in the simulation is the simulated results but the in practice; input impedance of the antenna may change a bit due to the fabrication errors. The change of input impedance leads the rectenna at 1.7 GHz reaching better matching than the rectenna at 2.0 GHz.

The measured conversion efficiency and output voltage of the rectenna for different input power density and frequency are depicted in Figs. 4.27 and 4.28. The optimum operating frequency range for the wideband cross dipole is found to be 1.7 to 2.5 GHz at a power density

range from 15 to 200 μW/cm^2. It is seen that the maximum conversion efficiency of 57% is achieved around 0.12 mW/cm^2 at 1.7 GHz. Over a higher frequency range (2.3 GHz- 2.8 GHz) conversion efficiencies decrease due to the material losses on the rectifier and a mismatch between the antenna and the rectifier caused by fabrication error. In addition, from 1.7 to 2.5 GHz the conversion efficiency of the rectenna is stay above 25%. Comparing with other wideband rectennas the proposed rectenna has relatively good conversion efficiency at wideband range. The Fig. 12 delivers the measured DC output voltage of the rectenna as a function of frequency and power density. The output voltage stays above 720 mW over the range of power densities of 15 to 200 μW/cm^2. In addition, as expected, the output voltage increases with the power density. The RF to DC conversion efficiency surface takes a very different shape than the DC output power surface shape. It is shown that small output power deviations translate to large changes in the efficiency since the rectenna conversion efficiency is very sensitive to the output voltage. Indeed, from the Equation (4.6), for the constant P_{RF} and R_L the conversion efficiency is directly proportional to the $V_{dc}{}^2$. Thus small changes of the voltage V_{dc} can be much affected the conversion efficiency.

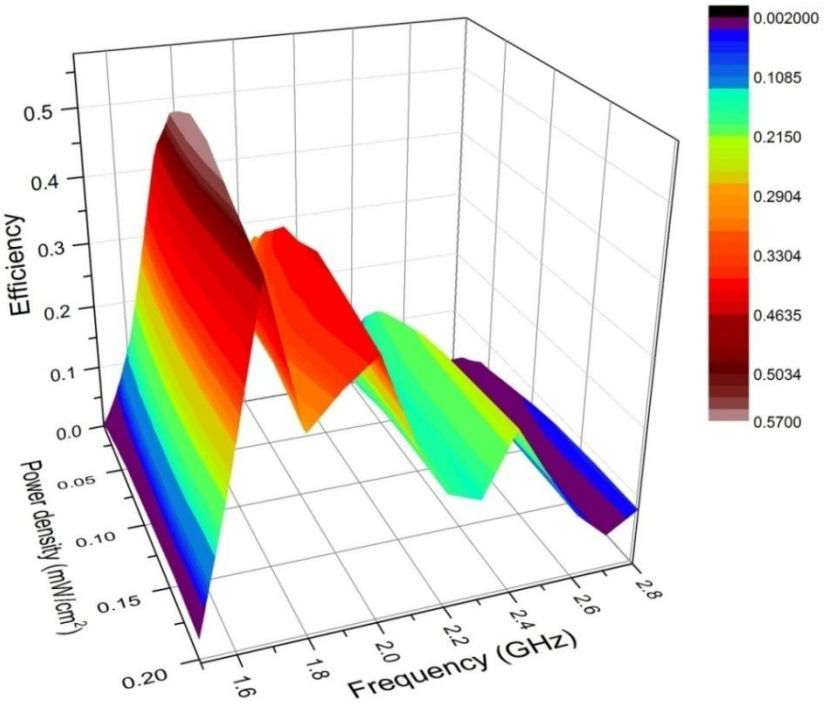

Fig. 4.27: Measured RF to DC conversion efficiency for wideband rectenna at broadside for power densities 15 to 200 μW/cm^2

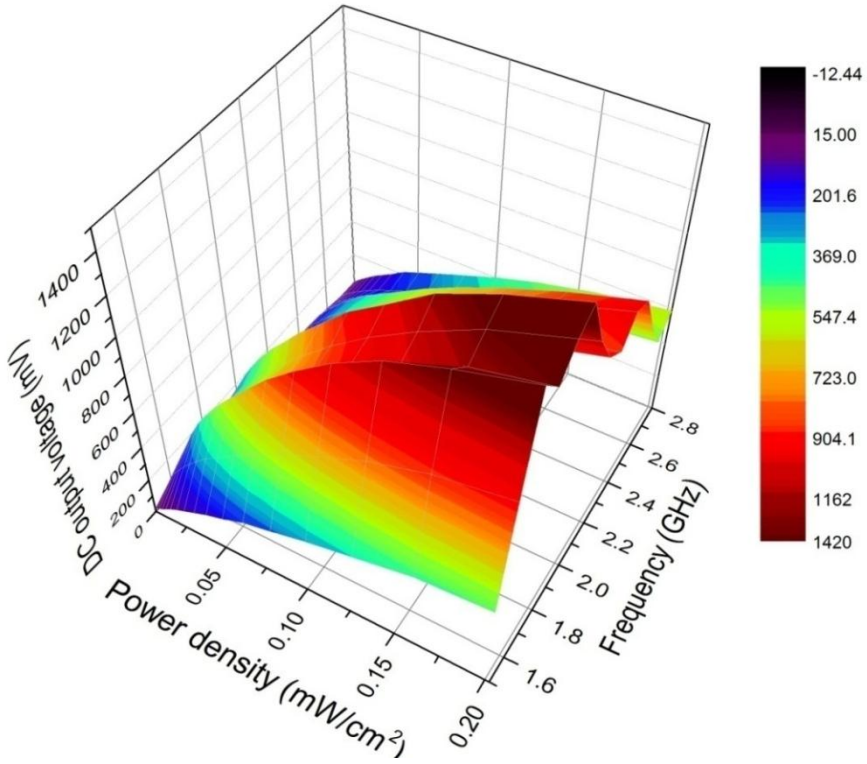

Fig. 4.28: Measured DC output voltage for wideband rectennaat broadside for power densities 15 to 200 μW/cm^2

4.7 Summary

In this chapter, a wideband cross dipole rectenna has been designed, simulated, fabricated and evaluated. The results have been provided. It has been demonstrated that the rectenna can effectively convert the RF energy between 1.7 and 3.0 GHz into DC energy. Due to the low diode conversion efficiency for the low input power density, our rectenna achieved maximum conversion efficiency around 75% for the maximum incident power density of 7.667mW/cm^2 at 2 GHz which is comparable with the results in [19, 22, 24]. Moreover, higher efficiency can be obtained if the incident power density is increased when the power density level below a certain value. It is noted that the diode should be protected from damage for a very high power density. In addition, it has been represented that how the power density and load impedance values can affect the power conversion efficiency in this structure.

Furthermore, the capabilities, potentials and performance of a wideband rectenna on FR4 substrate have been demonstrated and shown with experimental and simulations earlier in the chapter. The input impedance and rectifier conversion efficiency have also been investigated and the rectifier has been designed for low input power density. Additionally, the rectenna also has been optimized to match the rectifier for relatively low input power densities (15-200 μW/cm^2) The study has confirmed that the proposed rectenna has the maximum RF to DC conversion efficiency around 55% at single frequency and conversion efficiencies over 25% have been achieved over the frequency range from 1.6 to 2.5 GHz. This efficiency is comparable with other reported results[1, 19]but this rectenna has a much wider frequency bandwidth than the other designs.

References

[1] E Falkenstein, M Roberg, and Z. Popovic, "Low-Power Wireless Power Delivery," *Microwave Theory and Techniques, IEEE Transactions on,* vol. 60, pp. 2277-2286, 2012.

[2] E. Levine, S. Shtrikman, and D. Treves, "Double-sided printed arrays with large bandwidth," *Microwaves, Antennas and Propagation, IEE Proceedings H,* vol. 135, pp. 54-59, 1988.

[3] S. Barrette, S. K. Podilchak, and Y. M. M. Antar, "Ultrawideband double-sided printed dipole arrays," in *Ultra-Wideband (ICUWB), 2012 IEEE International Conference on*, 2012, pp. 232-235.

[4] B. G. Duffley, G. A. Morin, M. Mikavica, and Y. M. M. Antar, "A wide-band printed double-sided dipole array," *Antennas and Propagation, IEEE Transactions on,* vol. 52, pp. 628-631, 2004.

[5] T. W. Eubanks and Chang Kai, "A 4×4 radial dipole array fed by double-sided parallel-strip line," in *Antennas and Propagation Society International Symposium (APSURSI), 2010 IEEE*, 2010, pp. 1-4.

[6] T. W. Eubanks and Chang Kai, "Double-sided parallel-strip line-fed radial dipole," in *Antennas and Propagation Society International Symposium (APSURSI), 2010 IEEE*, 2010, pp. 1-3.

[7] Huang Jhin-Fang, Hsu Mao-Hsiu, and Wu Fu-Jui, "Design of a Double-Sided and Printed Wideband Dipole Array Antenna on 5.2GHz Band," in *ITS Telecommunications Proceedings, 2006 6th International Conference on*, 2006, pp. 430-433.

[8] Huang Jhin-Fang, Hsu Mao-Hsiu, and Liang Jia-Wei, "Wideband printed and double-sided dipole pair antennas with a parallel reflector," in *Microwave, Antenna, Propagation and EMC Technologies for Wireless Communications, 2005. MAPE 2005. IEEE International Symposium on*, 2005, pp. 1635-1638 Vol. 2.

[9] CST Microwave Stdio 2011 [Online].

[10] T. W. Yoo and Chang Kai, "Theoretical and experimental development of 10 and 35 GHz rectennas," *Microwave Theory and Techniques, IEEE Transactions on,* vol. 40, pp. 1259-1266, 1992.

[11] Suh Young-Ho and Chang Kai, "A novel dual frequency rectenna for high efficiency wireless power transmission at 2.45 and 5.8 GHz," in *Microwave Symposium Digest, 2002 IEEE MTT-S International*, 2002, pp. 1297-1300 vol.2.

[12] Y Suh and K. Chang, "A high-efficiency dual-frequency rectenna for 2.45- and 5.8-GHz wireless power transmission," *Microwave*

Theory and Techniques, IEEE Transactions on, vol. 50, pp. 1784-1789, 2002.

[13] J. Zbitou, M. Latrach, and Serge Toutain, "Hybrid rectenna and monolithic integrated zero-bias microwave rectifier," *Microwave Theory and Techniques, IEEE Transactions on,* vol. 54, pp. 147-152, 2006.

[14] Lozano-Nieto, *RFID design fundamentals and applications*. United State: CRC Press, 2011.

[15] J. A. Hagerty, F. B. Helmbrecht, W. H. McCalpin, R. Zane, and Z. B. Popovic, "Recycling ambient microwave energy with broad-band rectenna arrays," *Microwave Theory and Techniques, IEEE Transactions on,* vol. 52, pp. 1014-1024, 2004.

[16] M. Pinuela, P. D. Mitcheson, and S. Lucyszyn, "Ambient RF Energy Harvesting in Urban and Semi-Urban Environments," *Microwave Theory and Techniques, IEEE Transactions on,* vol. 61, pp. 2715-2726, 2013.

[17] H. J. Visser, A. C. F. Reniers, and J. A. C. Theeuwes, "Ambient RF Energy Scavenging: GSM and WLAN Power Density Measurements," in *Microwave Conference, 2008. EuMC 2008. 38th European*, 2008, pp. 721-724.

[18] H Sun, Y. Guo, M He, and Z. Zhong, "Design of a High-Efficiency 2.45-GHz Rectenna for Low-Input-Power Energy Harvesting," *Antennas and Wireless Propagation Letters, IEEE,* vol. 11, pp. 929-932, 2012.

[19] G. Monti, L. Tarricone, and M. Spartano, "X-Band Planar Rectenna," *Antennas and Wireless Propagation Letters, IEEE,* vol. 10, pp. 1116-1119, 2011.

[20] B. Strassner and Chang Kai, "5.8 GHz circular polarized rectenna for microwave power transmission," in *Energy Conversion Engineering Conference and Exhibit, 2000. (IECEC) 35th Intersociety*, 2000, pp. 1458-1468 vol.2.

[21] T. Yoo, J. McSpadden, and K. Chang, "35 GHz rectenna implemented with a patch and a microstrip dipole antenna," in *Microwave Symposium Digest, 1992., IEEE MTT-S International*, 1992, pp. 345-348 vol.1.

[22] Ren Yu-Jiun and Chang Kai, "5.8-GHz circularly polarized dual-diode rectenna and rectenna array for microwave power transmission," *Microwave Theory and Techniques, IEEE Transactions on,* vol. 54, pp. 1495-1502, 2006.

[23] Ren Yu-Jiun and Chang Kai, "New 5.8-GHz circularly polarized retrodirective rectenna arrays for wireless power transmission," *Microwave Theory and Techniques, IEEE Transactions on,* vol. 54, pp. 2970-2976, 2006.

[24] H. Takhedmit, B. Merabet, L. Cirio, B. Allard, F. Costa, C. Vollaire, *et al.*, "A 2.45-GHz low cost and efficient rectenna," in *Antennas and Propagation (EuCAP), 2010 Proceedings of the Fourth European Conference on*, 2010, pp. 1-5.

CHAPTER 5

WIDEBAND RECTENNA ARRAYS FOR LOW INPUT POWER WIRELESS ENERGY HARVESTING

5.1 Introduction

Since the ambient RF energy resources are usually a of low input power level, rectennas with high efficiency for low input power are in great demand. Wideband antennas have received much attention in mobile wireless communications and with a wideband antenna the rectenna can harvest ambient RF energy in the air at different operational frequencies. To provide adequate output power for some applications, a rectenna array is required which can also be used as an effective methods to increase the rectenna capability for a low input power. Most of rectenna elements and rectenna arrays are developed for single frequency or multi-frequencies for low input power levels, especially for ISM (industry- science-medical) bands [1-3]. Few rectennas are reported for wideband rectenna and low

input power applications and they are focused on single element performances for a narrowband rectenna [1, 4].

In this chapter, a wideband double-sided rectenna array for harvesting low power RF energy is presented. The RF to DC conversion efficiency for low input power is improved. Two types of high gain wideband antenna arrays are designed for the rectenna array. Since the effective aperture area of an antenna is proportional to its gain, the use of a high gain antenna can receive more power for the rectification to a great extent when the incident power density is low.

5.2 Antenna Array Design

5.2.1 A Single Rectenna Element

Different shapes of double-side dipoles have been investigated for wideband design [5-10]. The proposed wideband antenna for rectenna is shown in Fig. 5.1. The antenna is printed on FR4 substrate coated with 1 oz cooper (thickness of 0.036 mm), the relatively permittivity is 4.3 and the thickness of the substrate is 0.6 mm. The antenna is fed by the parallel strip-line. The characteristic has been reported in Section 4.2. The length of L is 40 mm, the length of feed line Lf is 40 mm, and the width of feed line Wf is 0.8 mm. The dimensions of double side dipole are optimised by using the 3D electromagnetic simulator CST MWS. Firstly, the simulated reflection coefficient and the gain of an antenna element without reflector are shown in Fig. 5.2 and 5.3 respectively, which is used to compare with the results from the proposed antenna. The result shows that the double-sided antenna without reflector can achieve a bandwidth of 60% and the average gain of the antenna is around 3 dBi.

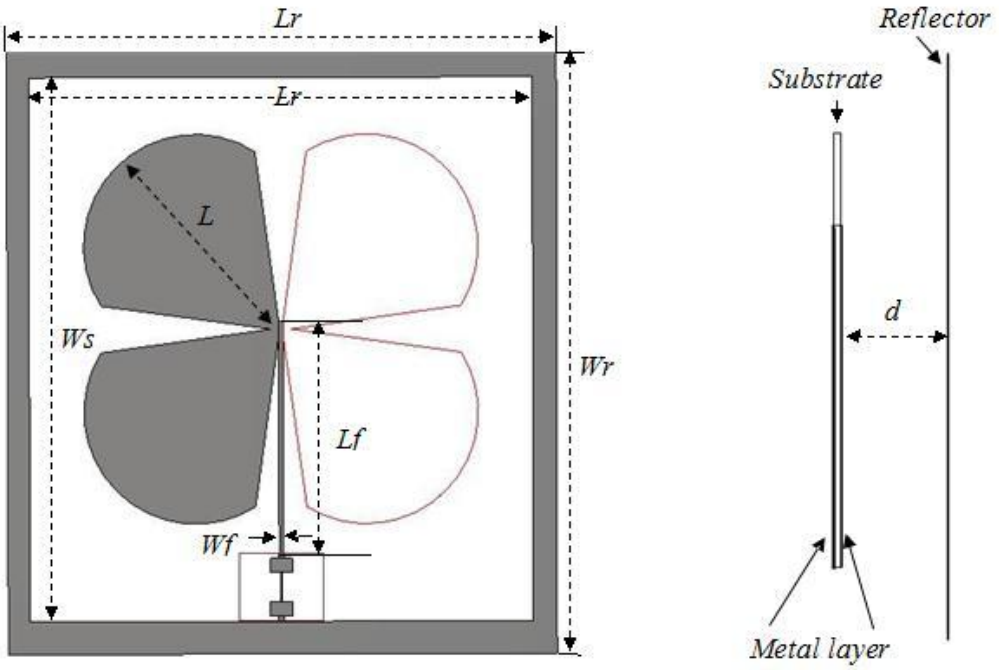

Fig. 5.1: The configuration of the proposed antenna

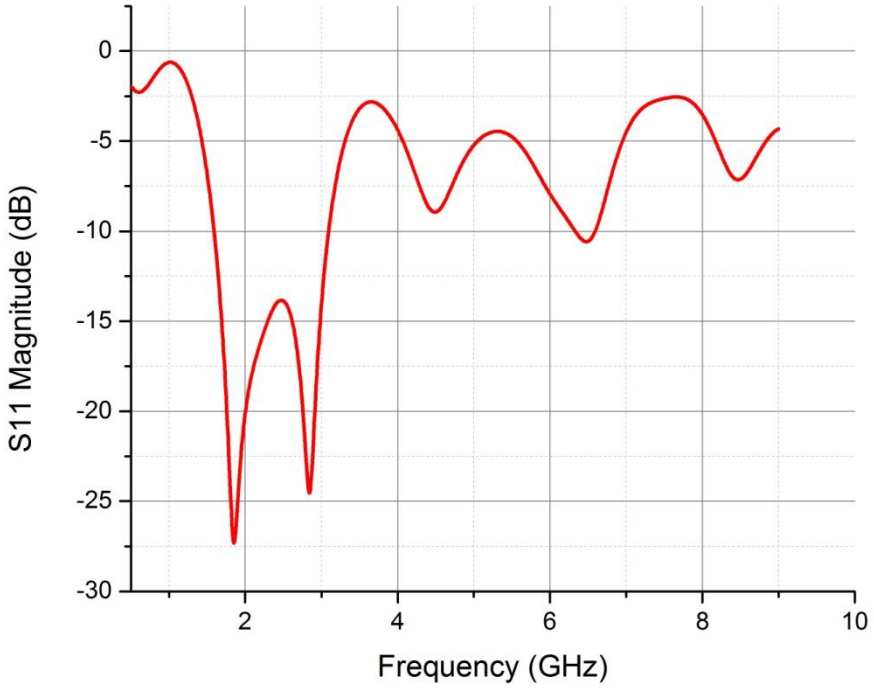

Fig. 5.2: The reflection coefficient for the antenna without a reflector

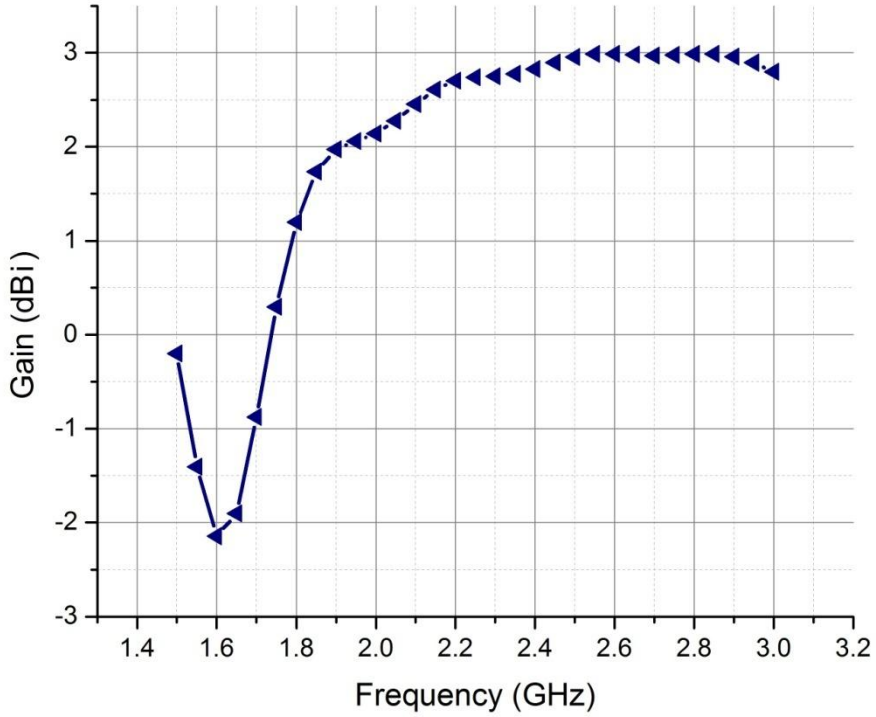

Fig. 5.3: The gain for the antenna without a reflector

In order to increase the gain, a reflector is added below the antenna. It has been found that the space *d* between antenna and reflector affected the operation bandwidth and input impedance of the wideband antenna. A parametric study is taken by using the simulation software as shown in Fig. 5.4;it is obvious that the antenna with the increase of *d* the antenna has wider bandwidth. On the other hand, the peak gain of antenna is another important aspect for this antenna and the peak gain value with various *d* is given in Fig. 5.5.It is important to note that with the increase of space *d* the gain of antenna decreases. So the space *d* of35 mm is chosen for a wide bandwidth and high gain in the final design. It is apparent that this wideband antenna has a S11=-10 dB bandwidth over 60%. An antenna with such a wide operation bandwidth can cover most of GSM applications and 3G, 4G Wi-Fi systems from 1.6 to 3.2 GHz. In addition, comparing with results for antenna without reflector the gain of the

antenna, the gain of antenna with the reflector is higher than that of antenna without reflector.

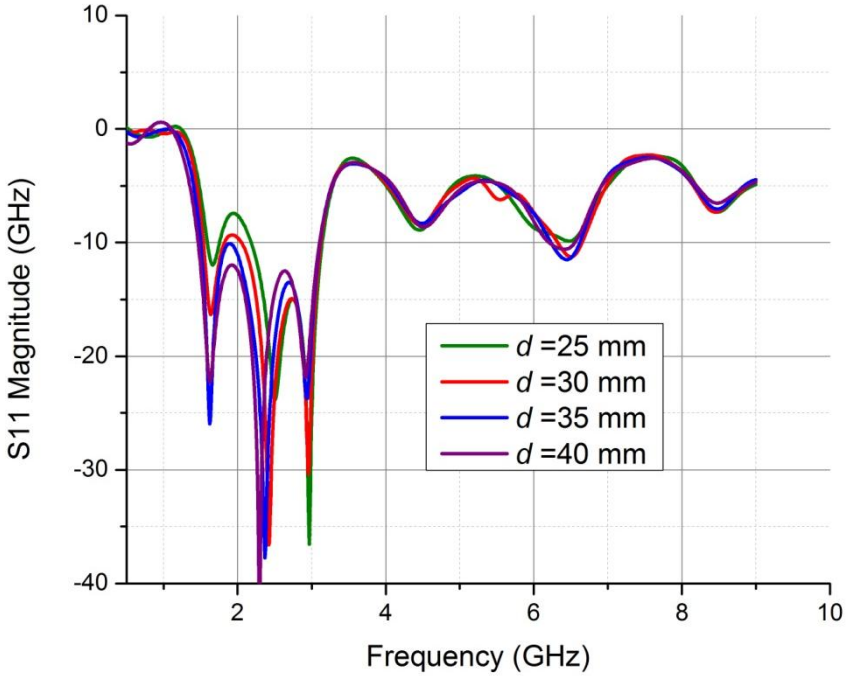

Fig. 5.4: The S11 of the proposed antenna with reflector

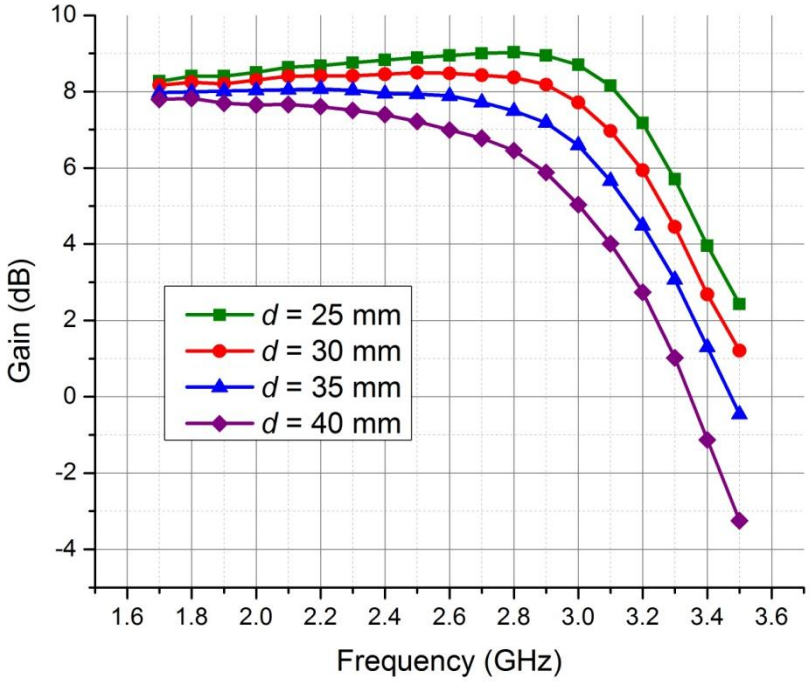

Fig. 5.5: The gain of the proposed antenna with reflector

There are some advantages of this design. The first is that it can be integrate with a low-pass filter and rectifier on the same substrate. The second is that it can control the wideband performance by tuning the feed line and reflector easily. This is helpful while designing the rectenna and the rectenna array for low input power.

For the rectenna design, a low-pass filter is connected with the antenna and the simulated optimum reflection coefficient of antenna with low-pass filter matching to 50 Ω is shown in Fig. 5.5. It shows that the -10 dB bandwidth is 65% for antenna with the low-pass filter. The deep around 5 GHz is caused by the strong coupling between antenna and filter. It is clear that the antenna with low-pass filter can blocks the high order harmonics in most of frequencies and the 3D radiation pattern for 2 GHz 2.4 GHz and 3GHz are shown in Fig. 5.6(a).Fig. 5.6(b) shows the 2D radiation pattern and it is shown that the broad beam-width can be observed and its half power beam width (HPBW) is about 60^{o} for both frequencies. The broad beam-width can overcome the sensitive of antenna to the direction. The radiation patterns for those frequencies do not change much. These results represent that the radiation patterns are quite stable within the operating bandwidth.

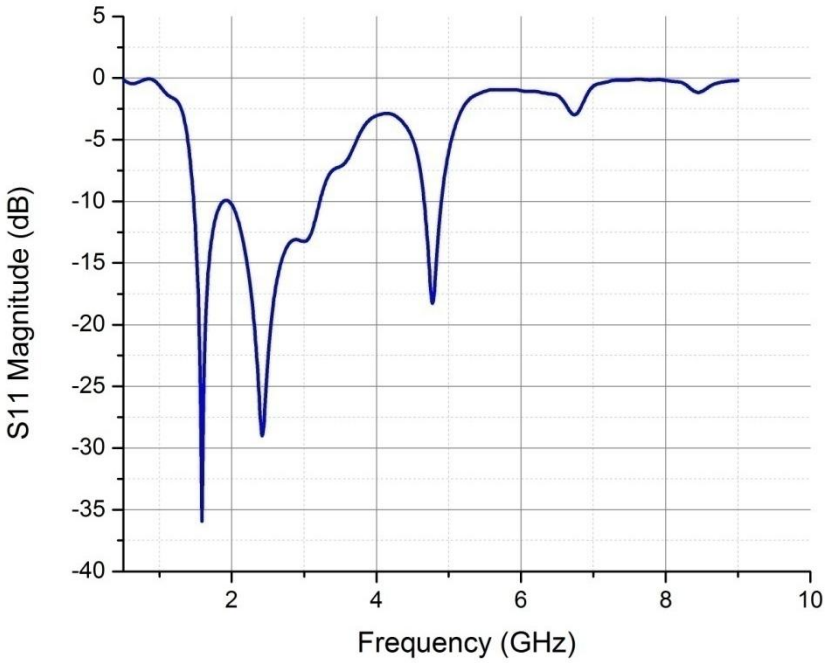

Fig. 5.5: The reflection coefficient for antenna with low-pass filter

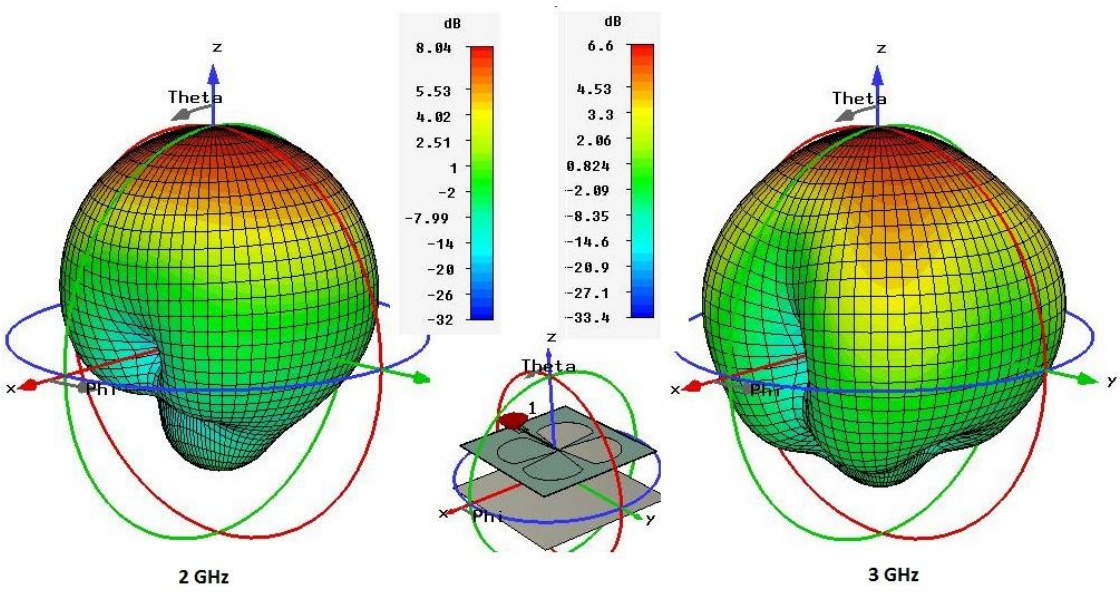

Fig. 5.6(a): The 3D radiation pattern for the proposed antenna at 2 GHz and 3 GHz.

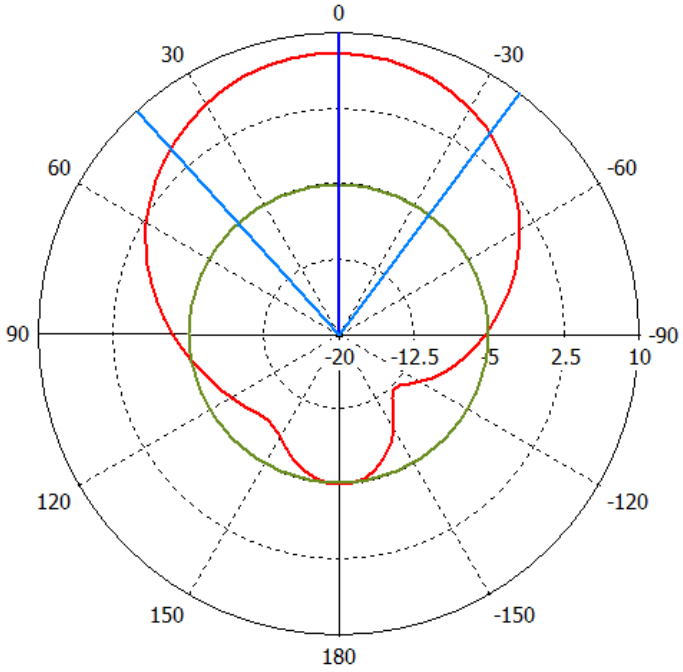

(b) 2 GHz yoz plane

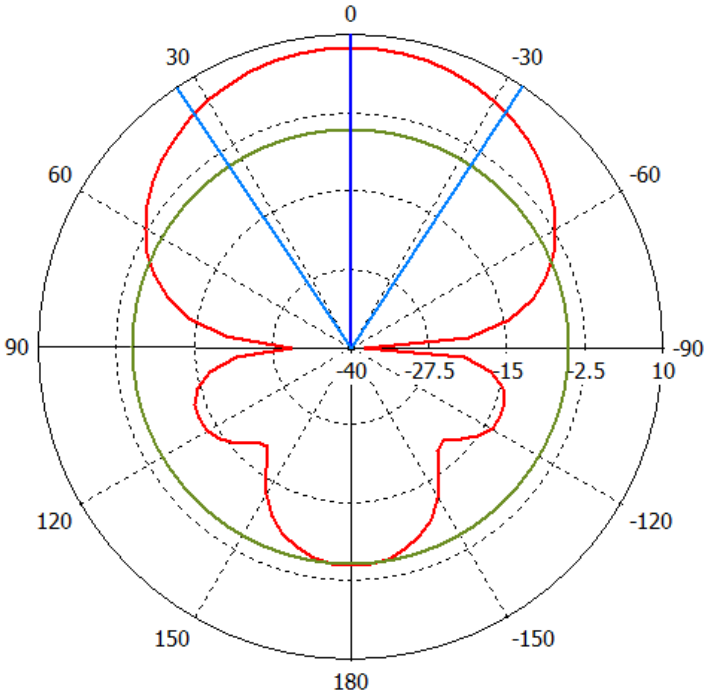

(c) 2GHz xoz plane

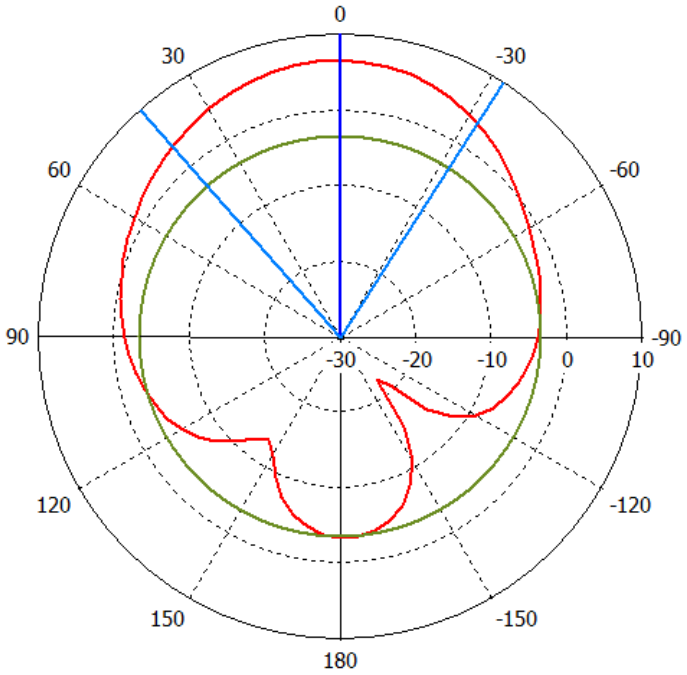

(d) 3GHz yoz plane

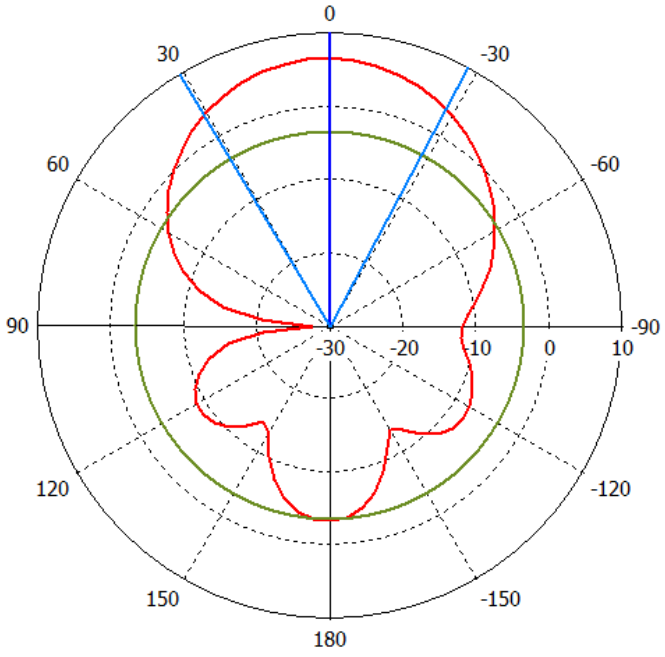

(e) 3GHz xoz plane

Fig. 5.6 Simulated radiation pattern at 2 GHz and 3 GHz for antenna with the low-pass filter

The rectifier consists of a schottky diode, a DC-pass filter and a resistive load. The input impedance for antenna is shown in Fig. 5.7. The antenna is designed self-matching with the rectifier. Because the input impedance of the rectifier strongly depends on the frequency, the input power and output load which has been discussed in Chapter 4. Although the antenna is optimised to conjugating match with rectifier at all operation frequencies it may still mismatches with rectifier in some specific frequencies.

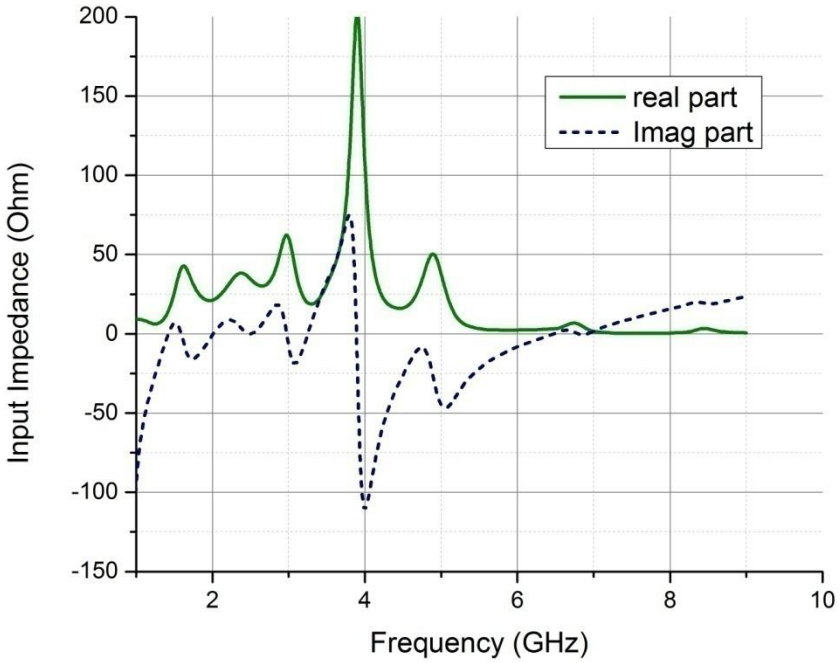

Fig. 5.7: Simulated input impedance for proposed antenna with the low-pass filter

The conversion efficiency is calculated by

$$\eta = \frac{V_{DC}^2}{R_L} \times \frac{1}{P_{in}} \tag{5.1}$$

Where V_{DC} is the DC output voltage and P_{in} is the input power level sensed by the rectenna.

The simulated rectenna conversion efficiency as a function of frequency and power density is plotted on Fig. 5.8. It is worth to note that

the highest RF to DC conversion efficiency for whole frequencies occurs when the power density is 0.07 mW/cm^2. Also, the maximum conversion efficiency for the proposed rectenna is around 60%. In addition, in the same power density level, the conversion efficiency is lower at 1.6 to 2.0 GHz is due to the mismatching between antenna to the rectifier. At power density of 0.07 mW/cm^2, the RF to DC conversion efficiency is over 40% from 1.9 to 3.2 GHz

The DC output voltage simulated by using ADS software is given in Fig. 5.9. It is obvious that the DC voltage is increase with the increase of input power density. In the same power density the value of DC output voltage does not change too much at 2.0 to 3.2 GHz. It is confirmed that the rectenna conversion efficiency is very sensitive to the changes on the DC output voltage. The output voltage is low in the lower frequency is due to the strong mismatching as we mentioned above.

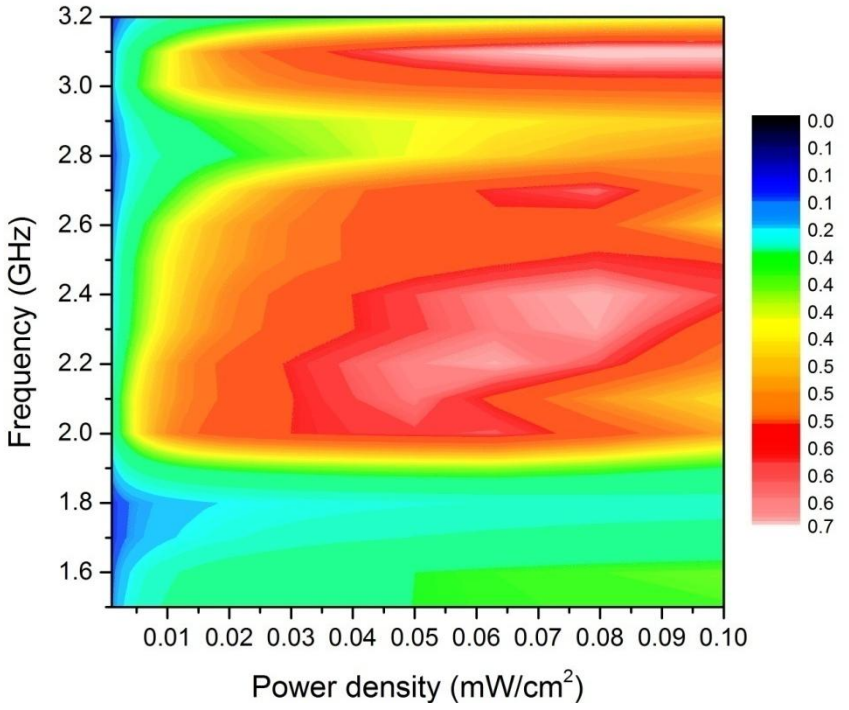

Fig. 5.8: Calculated RF to DC conversion efficiency for the proposed rectenna at broadside for power density 5 to 100 μW/cm^2

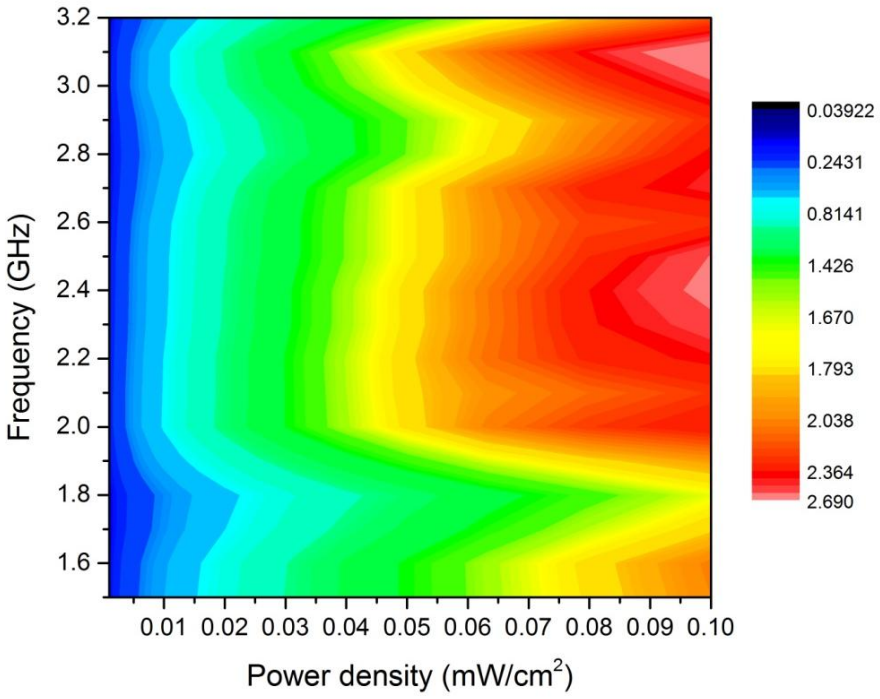

Fig. 5.9: Simulated DC output voltage for the proposed rectenna at boeadside for power density 5 to 100 μW/cm^2

5.2.2 Rectenna Array Designs

Typically, a single rectenna is not sufficient in supplying energy for reliable device operation. Properly interconnecting several antennas could provide for sufficient power. There are two basic methods for rectenna array energy collectors. The first approach is that each antenna element supplies its own rectifier and the DC output voltage is combined in parallel, series or a hybrid manner shown in Fig. 5.10 (a). On the other hand, combined the electrical oscillations from many antenna elements in a particular phase relationship and delivered their combined output to a rectifier shown in Fig. 5.10 (b). This configuration is suitable for large rectenna array which can effectively avoid the complex feeds. The first method is called DC combiner method and the latter method is called RF combiner method [11].

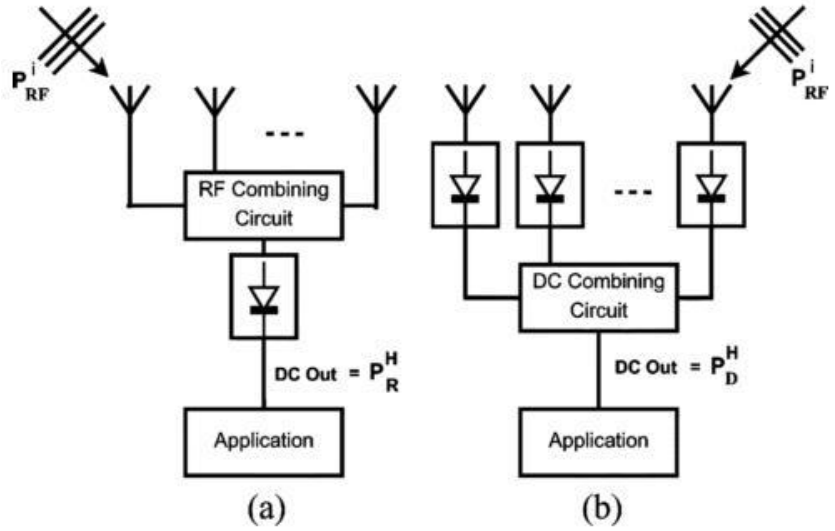

Fig. 5.10: (a) RF combiner (b) DC combiner

Schematics of the investigated rectenna array configurations[11]

5.2.2.1 The RF Combiner Rectenna Array

The two element wideband printed dipole array is shown in Fig. 5.11 and the antenna printed on a low-cost RF4 substrate with the relatively permittivity of 4.3, thickness of 0.6 mm. The length of *L* is 40 mm, the distance between two antenna is *d1* and a reflector place below the antenna with an optimised space of *d* of 25 mm.

The two feed line are then connected to the output ports of a power combiner circuit. Power dividers/ combiners are passive devices which are widely used in microwave systems. It is used to distribute input signal power to two or more parts. T junction power divider is the simplest power divider /combiner which behaves similarly to a three-port Wilkinson except there is no isolation between two input ports. Isolation is one of the most important qualities of a network. The most common problem of poor isolation in a combiner is that the interaction between two input ports might significantly affect the performance of the power combiner. The load resistant can be used between two input ports to provide good isolation like Wilkinson power combiner but it also causes power loss on the resistant. Hence, in the rectenna design we choose the T

junction power combiner. In practice, the measured results would lower than the theoretical results due to the poor isolation.

The characteristic impedance of the parallel strip-line which feed every element is 100 ohm. Neighbour antennas are connected through a T-junction power combiner that is used to combine the power from each antenna element and transfer it to the low-pass filter and rectifier. To optimise the antenna match 100 ohm can avoid using quarter wavelength transmission line which can be narrow the bandwidth. The whole array is fed from a conversional 50 Ohm transmission line and this design can combine the power over wide bandwidth.

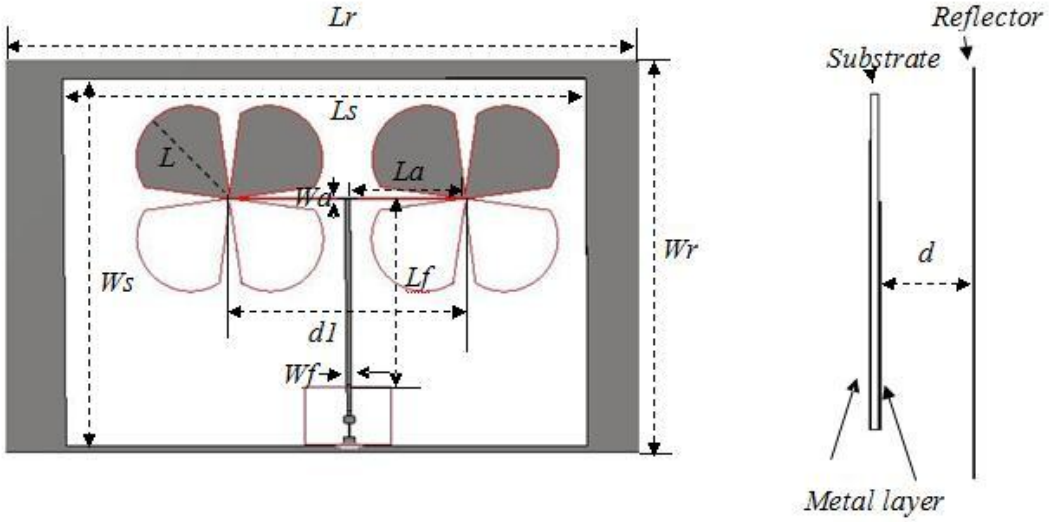

Fig. 5.11: The layout of the proposed rectenna array

When antenna elements are placed in an array, they interact with each other. The interactions between elements due to their close proximity is called mutual coupling, which affects the current distribution and hence the input impedance as well as the radiation pattern [12]. Therefore a parametric study is taken by using CST MWS to optimise the distance *d1* and reflection coefficient and gain are depicted in Fig. 5.12 and 5.13. It is important to note that the gain and the bandwidth do not have much

changes with various *d1*. So the average *d1* of the proposed antenna array is 90 mm.

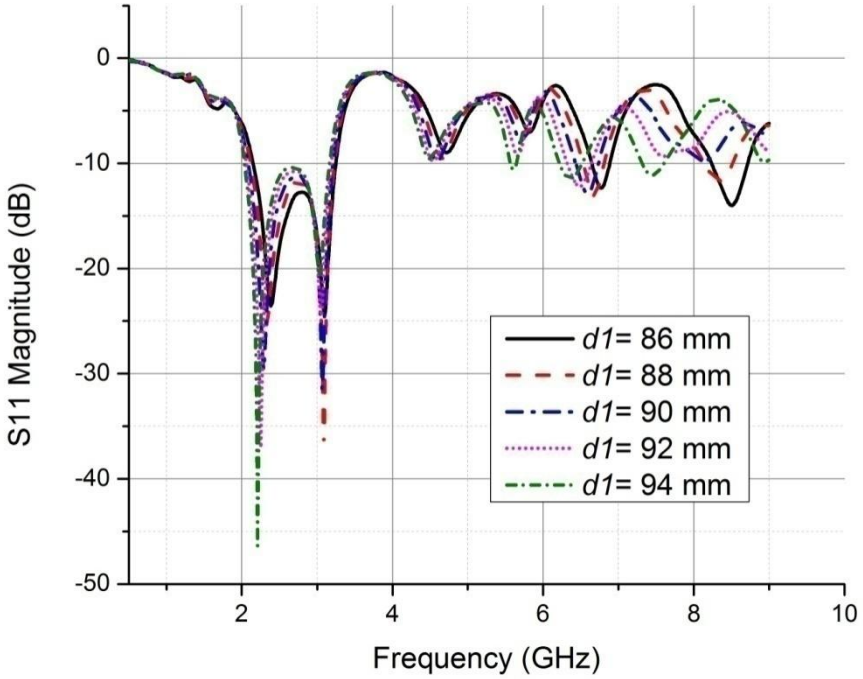

Fig. 5.12: The S11 of proposed antenna without reflector for various *d1*

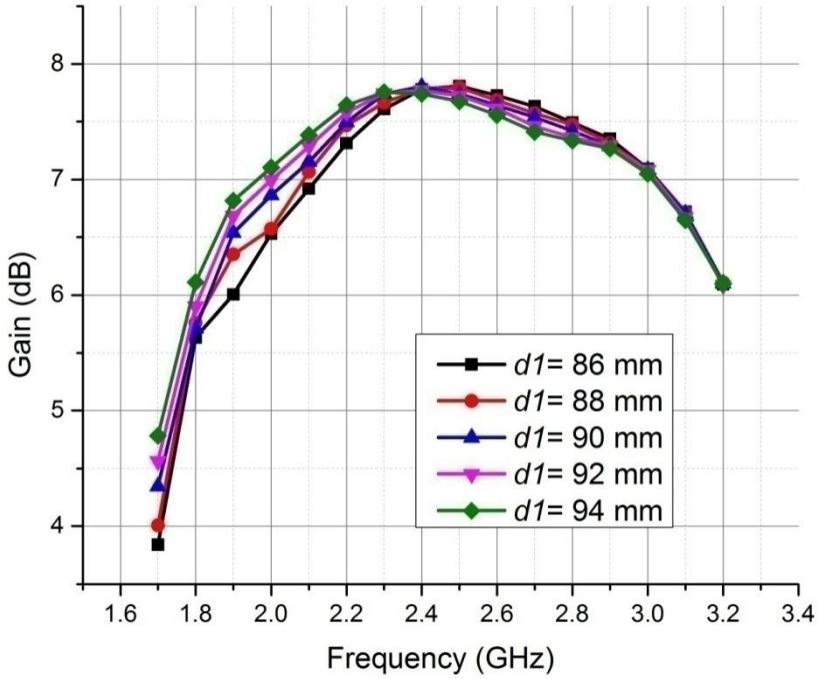

Fig. 5.13: The gain of proposed antenna without reflector for various *d1*

Results for antenna array with low-pass filter are shown in Fig. 5.14. From Fig. 5.14 (a) the maximum gain in main lobe of antenna is 12.8 dB at 2.5 GHz and the average gain is 12 dB. The reflection coefficient shown in Fig. 5.14 (b) represents that the antenna array with reflector covers the bandwidth from 2 to 3 GHz. There are two deeps at 4.3 and 5 GHz due to the coupling between antennas with low-pass filter which cannot be avoid. It is obvious that the low-pass filter block most of high order harmonics foe the proposed antenna array which can increase the conversion efficiency of the rectenna array. In addition, the 3D antenna radiation patterns are plotted in Fig. 5.15. It is obvious that the antenna array has narrow beam-width due to the high gain obtained. Thus, the antenna has a strong dependence upon the antenna direction.

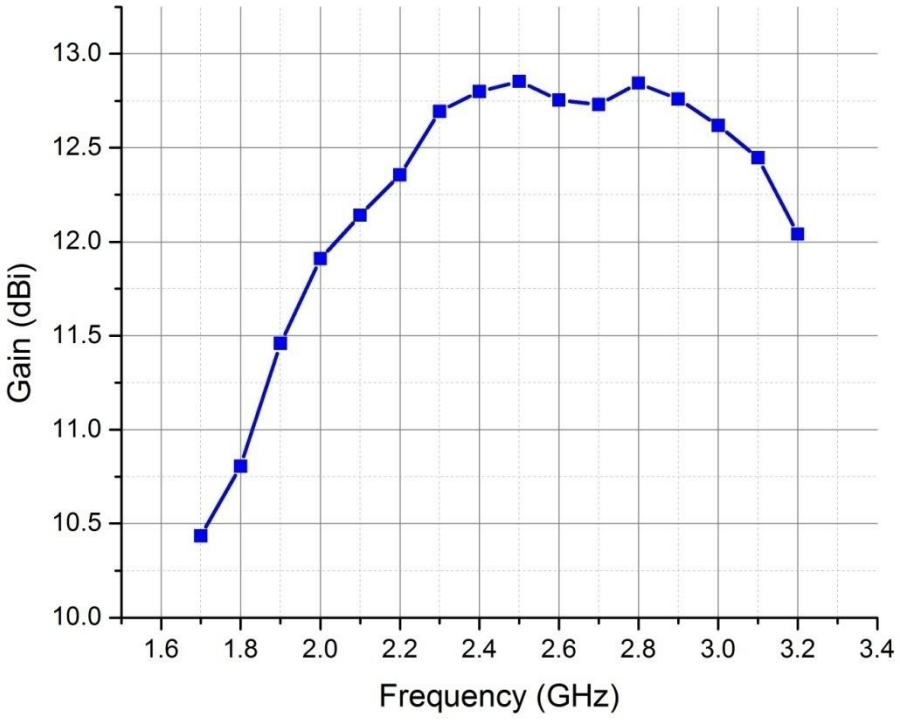

(a) optimum gain of the proposed antenna array with the low-pass filter.

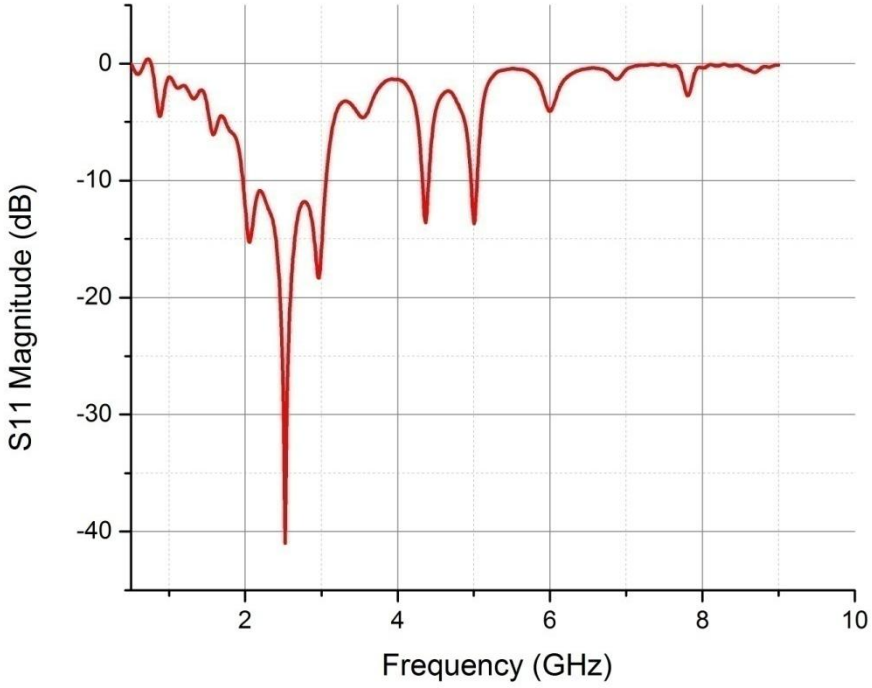

(b) The simulated S11 for the proposed antenna array with low- pass filter.

Fig. 5.14: The optimised antenna performance of the proposed antenna array

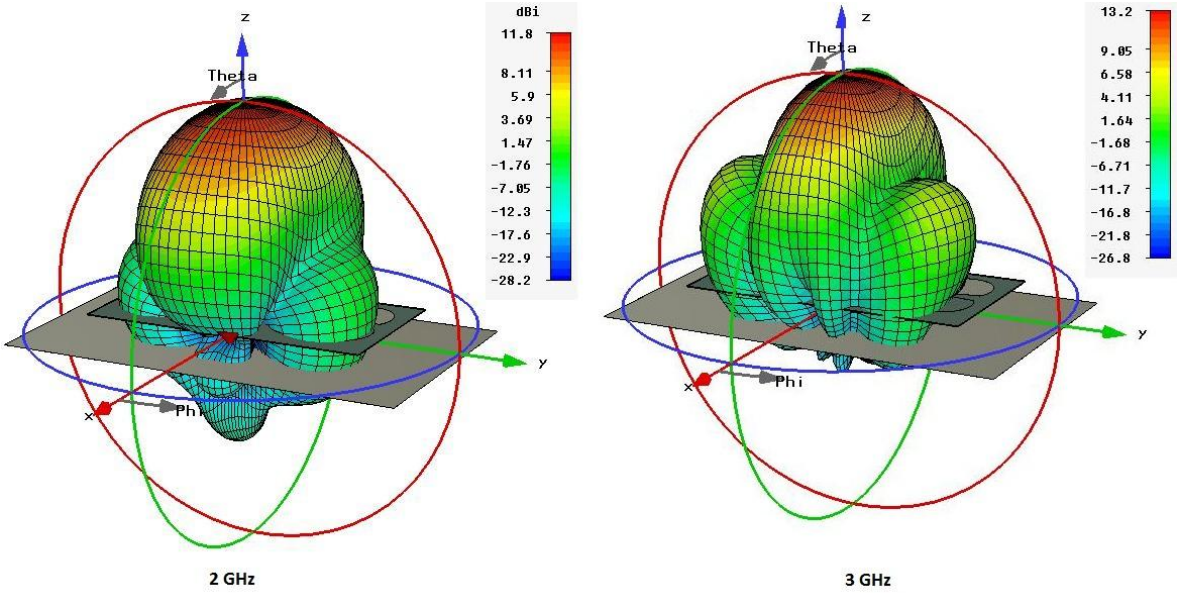

Fig. 5.15: The simulated 3D radiation pattern for the proposed rectenna array

The DC output voltage and RF to DC conversion efficiency for the rectenna array is given in Fig. 5.16. At the same power density the efficiency is higher than that of a single rectenna because it inherently has

a higher gain. From 1.9 to 3.2 GHz the rectenna array has high conversion efficiency over 40% for power density 5 μW/cm^{2}to 38 μW/cm^2. The highest conversion efficiency of 66% occurs when the input power density is around 25 μW/cm^2. It means this rectenna array effectively increase the rectenna conversion efficiency for low power density over the whole frequency range.

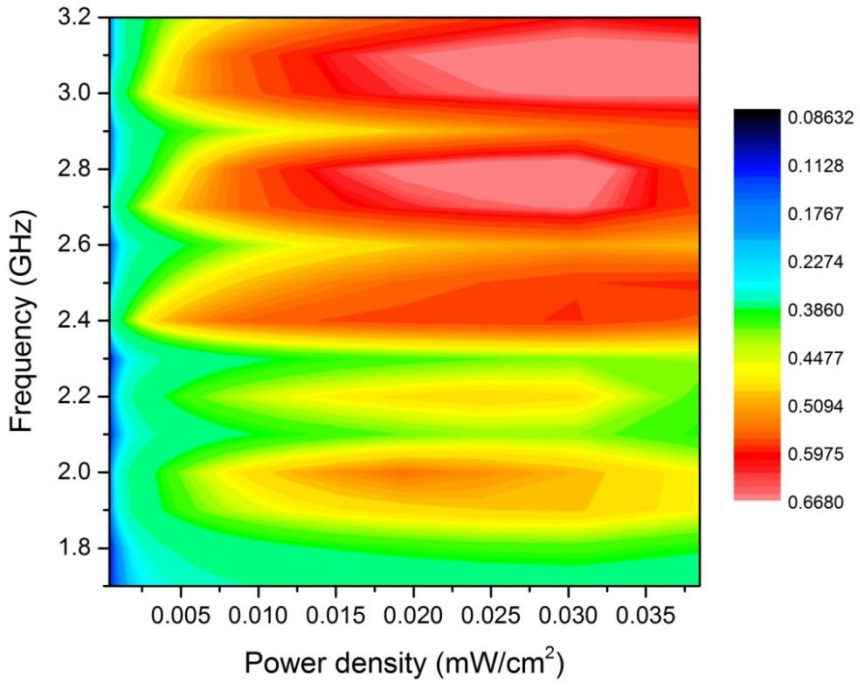

Fig. 5.16: Calculated RF to DC conversion efficiency for the proposed rectenna at broadside for power density 0.3 to 35μW/cm^2

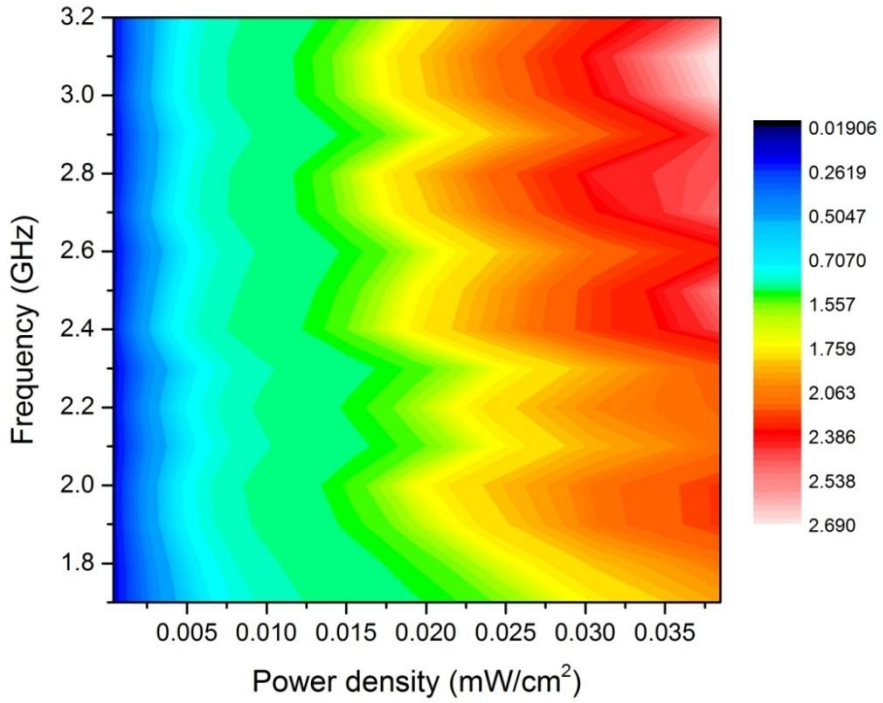

Fig. 5.17: Simulated DC output voltage for the proposed rectenna at broadside for power density 0.3 to 35μW/cm^2

From Fig. 5.17, as we expect, the DC output voltage increase together with the power density. In addition, higher frequencies achieve higher output voltage is due to the good matching in higher frequencies. At power density of 0.03 mW/cm^2, DC output voltage for the single rectenna and the rectenna array are 1.2 V and 2.3 V, respectively. Comparing the rectenna array output voltage with the single element output voltage it is important to note that the output voltage for the rectenna array significantly increases. Furthermore, it almost once higher than the output voltage for a single rectenna. The only limitation of this design is that the rectenna is very sensitive to the direction as we mentioned above.

5.2.2.2 The DC Combiner Rectenna Array

The second two-element wideband printed dipole array is shown in Fig. 5.18. The length of *L* is 40 mm; the distance between two antennas is *d1* and a reflector place below the antenna with an optimised space of *d* of 35 mm. The characteristic impedance of the parallel strip-line which fed every element is 50 ohm and connected to the low-pass filter and rectifier.

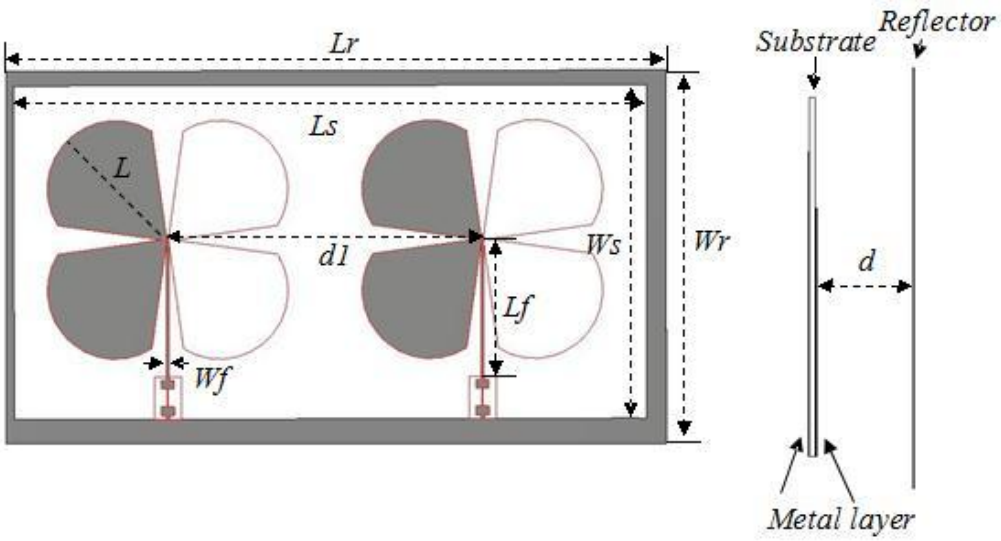

Fig. 5.18: The layout of the proposed rectenna array

The optimised reflection coefficient and gain for each antenna element are shown in Fig. 5.19 and 5.20. This two antenna element is the same and has the same antenna performance. From Fig. 5.19 the antenna has the bandwidth of 61%, which cover frequencies from 1.7 GHz to 3.2 GHz. The low-pass filter blocks the high order harmonics but due to the coupling between antenna and low-pass filter there is a deep at 5 GHz. The gain of proposed antenna shows that the antenna maximum gain is 7.6 dB at 2.2 to 2.8 GHz and the average gain is 7 GHz at whole frequency range. Comparing the gain of the antenna element to the gain of the single antenna, the decrease of the gain may cause by the mutual coupling between two elements. The DC output is parallel combined in the rectifier and the theoretical analysis is discussed as follows.

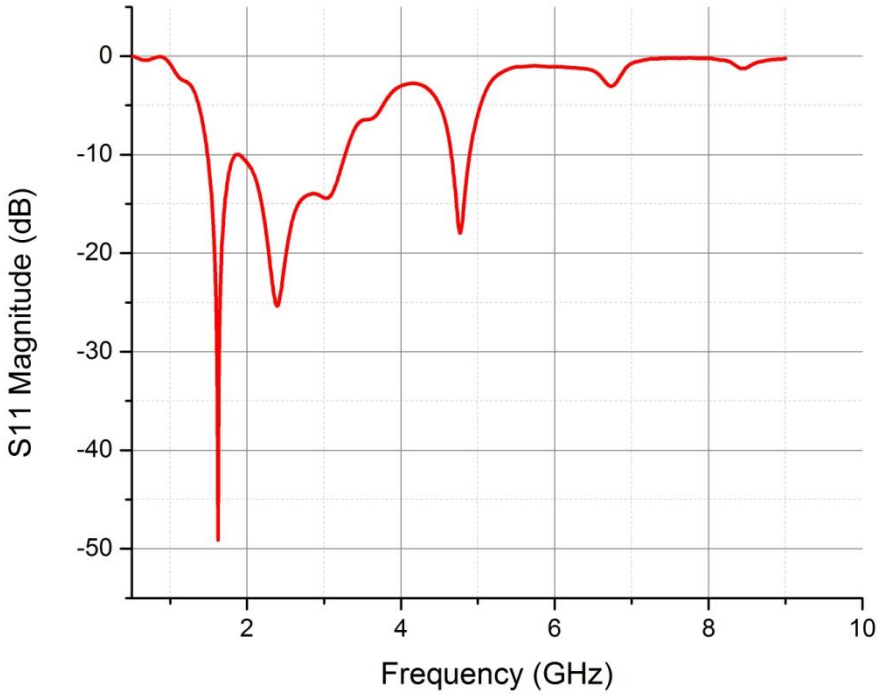

Fig. 5.19: Simulated S11 for proposed antenna with low-pass filter

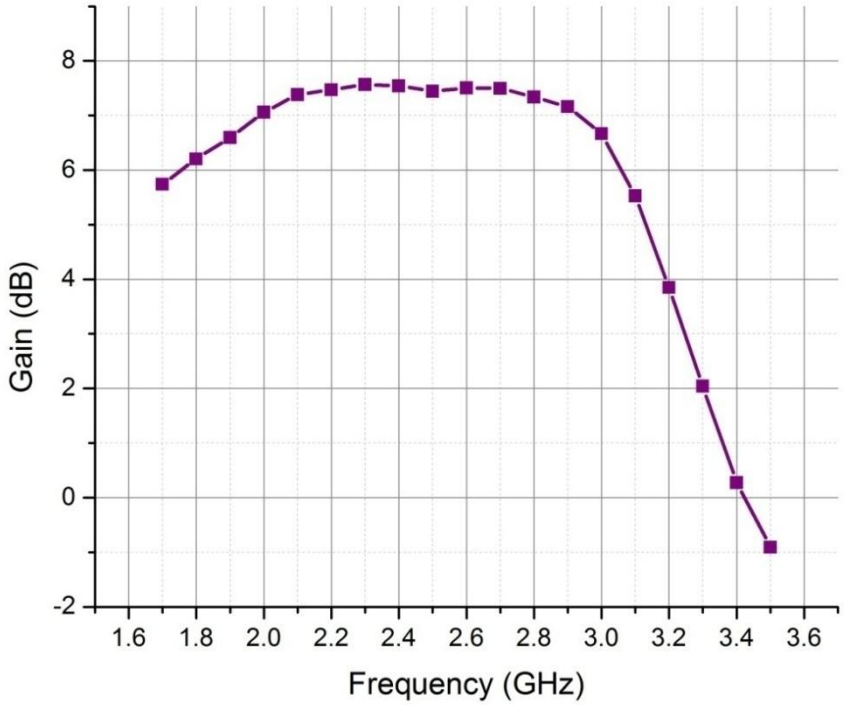

Fig. 5.20: Simulated gain for each proposed antenna element with the low-pass filter

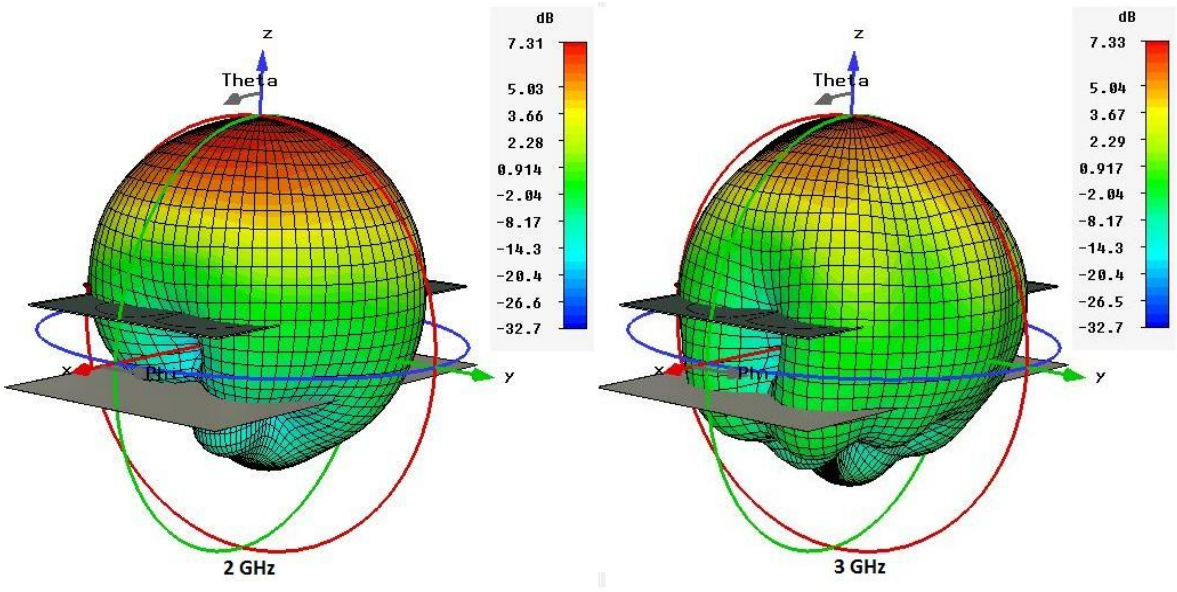

Fig. 5.21: The radiation pattern for one of the proposed antenna with the low-pass filter in the array

The 3D radiation pattern of the antenna array at 2 GHz and 3 GHz are depicted on Fig. 5.21. The radiation patterns display nearly unidirectional radiation patterns and the antenna has HPBW over 60% which means the antenna has a wide beam-width and each element in the array has independent radiation pattern.

Each rectenna is a non-linear device so using a non-linear model to analyze the circuit behaviour is preferred. Theoretically, the non-linear model should be able to describe the characteristics for the whole range of loadings. In our study, for the purpose of easy analysis, the rectenna is modelled as a linear device. The simple equivalent linear model of single rectenna element is shown in Fig. 5.22(a). Using the equivalent circuit, an analytical model of a parallel connection can be built. The load voltage V_{D0}, current I_0 and power P_L of a load is calculated by

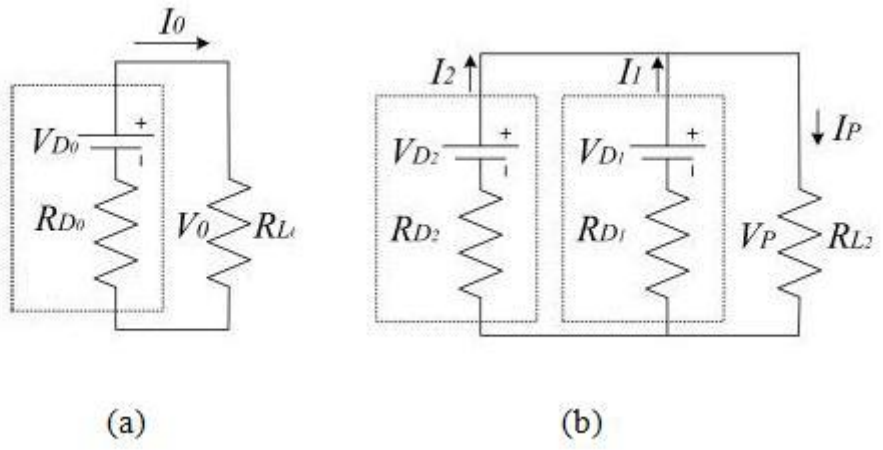

Fig. 5.22: simple equivalent circuit of rectennas (a) single rectenna (b) the rectenna array connected by parallel

$$I_0 = \frac{V_{D0}}{R_{D0}+R_{L0}} \tag{5.1}$$

$$V_0 = \frac{V_{D0}\cdot R_{L0}}{R_{D0}+R_{L0}} \tag{5.2}$$

$$P_L = \frac{V_{D0}^2\cdot R_{L0}}{(R_{D0}+R_{L0})^2} \tag{5.3}$$

The power reaches a maximum when the condition of $R_S = R_L$. The circuit parameters of the parallel connection as shown in Fig. 5.20(b) we assume R_{L1}=R_{S1} and R_{L2} = R_{S2}, the maximum power transfer when $R_{D0} = {}^{1}\Big/\left({}^{1}/_{R_{D1}} + {}^{1}/_{R_{D2}}\right) = {}^{R_{D0}}/_{2}$ are given by

$$I_P = (I_1 + I_2) = \frac{V_{D1}+V_{D2}}{R_{D0}+R_{Ls}} \tag{5.4}$$

$$V_P = \frac{V_{D1}+V_{D2}}{2} = \frac{V_{D1}+V_{D2}}{R_{D0+}R_{Ls}} \cdot \frac{R_{L0}}{2} \tag{5.5}$$

$$P_P = V_p \cdot I_P \tag{5.6}$$

In theory the DC output voltage for the antenna array is the same with the output voltage for single rectenna. The simulation is undertaken to simulate the RF to DC conversion efficiency and DC output voltage reported in Figs. 5.23 and 5.24.

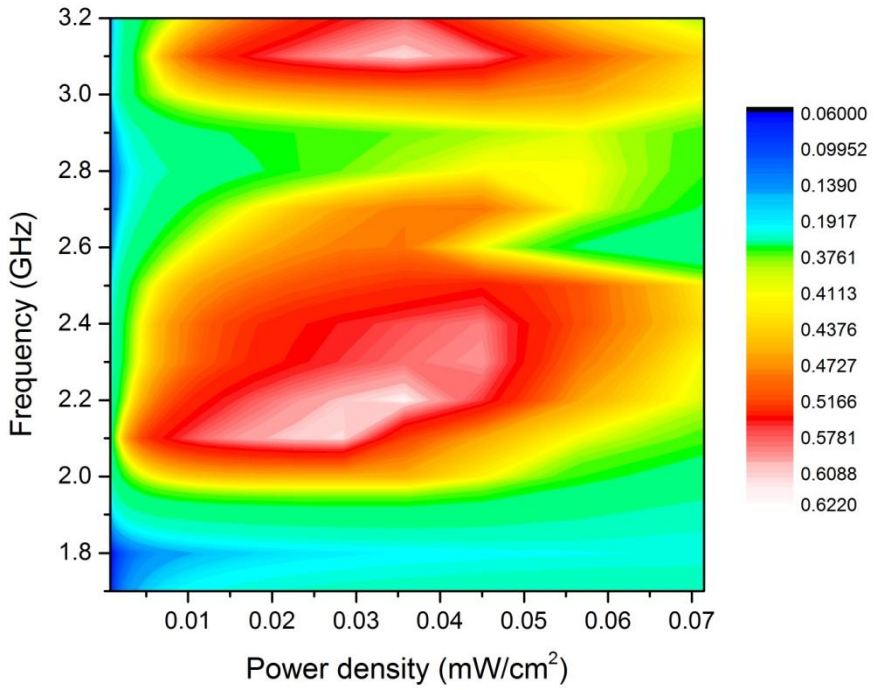

Fig. 5.23: Calculated RF to DC conversion efficiency for the proposed rectenna at broadside for power density 0.7 to 72μW/cm^2

Fig. 5.23 shows the RF to DC conversion efficiency for the rectenna at range of power density 7μW/cm^{2}to 70μW/cm^2 at whole operation frequencies. As the impedance deviates from the optimum, the rectenna conversion efficiency decreases significantly around 2.8 GHz due to the big mismatching between antenna and rectifier. At single frequency the rectenna has highest RF to DC conversion efficiency of 62% for power density of 30 μW/cm^2 which almost the same as the maximum conversion efficiency of the RF combiner rectenna array. It is clear that the rectenna has high conversion efficiency for low input power density.

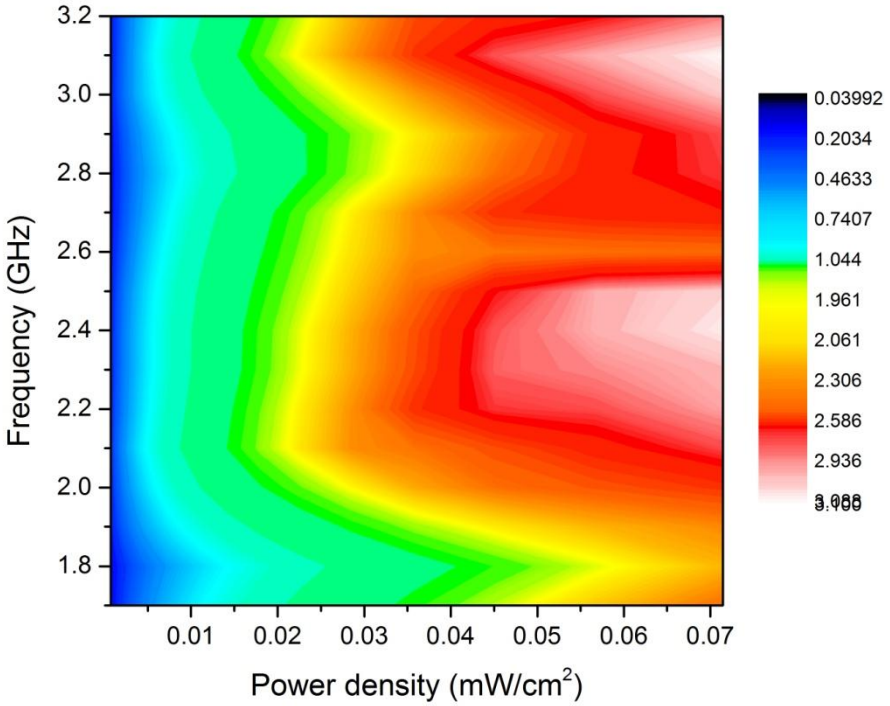

Fig. 5.24: Simulated DC output voltage for the proposed rectenna at broadside for power density 0.3 to 35μW/cm^2

As we expected, there are the same trend for all frequency, the output voltage increases with the power density. In addition, comparing with the output voltage between the single rectenna and the rectenna array at 30 μW/cm^2. The output voltage of the array is slightly higher than that of the single antenna.

Comparing the results of DC combiner rectenna array to the RF combiner rectenna array, the later one has high conversion efficiency over wider bandwidth. In addition, the output voltage of the RF combiner rectenna is also higher than that of the DC combiner rectenna.

For a conclusion, although both of these two rectenna arrays can effectively increase the RF to DC conversion efficiency for the rectenna for low input power density and output voltage, the RF combiner rectenna array is better than the DC combiner rectenna array. However, it is worth

to note that the RF combiner rectenna array has a narrow beam-width to the high gain which means the rectenna array is very sensitive to the direction. A further study of wideband rectenna array design is needed to solve this problem.

5.3 The Rectenna Implementation

The propose RF combiner rectenna was made and then tested in an anechoic chamber. The measurement system is illustrated in Fig. 5.25(a) and the photograph of the fabricated rectenna is given in Fig. 5.25(b). The source in the measurement was a signal generator connected a power amplifier, allowing far field measurements to be performed for a range of incident power density on the integrated rectenna at the normal incidence. A standard horn antenna was used for transmitting the power from 1.4 to 3 GHz. In addition, the proposed rectenna was placed in a fixed position and by measuring the output voltage V_{dc} over the load R, then the conversion efficiency can be obtained.

The measured conversion efficiency and output voltage of the rectenna for different input power densities and frequencies are depicted in Figs. 5.26 and 5.27. The optimum operational frequency range for the wideband rectenna is found to be 1.5 to 3.0 GHz at a power density range from 0.1 to 120 μW/cm^2. It is seen that the maximum conversion efficiency of 37% is achieved around 80 μW/cm^2 at 2.2 GHz. Over a higher frequency range (2.4 GHz-3.0 GHz) conversion efficiencies decrease due to the material losses on the rectifier and a mismatch between the antenna and the low-pass filter and the rectifier caused by fabrication errors. In addition, from 1.5 to 3 GHz the overall conversion efficiency of the rectenna is above 20 %. Comparing with other wideband rectennas, the proposed rectenna has relatively good conversion efficiency over a wideband range. The Fig. 5.27 shows the measured DC output voltage of the rectenna as a function of the frequency and power density.

The output voltage stays above 500 mV over the range of power densities from 10 to 120 μW/cm^2. In addition, as expected, the output voltage increases with the power density.

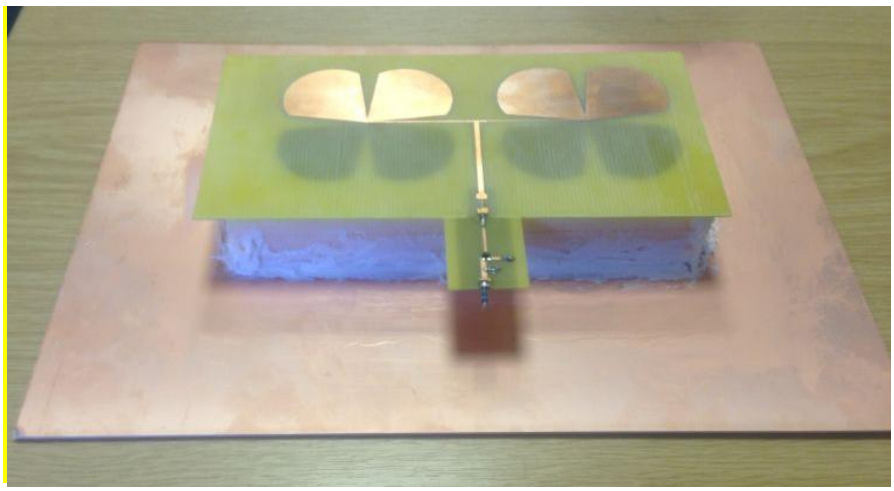

(a)

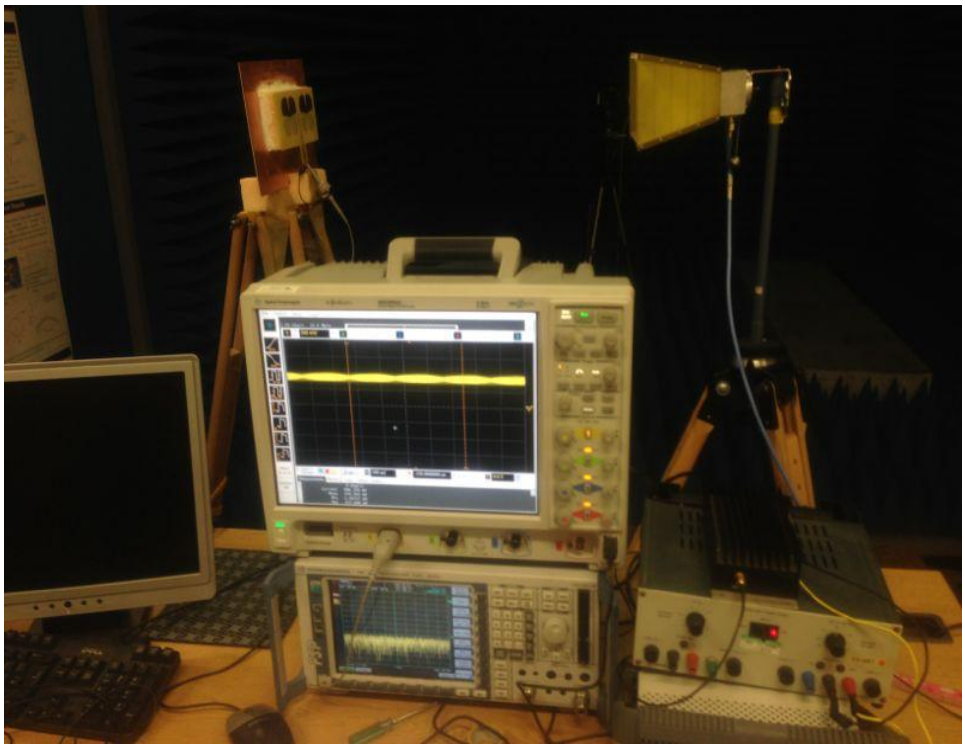

(b)

Fig. 5.25. (a) The photographs of proposed rectenna under test. (b) the measurement system in anechoic chamber.

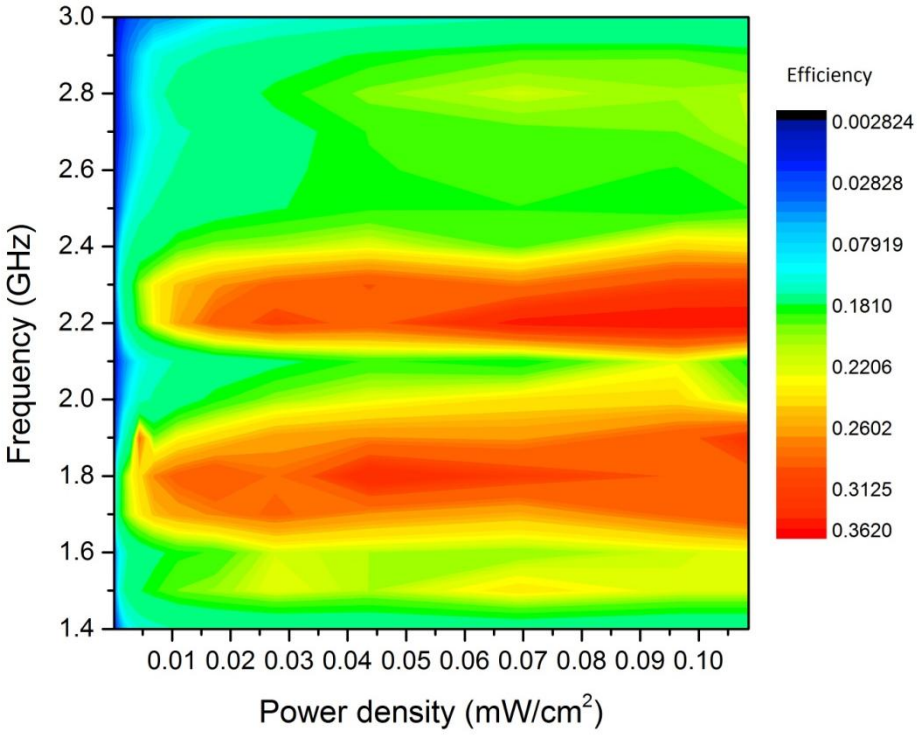

Fig. 5.26. Measured conversion efficiency for wideband rectenna at broadside for power densities up to 120 μW/cm^2

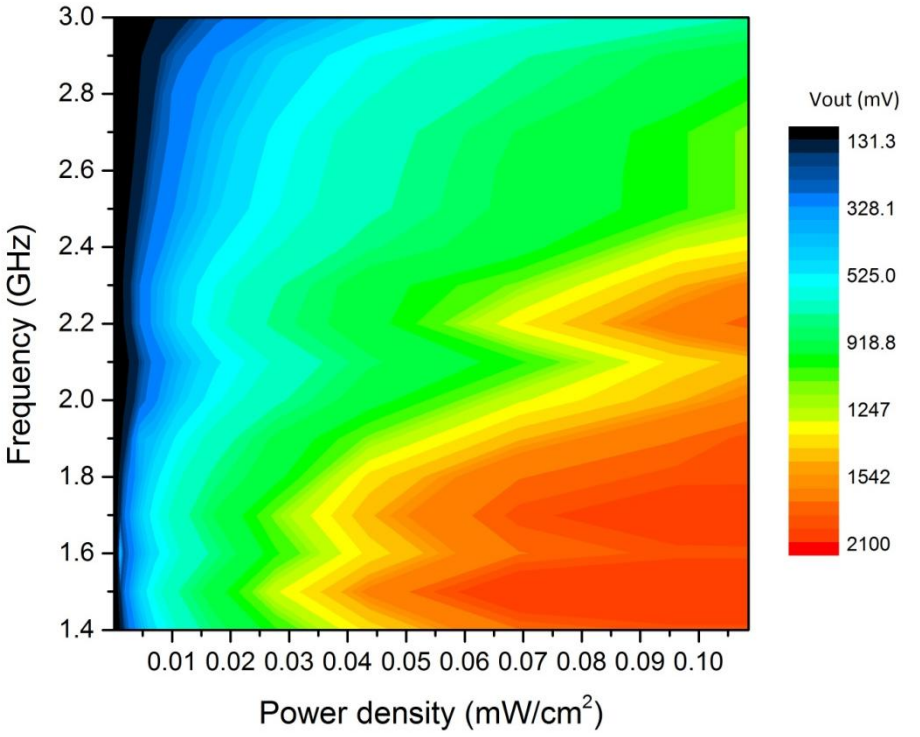

Fig. 5.27. Measured DC voltage for wideband rectenna at broadside for power densities up to 120 μW/cm^2

From Fig. 5.26 and 5.27, it is shown that the output voltage and RF to DC conversion efficiency are lower than the simulated results. The disagreement is cause by three factors. Firstly, the FR4 substrate cause material loose at high frequency (>1.5GHz). Secondly, the fabrication error and the connection between antenna and rectifier affect the rectenna performance. Finally, the poor isolation combiner affected the antenna performance. Therefore, in my future work, the rectenna performance can be increase by overcoming these three factors.

5.4 Summary

In this chapter, a wideband rectenna array for wireless energy harvesting for low input power density has been addressed. Two connection methods were used to form the rectenna array and the RF combiner rectenna is better than the DC combiner rectenna due to the wider rectification bandwidth and higher DC voltage supply. Methods have demonstrated in simulation on the wideband rectennas with voltage doubler rectifying circuits. Results has represented that the rectenna array with reflector can effectively increase the rectenna conversion efficiency and output voltage for low power density at wide frequency range by increasing the gain of antenna. The study has also confirmed that the RF combiner method can has good performance for efficiency and output voltage but limited by the rectenna direction. It is comparable with the results in [1, 3, 13, 14] and the rectenna array even has higher efficiency than wideband rectenna array designs.

A wideband rectenna array has been fabricated and tested. The overall conversion efficiency over 20% has been achieved from 1.5 to 3 GHz with the incident power density from 5 to 120 μW/cm^2. In addition the maximum conversion efficiency is 37% at 1.8 and 2.2 GHz

respectively. The shining point of this design is that the rectenna array provides good conversion efficiency even with very low incident power (around 5 μW/cm^2) and the rectenna operation bandwidth are very 60%.

References

[1] H Sun, Y. Guo, M He, and Z. Zhong, "Design of a High-Efficiency 2.45-GHz Rectenna for Low-Input-Power Energy Harvesting," *Antennas and Wireless Propagation Letters, IEEE,* vol. 11, pp. 929-932, 2012.

[2] M. Pinuela, P. D. Mitcheson, and S. Lucyszyn, "Ambient RF Energy Harvesting in Urban and Semi-Urban Environments," *Microwave Theory and Techniques, IEEE Transactions on,* vol. 61, pp. 2715-2726, 2013.

[3] H. Sun, Y. Guo, M. He, and Z. Zhong, "A Dual-Band Rectenna Using Broad-Band Yagi Antenna Array for Ambient RF Power Harvesting," *Antennas and Wireless Propagation Letters, IEEE,* vol. PP, pp. 1-1, 2013.

[4] E Falkenstein, M Roberg, and Z. Popovic, "Low-Power Wireless Power Delivery," *Microwave Theory and Techniques, IEEE Transactions on,* vol. 60, pp. 2277-2286, 2012.

[5] S. Barrette, S. K. Podilchak, and Y. M. M. Antar, "Ultrawideband double-sided printed dipole arrays," in *Ultra-Wideband (ICUWB), 2012 IEEE International Conference on*, 2012, pp. 232-235.

[6] B. G. Duffley, G. A. Morin, M. Mikavica, and Y. M. M. Antar, "A wide-band printed double-sided dipole array," *Antennas and Propagation, IEEE Transactions on,* vol. 52, pp. 628-631, 2004.

[7] T. W. Eubanks and Chang Kai, "A 4×4 radial dipole array fed by double-sided parallel-strip line," in *Antennas and Propagation Society International Symposium (APSURSI), 2010 IEEE*, 2010, pp. 1-4.

[8] T. W. Eubanks and Chang Kai, "Double-sided parallel-strip line-fed radial dipole," in *Antennas and Propagation Society International Symposium (APSURSI), 2010 IEEE,* 2010, pp. 1-3.

[9] Huang Jhin-Fang, Hsu Mao-Hsiu, and Wu Fu-Jui, "Design of a Double-Sided and Printed Wideband Dipole Array Antenna on 5.2GHz Band," in *ITS Telecommunications Proceedings, 2006 6th International Conference on*, 2006, pp. 430-433.

[10] Huang Jhin-Fang, Hsu Mao-Hsiu, and Liang Jia-Wei, "Wideband printed and double-sided dipole pair antennas with a parallel reflector," in *Microwave, Antenna, Propagation and EMC Technologies for Wireless Communications, 2005. MAPE 2005. IEEE International Symposium on*, 2005, pp. 1635-1638 Vol. 2.

[11] U. Olgun, Chen Chi-Chih, and J. L. Volakis, "Investigation of Rectenna Array Configurations for Enhanced RF Power Harvesting," *Antennas and Wireless Propagation Letters, IEEE,* vol. 10, pp. 262-265, 2011.

[12] Huang Yi, Kevin Boyle, *Antennas: from theory to practice*. UK: Wiley, 2008.

[13] Pham Binh, J. C. S. Chieh, and Pham Anh-Vu, "A wideband composite right/left hand rectenna for UHF energy harvesting applications," in *Antennas and Propagation Society International Symposium (APSURSI), 2012 IEEE*, 2012, pp. 1-2.

[14] J. A. Hagerty, F. B. Helmbrecht, W. H. McCalpin, R. Zane, and Z. B. Popovic, "Recycling ambient microwave energy with broad-band rectenna arrays," *Microwave Theory and Techniques, IEEE Transactions on*, vol. 52, pp. 1014-1024, 2004.

CHAPTER 6

CONCLUSION AND FUTURE WORK

6.1 Summary

With the rapid development of wireless communications, a large number of wireless systems radiate electromagnetic energy into the air but most of them are wasted. The rectenna has attracted great attention to recycle the ambient power radiated by wireless systems. Accordingly, the major goals of this thesis are on investigating wideband antenna performance, designing novel wideband rectennas for RF wireless energy harvesting and improving wideband rectenna conversion efficiency for low input power density.

In the first part of chapter 3, different shapes of broadband dipole antennas with unidirectional radiation pattern are developed for wireless harvesting and UWB applications. Both simulation and measurement have confirmed that circular dipole can covers the bandwidth from 2.4 to 10

GHz with unidirectional radiation pattern which is a good candidate to form a array for wireless energy harvesting application.

In the second part of chapter 3, a simple rectenna and duel-polarised rectenna arrays has been designed. A theoretical analysis has been presented to investigate diode performance. In addition, although the rectenna became narrowband due to the limitation on gap size of antenna it has shown that the maximum RF to DC conversion efficiency for the rectenna is around 16%. Furthermore, with a cascade interconnection, rectenna element has been built as two-element and three-element rectenna arrays. Measurements have been taken in the anechoic chamber. The result provided that the output voltage of the rectenna array is much higher than that of a single rectenna element. At the same time due to the distribute element characteristics the rectenna output voltage is sensitive to the measured position.

In chapter 4, two novel wideband cross dipole rectennas have been designed. The first design is a double-sided structure on Arlon Cu217 substrate. The rectenna has been demonstrated that the rectenna conversion efficiency is significantly affected by the input power density and output load of rectenna. It is obvious that that the peak RF to DC conversion efficiency is over 70% for high input power density levels. In addition, the second rectenna built on FR4 substrate has been investigated, fabricated and measured. The further investigation for the input impedance of rectifier has been analyzed and the wideband antenna is designed self-match to the rectifier. Experimental results have represented that the rectenna has wideband rectification performance and the maximum rectenna conversion efficiency at 1.7 GHz is more than 50% for power density of 0.1 mW/cm^2.

In chapter 5, a newly wideband rectenna array is developed to increase the rectenna conversion efficiency and output voltage for low input power density. In addition, two connection methods has been used to

build the rectenna array and compared with the single rectenna element. Connecting more antenna elements the receiving antenna of the rectenna can form a broadside array with higher gain. The RF combiner method can much increase the conversion efficiency for the rectenna and the maximum conversion efficiency is around 66%. In addition, the DC output voltage for the rectenna array is twice of that of the single element but the array is limited by the orientation. Comparing RF power combiner rectenna with the DC power combiner rectenna, the former one has high conversion efficiency at wider bandwidth and higher DC voltage absorption.

6.2 Future Work

Regards to the conclusions drawn and the limitations of the work presented, future work can be carried out in the following area:

- It is necessary to improve the rectenna array performance. A substrate material suitable for high frequency should be used to build the rectifying circuit. In addition, there is a strong demand for broadband duel-polarized rectenna design with for low input power density. It would be desirable is one can design a broadband duel polarisation rectenna array able to harvest and recycle ambient electromagnetic wave for low power density.

- An integrated device with rectennas, power management, storage andcontrol is desired. The energy collected from integrated rectenna must be converted to a form that can be stored for later use. In remote sensor systems or portable device applications that use energy harvesting a small rechargeable battery or storage capacitor is often employed to store the collected energy the system needs for operation.

- It is important to explore commercial applications for rectenna and rectenna arrays. Especially combining with other components or devices as a DC voltage source such as communications, RFID, embedded sensors.For example, the rectenna should be able to charge the battery of mobile device such as the cellular phone and the laptop. Besides the basic rectenna element, a recharging control circuit using a fixed voltage regulator is needed to provide a stable and constant voltage or current flowing into the battery.

END